Modelling Evaporation from a Subarctic Sedge Wetland

MODELLING EVAPORATION FROM A SUBARCTIC SEDGE WETLAND

By

David Alan Wessel, B.Sc.

A Thesis

Submitted to the School of Graduate Studies

in Partial Fulfillment of the Requirements

for the Degree

Master of Science

McMaster University

August 1992

MASTER OF SCIENCE (1992) (Geography)

McMASTER UNIVERSITY
Hamilton, Ontario

TITLE: **Modelling Evaporation from a Subarctic Sedge Wetland**

AUTHOR: David Alan Wessel, B.Sc. (McMaster University)

SUPERVISOR: Dr. Wayne R. Rouse

NUMBER OF PAGES: xi, 169

ABSTRACT

Evapotranspiration is a major constituent of both the energy and water balances of wetland tundra environments. Reliable estimates of evapotranspiration are required in the analysis of specific climatological and hydrological problems occurring within a wetland. As a result, where direct measurements are unavailable, models designed to accurately predict evapotranspiration for a particular wetland are highly desirable.

This paper evaluates the limitations, sensitivity and performance of four physically-based one-dimensional models in the simulation of evaporation from a subarctic tundra sedge wetland in the Hudson Bay Lowland near Churchill, Manitoba (58°45'N, 94°04'W). The surface of the study site consists of near-saturated peat soil with a sparse sedge canopy and a constantly varying coverage of open water. Measured evaporation was determined using the Bowen ratio approach to which the results of the models were compared. The comparisons were conducted with hourly and daily simulations over dry, wet and moderately wet surface conditions.

The four models comprised two previously developed and tested models and two modified versions of these models. All four are based on the well-known Penman-Monteith combination formula. The first two are the Penman-Monteith model and the Shuttleworth-Wallace sparse canopy model. The third is an extension of the Penman-Monteith model which is weighted for surface area of the evaporation sources. The fourth is a modified version of the Shuttleworth-Wallace model which includes open water as an additional component to sparse canopy and bare soil as a contributor to the evaporation stream.

Results from the study suggest that the weighted Penman-Monteith model has the highest potential for use as a predictive tool. In all four cases, the importance of accurately measuring the surface area of each evaporation source is recognized. The difficulty in determining a representative surface resistance for each source and the associated problems in modelling without it is also stressed. An analysis of the role and impact of feedbacks within the models is recommended as an important direction for future research.

ACKNOWLEDGEMENTS

First of all, I am sincerely grateful to my supervisor, Dr. Wayne Rouse, for his guidance and support through the research and writing of this paper. His vivid and active interest in my work was very encouraging and always kept me going through the hard times. I would also like to thank him for the unlimited use of his 486, which increased the running time of my models a hundredfold over my "dinosaur" of a computer.

A special thanks go to the other "climos" in GSB 413. Pete Blanken always provided unique insights and an endless source of humour, particularly when times were scary or when I was getting physically hurt by sliding doors. Dale Boudreau contributed very useful suggestions toward the presentation of past papers as well as the Big One. In addition to this, I couldn't have survived the past two years without occasionally using his Mac, even if it did crash alot (many times at my own unintentional doing). Derek Carlson applied his experience in the field as well as keeping me on the straight and narrow during the Early Years. I greatly appreciate their support.

I would also like to thank Dr. Peter Lafleur for his advice on the application of the models, with particular reference to his experience with the SW model. Thanks also to

Dr. John Davies for his comments and suggestions near the end of this research.

Finally, I would like to express my gratitude to my family and close friends who supported and encouraged me. There is no way I could have gotten this far without them.

TABLE OF CONTENTS

LIST OF FIGURES

LIST OF TABLES

Chapter 1

Introduction

The reliable estimation of evapotranspiration is required for many hydrological and climatological studies. This is mainly due to the fact that, depending on the region being studied, evapotranspiration is often the largest component of the water balance and it can be strongly influenced by climate change (Morton, 1983). This is especially true in wetland regions where the water table is quite often at or above the surface in the summer, which results in a reduction of surface resistance and an increase in the rate of evaporation (Roulet and Woo, 1986).

The Hudson Bay lowland is an extensive, flat, poorly-drained region along the southwestern coasts of Hudson and James Bay. It has been estimated that over 85% of the lowland is covered with a saturated peatland plain, much of which occurs as a fen wetland (Sims et al., 1979; Riley, 1982). Ponds and near-saturated peaty soil are the most common surface types and the largest contributors to evaporation. The vegetative canopy is sparse and the predominant plant types are grasses and sedges, particularly <u>Carex aquatilis</u> which is widely distributed from temperate regions to the high arctic (Riley, 1990). Open water, bare soil and vegetation combine to produce a latent heat flux which is a highly significant component of the energy balance of tundra (Lafleur et al, 1992).

The importance of evapotranspiration in water balance and climate change studies has prompted the development of physically-based mathematical models. The primary advantage of these models is their potential to predict the hydrological, meteorological and physiological responses to a variety of hypothetical climate change scenarios. However, the model must first be able to accurately simulate evapotranspiration from the surface it is representing before it can be accepted as a predictive tool. In most cases, evapotranspiration models have been developed for agricultural purposes and there has been relatively little testing in naturally vegetated areas. The specific goal of this thesis is to examine the ability of four physically-based models to simulate evaporation from sparsely-vegetated, hummocky, wetland sedge tundra and to assess their usefulness in a predictive role.

The first model is the well known and much used Penman-Monteith combination model, developed by Penman (1948) and modified by Monteith (1965). This one-dimensional model simulates evaporation from a surface covered by a closed canopy of vascular plants and assumes that contribution from the substrate is negligible. The driving variables within the model are available energy and vapour pressure deficit, with evaporation being restricted by aerodynamic and physiological resistances. The entire canopy is treated as a single large leaf such that all stomata within the canopy act in parallel.

The second model is the one-dimensional Shuttleworth-Wallace (1985) combination model which simulates the individual contributions of two sources of evaporation: canopy and bare soil. It takes a Penman-Monteith approach with both sources and assumes that the total evaporative flux is the sum of the two evaporation streams. Thus, the model theoretically accounts for sparse canopies, where substrate evaporation usually cannot be ignored. The same Penman-Monteith driving variables and resistances are used, except that the model also incorporates the less familiar concept of soil surface resistance.

The third model, developed within this thesis, is a modification of the Shuttleworth-Wallace model with open water included as an additional evaporation source. The sum of the contributions of canopy, bare soil and open water is assumed to produce the total evaporation stream. This reinterpretation provides a better analogy for wetland environments than the Shuttleworth-Wallace model.

The fourth model estimates total evaporation by using the Penman-Monteith model separately for each surface type. These component evaporation calculations are then weighted for surface area of canopy, bare soil and open water and summed to give the combined evaporation from the site. Theoretically, this is the best approach for representing evaporation from a site which has any number of surface types.

These three models are evaluated in this thesis through the comparison of their results to the latent heat flux as determined by the Bowen ratio-energy balance approach. The assumptions, sensitivities, limitations and advantages of each model are discussed and suggestions for predictive modelling are outlined.

Chapter 2

Site and Methods

This chapter describes the study site and the methods used to collect the meteorological, hydrological and physiological data.

2.1 Site Description

The research site is located in a low arctic sedge wetland near Churchill, Manitoba (58°45′N, 94°04′W) which is situated in the northern part of the Hudson Bay Lowlands (figure 2.1). This lowland region is typically flat and poorly drained and is predominantly composed of wetland tundra with hummocky terrain. It is often described as fen or tussock tundra (Cowell, 1982; NWWG, 1987). The site is 12.5 km south of the Hudson Bay coastline and 21 km east of the Churchill River.

In the area of the study site, the soil profile is composed of highly porous peat soil between 0.2 m to 0.4 m thick covering a thick layer of glaciomarine silty clays. A thin layer of carbonate cobbles, at least 0.1 m thick, exists within the clays. The entire area is underlain with permafrost which decreased from 0.3 m deep near the beginning of the study period in early July to greater than 1.0 m deep in late August. Frost hummocks ranging from 7 cm to 44 cm in

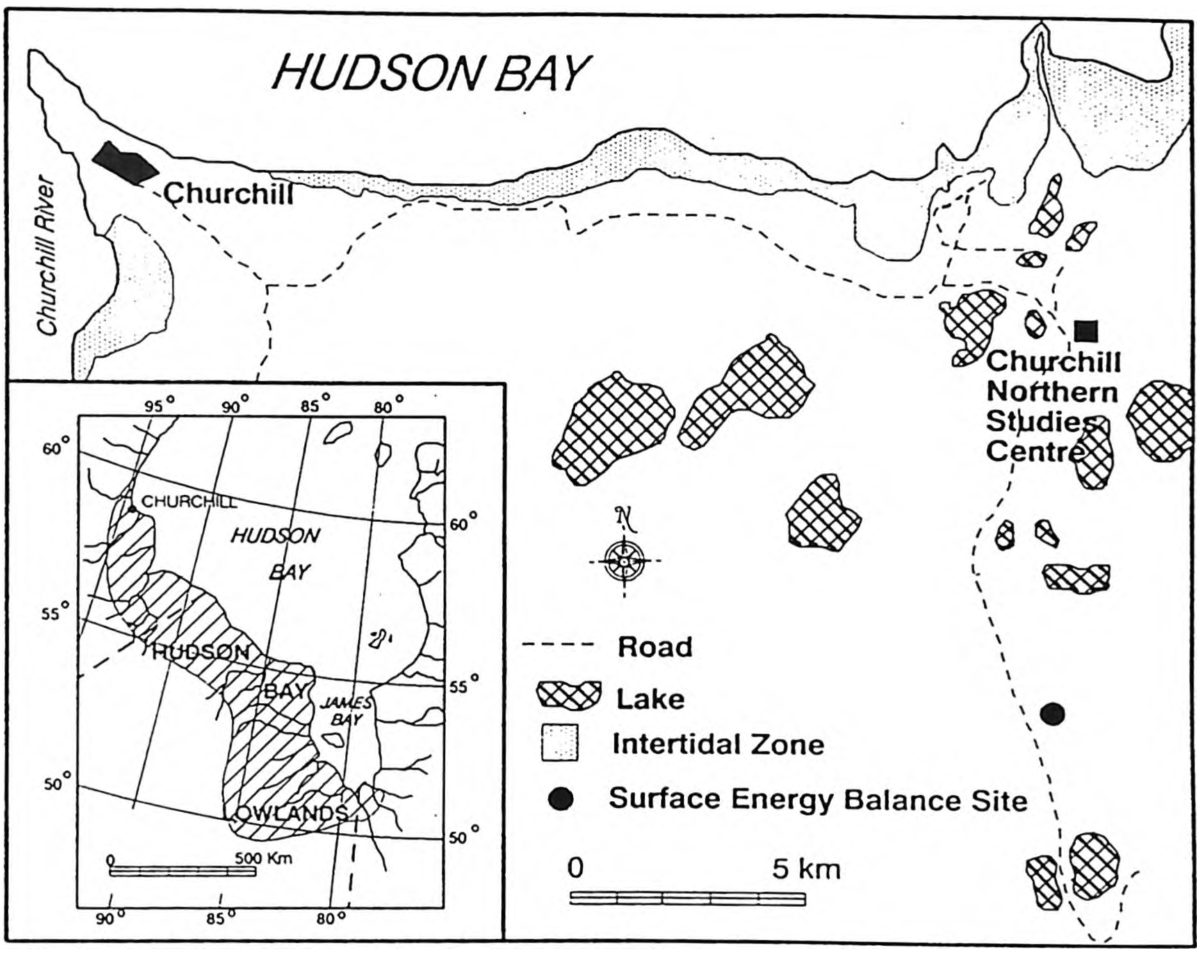

Figure 2.1 Location of the study area and the study site.

height are the features with the greatest relief in the area. These hummocks are separated by near-saturated patches of bare soil and by ponds generally less than 1 m in diameter.

The most common species of vegetation in the partial canopy at the site is Carex aquatilis, which grows both on hummocks and in hollows and can reach a height of 0.3 m. It is the largest and most common sedge in the region (Johnson, 1987). Other species of sedges, particularly Carex saxatilis and Carex gynocrates, and many unidentified species of grasses also exist on hummocks and in hollows but are less common. Isolated plants of Salix arctophila and Betula glandulosa, which reach maximum heights of 0.1 m and 0.5 m respectively, grow only on the hummocks. Andromeda polifolia is also a very common hummock vegetation type. Species of lichens and mosses, particularly Sphagnum, were also found at the site.

2.2 Instrumentation

Monitoring of a variety of microclimate variables was conducted through the use of instruments mounted on a 3.5 m tall mast. Signals from all sensors were sampled every 10 seconds and averaged for every half hour by a datalogger (Campbell Scientific CR7), which was housed in a protective shelter approximately 30 m from the mast. The datalogger operated from an unregulated 12 volt battery which was charged when needed by a solar panel (Solarex). The half hour averages were downloaded from the datalogger to a laptop computer (Zenith SUPERSport with PC206 Datalogger Support Software) every three days and stored on computer discs. Corresponding manual measurements of vegetation growth and activity were also conducted. Data were collected in these formats from June 16 to August 23, 1991, which included all of the growing season.

Maintenance of the climatological instruments and datalogger was conducted on a daily basis. Psychrometers were inspected regularly for drying or soiled wicks and all mast instruments were checked periodically for levelling. Water table and permafrost depth readings, surface cover surveys and the collection of soil moisture samples were carried out systematically.

2.2.1 Solar and Net Radiation

Solar radiation was measured with two Black and White pyranometers (Eppley Laboratory). An upfacing pyranometer was used to measure incoming solar radiation and a downfacing sensor was mounted on the mast at a height of 3.0 m to measure reflected solar radiation.

A net pyrradiometer (Middleton) for measuring net radiation was mounted on the mast at the same height as the inverted pyranometer. It was oriented facing southward to avoid the shadow effects caused by the mast during the day. The polyethylene hemispheres were aspirated with desiccated air pumped by a rubber inner-tube.

A second pyrradiometer (Middleton) was positioned near the surface to obtain net radiation periodically for open water, hollows and hummocks. The maximum height of the instrument was 15 cm.

2.2.2 Ground Heat Flux

The ground heat flux was measured with three soil heat flux transducers (Middleton), with one sensor placed in the substrate for each of the three surface types of canopy, bare soil and open water. All transducers were buried approximately 1 cm into the soil. Since individual ground heat flux values were required for each surface type, the transducers were moved periodically when the fluctuation of the water table changed the surface type being measured.

Rouse (1984) and Halliwell and Rouse (1987) have found that transducers tend to underestimate true ground heat flux, particularly for near-saturated, organic material. To correct the transducer data, they used a calorimetric method which calculates ground heat flux using knowledge of soil characteristics at depth and measurements of subsurface temperatures. For application to this study, a ground temperature rod with thermocouples at regular depth intervals was used to measure the subsurface temperatures. For the first half of the season, from July 4 to July 24, the rod was accidentally frozen partially out of position into the permafrost. As a result, for this period the rod recorded temperatures at depths of 0.05, 0.25, 0.35, 0.45, and 0.65 m. In the period following the proper positioning of the rod, from July 24 to August 23, temperatures were recorded at depths of 0.05, 0.15, 0.25, 0.45, 0.55, 0.65 and 0.85 m.

Correction of the ground heat flux (Q_g) data was done by determining the ratio between the transducer measurements and the calorimetric calculations. This ratio, referred to as the correction factor (CF), was determined for each surface type and assumed to be constant for the duration of the period that the transducer was in place. This method of correction, which produces a smooth trend of Q_g with time, is preferred to the direct application of the calorimetric method, which tends to behave erratically (Halliwell and Rouse, 1987). For the 1991 season, a new correction factor was calculated every time a transducer was moved. The correction factors for the canopy (CF_c), bare soil (CF_s) and open water (CF_w) averaged to 1.73, 1.65 and 1.36 respectively. For the same site in 1987, no correction factors were used (Weick, 1989) and in 1989, factors of 1.41, 1.49 and 1.24 were used for dry, mesic and wet locations respectively (Carlson, 1991).

The value of Q_g for the ponds required an additional calculation of change in storage, ΔQ_{st}, which was added to the corrected transducer measurement to provide a true value of ground heat flux for the water. For final overall calculation, the canopy, bare soil and open water fluxes were weighted by surface area and summed to give the representative

Q_g of the site. If d_w is the mean depth of the open water layer, C is the heat capacity of water, $\Delta T_w/\Delta t$ is the change in mean water temperature over a given time interval and Q_{gc}, Q_{gs} and Q_{gw} are the ground heat fluxes for canopy, bare soil and open water, respectively, then

$$\Delta Q_{st} = C \cdot \frac{\Delta T_w}{\Delta t} \cdot d_w \qquad (2.1)$$

$$Q_{gw} = W \cdot (\Delta Q_{st} + CF_w \cdot Q_{g3}) \qquad (2.2)$$

$$Q_{gc} = H_u \cdot CF_c \cdot Q_{g1} \qquad (2.3)$$

$$Q_{gs} = H_o \cdot CF_s \cdot Q_{g2} \qquad (2.4)$$

and

$$Q_g = Q_{gc} + Q_{gs} + Q_{gw} \qquad (2.5)$$

where H_u, H_o and W are the surface weighting factors and Q_{g1}, Q_{g2} and Q_{g3} are the transducer measurements for canopy, bare soil and open water, respectively. The surface weighting factors give the proportion of hummocks (H_u), hollows (H_o) and water (W) on the surface. For simplicity, Q_{gc} was weighted by

H_u since the canopy existed only on the hummocks whereas Q_{gs} was assumed to be represented by hollow soil only and was weighted by H_u.

2.2.3 Temperature and Vapour Pressure

Temperature and humidity were measured at six levels with a wet and dry bulb aspirated psychrometer system. The instruments were positioned on the mast at heights of 0.4, 0.8, 1.1, 1.3, 1.7 and 2.1 m above average ground height. Wet and dry bulb temperatures were measured with copper-constantan thermocouples sealed inside stainless steel tubing and shielded from the elements inside a styrofoam housing covered in reflective tape. Each psychrometer was aspirated with a fan rotating at a speed of about 5 ms^{-1} and powered by a 12 v battery. To prevent the fans from slowing down at low voltage, the battery was continuously recharged by a solar panel (Solarex) for the duration of the measurement period.

Each wet bulb thermocouple was referenced to the corresponding dry bulb thermocouple positioned at the same height. Each dry bulb thermocouple was referenced to a ground temperature plug which was referenced to the panel temperature of the datalogger. This process was considered necessary to avoid error in the temperature measurements due to slight temperature differences across the input cards in the datalogger (Halliwell, 1989).

2.2.4 Wind Speed and Direction

Wind speed was measured with three 3-cup analogue output anemometers (R.M. Young Company) positioned at the same heights as the top three psychrometers. The anemometers were mounted 0.8 m away from the main mast, where interference from the other instruments on the mast was considered to be negligible. Wind direction was measured using a wind vane (R.M. Young Company) mounted at the top of the mast, approximately 3.5 m above the ground surface.

The validity of the measurements from the instruments on the mast is dependent on the fetch of the site. The standard minimum fetch requirement is a distance of 100 m from a change in surface roughness for every 1 m of height of the highest instrument, which was the wind vane in this study. The fetch at the study site was at least 600 m in all directions.

2.2.5 Surface Temperature

Surface temperatures were measured for all three surface types using sensors comprised of two sizes of copper-constantan thermocouples. One sensor consisted of three 30-gauge, fine wire thermocouples attached in parallel to a larger 24-gauge thermocouple which was wired into the datalogger and referenced to the CR7 panel temperature. Nine sensors were used in the study with five in hummocks, two in hollows and two in open water. The sensors were checked daily to ensure that a change in the water table did not change the surface type that a sensor was measuring. All nine sensors were placed at a depth of about 1 cm below the substrate to shield the thermocouples from direct sunlight. For simplicity, ponds were assumed to approach isothermal conditions so that the open water sensors represented true water temperature. This seemed to be a reasonable assumption for the purposes of this study considering the shallow depths of the ponds, which reached a maximum of 0.29 m.

2.3 Manual Measurements

2.3.1 Precipitation and Water Table

Precipitation was measured diurnally at about the same time every day using a standard rain gauge. The water table depth with respect to an arbitrary datum was recorded diurnally at the same time as the precipitation measurement. The level of the water table was monitored using a hollow PVC tube with drilled holes of 7.5 mm in diameter along its length. The bottom of the tube was approximately 0.5 m below the surface and the top, which represented the datum, was 0.5 m above the surface. The top of the tube was accurately surveyed with respect to the rest of the site to determine the relative position of the water table as compared to the surface. The height of the surface was considered to be the average depth of the hollows; when the water table rose above this depth, it was considered to be above the surface.

2.3.2 **Surface Cover**

The percentage of hummock, hollow and open water was determined through surveys at regular intervals throughout the season. The surveys employed eight transects of 20 m in length extending in the eight cardinal directions from a centre point approximately 50 m south of the instrument mast. Surface type was recorded every 1 m along each transect. A patch of surface was considered to be a hummock if it had a distinct boundary with a greater relief than the surrounding area. Hollows were patches of soil at low relief.

For each day that a survey was conducted, a percentage of surface cover of each surface type was determined based on the total number of observations. Interpolation of the surface cover percentage over the rest of the season was done by regressing the percentage covers of open water and hollows against the depth of the water table. Both regressions produced linear relationships shown in figure 2.2. By knowing the percentage cover of open water and hollow for each day, the percentage cover of hummock was taken as a residual. The total surface cover percentage for the season is illustrated in figure 2.3.

2.3.3 **Vegetation Survey**

To determine the spacial distribution of vegetation on a smaller scale, a 0.5 m by 0.5 m sampling square was used on 10 separate occasions throughout the season. The square was

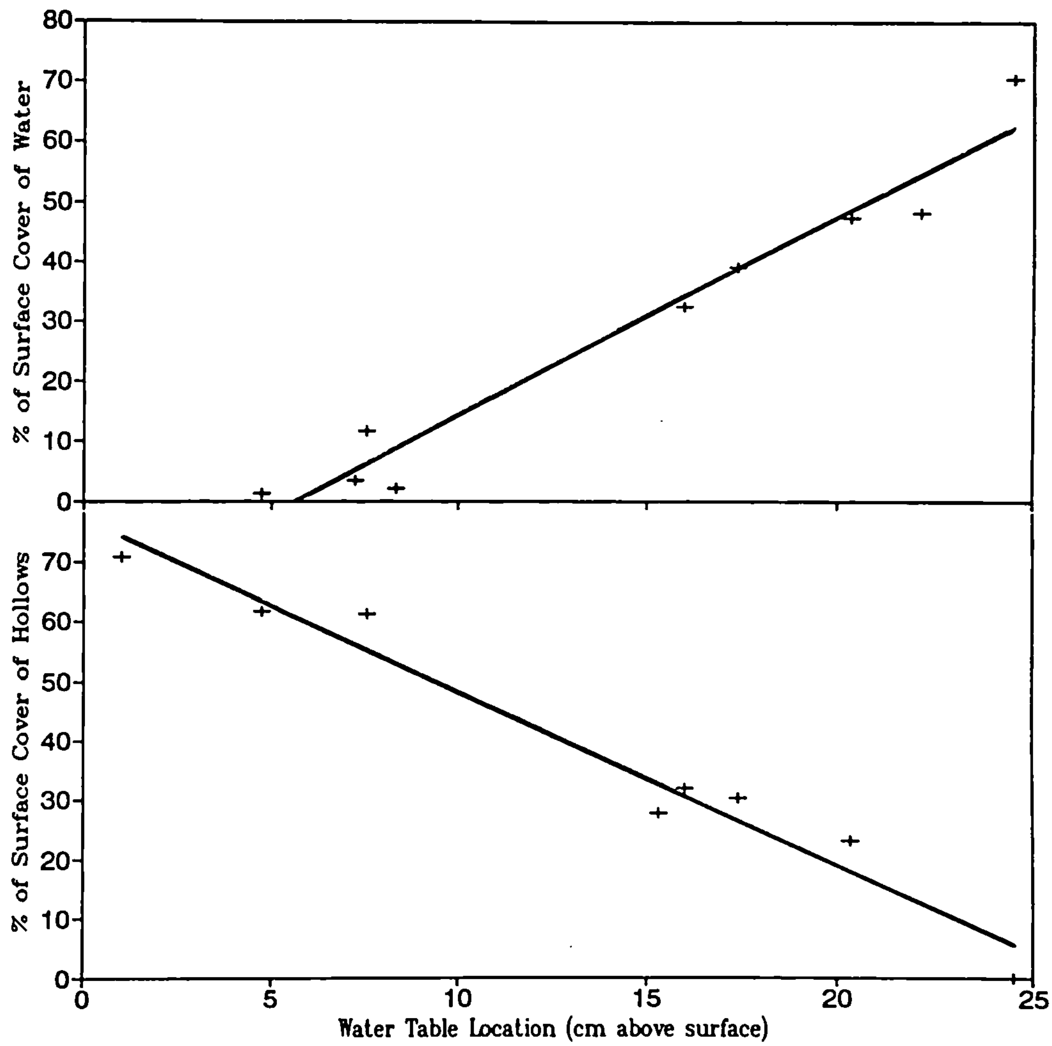

Figure 2.2 Linear regression of surface coverage (%) against water table location (in cm above the surface) for a) open water and b) hollow. Both regressions had an r^2 value of 0.96.

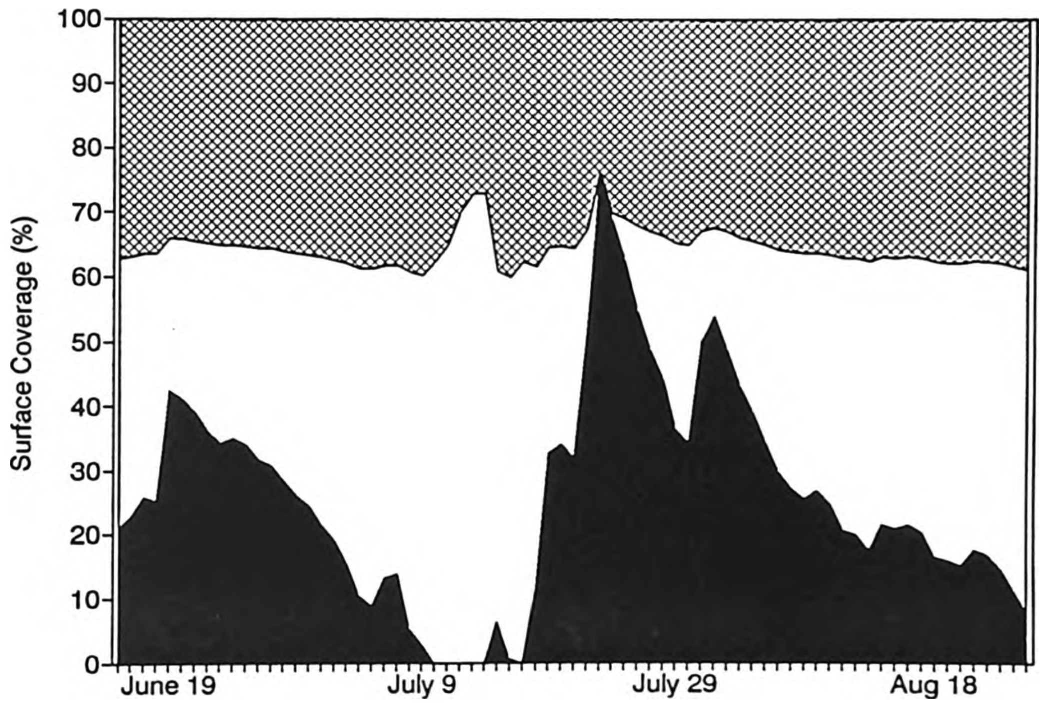

Figure 2.3 Surface cover percentage of open water, hollows and hummocks. The solid portion represents open water, the empty represents hollows and the cross hatch represents hummocks.

composed of 100 smaller 5 cm by 5 cm openings defined by strings tied in a checkerboard format across the square. Sampling was conducted by recording the most abundant surface type in each opening and calculating a percentage of the total square. This was done separately for hummocks and hollows, with all data being totalled to find the spatial distribution for the entire site.

Seasonally, the most dominant surface type at the site was bare soil (table 2.1). This included a sparse representation of mosses and lichens. The most abundant living vegetation was *Carex aquatilis*, which comprised one quarter of the total live vegetation. All of the living sedges and grasses comprised 67% of the total live vegetation.

2.3.4 Surface Soil Moisture

Surface soil moisture was measured volumetrically on a daily basis over the season. Peat soil was the only soil type sampled in the analysis and 5 samples were taken from both hummocks and hollows in the vicinity of the site for each daily sampling period. The samples were taken from just below the ground surface and no hummock or hollow was ever sampled more than once. Initial measurements of mass of the collected samples were conducted at the site with a portable mass balance (Ohaus CT series) with a precision of ± 0.1 g. Following a period of oven drying, the samples were again weighed by the same balance.

Surface Type	**Hum %**	**Hol %**	**Total %**
Bare Soil	29.1	22.6	25.9
Water	0.0	45.5	22.8
Dead Grass	22.8	10.6	16.7
Carex aquatilis	12.2	4.0	8.1
Andromeda polifolia	12.2	0.0	6.1
Scirpus caespitosus	6.7	0.2	3.5
Salix arctophila	5.5	0.0	2.8
Carex gynocrates	2.5	1.2	1.9
Carex saxatilis	2.0	1.8	1.9
Betula glandulosa	2.7	0.0	1.4
Carex capitata	1.0	1.3	1.2
Salix pedicellaris	1.0	0.0	0.5
Vaccinium uliginosum	1.0	0.0	0.5
Carex capillaris	0.4	0.0	0.2
Unknown grass/sedge	0.9	12.8	6.5

Table 2.1 Surface coverage (%) of bare soil, open water and vegetation found on hummocks, in hollows and over the total surface as determined from the small-scale surface cover survey.

Volumetric soil moisture analysis showed a consistent temporal trend (figure 2.4). Hummocks ranged from 42 to 52% water by volume and hollows ranged from 78 to 87% water by volume. The average of the two surface types ranged from 55 to 75% water by volume. In a typical drainage basin near the site, volumetric soil moisture analysis revealed a spatially consistent trend for hollows, with soil moisture ranging from 78 to 91% water by volume (D. Boudreau, pers. comm.).

2.4 Vegetation Growth Measurements

2.4.1 Leaf Area Index

Leaf area index (LAI) for the site was measured periodically throughout the 1990 growing season using a destructive method and once in 1991 using a non-destructive method. All measurements of LAI were of the sedges and grasses growing on hummocks. The sampled vegetation was both living and dead.

The destructive method was used primarily to determine the dead area index of the dead vegetation (DAI). However, living vegetation was also sampled to provide a total foliage area index (FAI) for comparison with the non-destructive method. If LAI represents the leaf area index of living vegetation only, then it follows that

$$FAI - LAI + DAI \qquad (2.6)$$

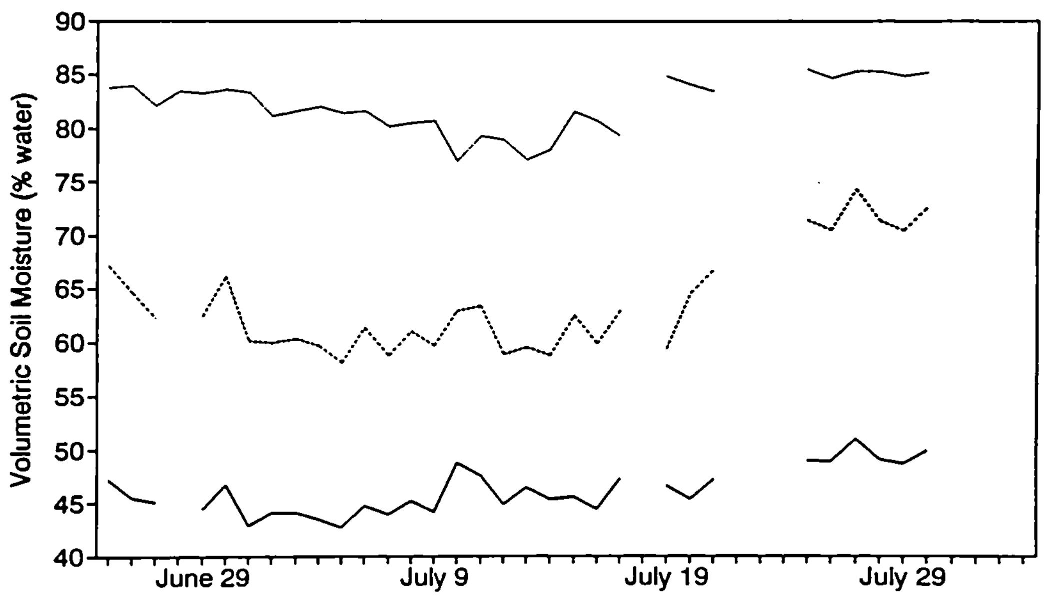

Figure 2.4 Volumetric soil moisture (% volume of water) of peat soil on the hummocks (solid), the hollows (dotted) and overall (dashed).

The destructive method involved the harvesting of a 0.25 m by 0.25 m plot once during the 1991 season. A sample of 50 blades of sedges and grasses were chosen from the bulk sample and traced onto graph paper. All of the harvested sedges and grasses were sealed in paper bags and returned to McMaster University for drying and weighing. Following the drying, the 50 blades and the bulk sample were weighed on an electronic scale to the nearest 0.1 mg. The graph paper traces were then cut out, weighed and compared to the weight of the 50 blades to obtain a linear area-to-dry weight standard such that

$$Area = 0.013 \cdot Mass \tag{2.7}$$

where area is in m^2 and mass is in grams. This was applied to the bulk sample and related to the size of the plot to obtain values for FAI, DAI and LAI, which were 0.27, 0.14 and 0.13 respectively.

The non-destructive method employed the use of a plant canopy analyzer (LI-Cor LAI-2000). This instrument measures foliage area index only and is unable to discern between living and dead vegetation. It determined FAI by measuring the degree of attenuation of diffuse sky radiation caused by the foliage in the vegetative canopy. To ensure that diffuse sky conditions existed, FAI measurements were only taken on overcast days. Five measurements taken during the 1990 growing season were used to find the seasonal trend of FAI for the hummocks. The instrument was unable to compute a foliage area index for the hollows due to the short stature and sparseness of the canopy. Standard error of the FAI determinations ranged from 0.02 to 0.11. No measurements were taken using the canopy analyzer during the 1991 season.

The destructive method was highly consistent with the non-destructive method (figure 2.5). Since there were not enough data available to plot a seasonal trend in DAI, it was assumed to be a constant value of 0.14, the only measured value available. To obtain the LAI (living vegetation), the DAI was subtracted from each value of FAI measured with the canopy analyzer. The living data from the growing season were fitted to a third order polynomial.

2.4.2 Stomatal Conductance

Stomatal conductance was measured using a steady state porometer (LI-Cor LI-1600). This instrument consists of two parts, a console microcomputer and a sensor head which has a sampling cuvette. Conductance is calculated using changes in leaf and air temperature and relative humidity in the cuvette. Leaf temperature is measured when a leaf sample comes in contact with a chromel-constantan thermocouple as it is clamped into the sensor head aperture. Air temperature is measured by a thermistor inside the cuvette and relative humidity was measured using a Vaisala HUMICAP. Changes in these variables are monitored by the microcomputer, which

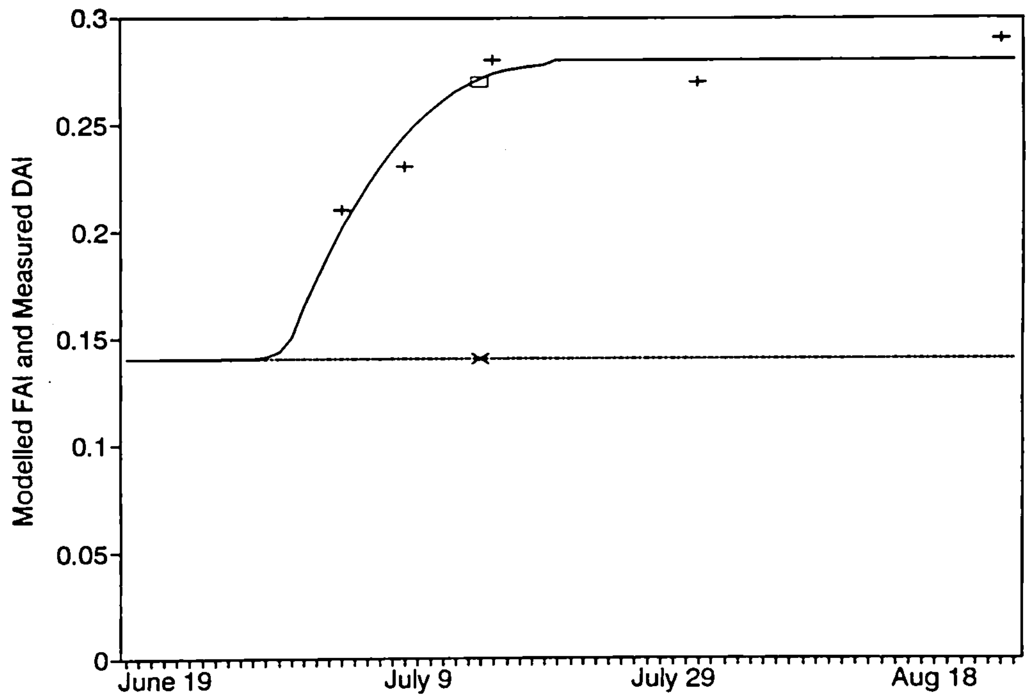

Figure 2.5 Seasonal trend of foliage area index and dead area index. Individual values of foliage area index as measured by the LAI-2000 Plant Canopy Analyzer (+) in 1990 were used to plot the growth curve of vegetation (solid). Individual values of FAI (□) and DAI (x) as measured using the manual method in 1991 are also given, with the DAI value providing a constant dead area trend (dashed). The leaf area index is the difference between the FAI and the DAI.

computes and adjusts the rate of desiccated air needed to maintain a constant relative humidity. This flow rate determines the water loss from the leaf. The porometer has an accuracy of ± 10%.

Hourly measurements of stomatal conductance were taken from sunrise to sunset on three days during the season. Only days with fair weather conditions were selected and no measurements were made on hours where fog or rain occurred since these could damage the instrument. Prior to each daily session, the thermocouple and thermistor were calibrated and the porometer was allowed to acclimate to ambient conditions as suggested by the manufacturer. Carex aquatilis was the only plant to be sampled since the width of all other sedges and grasses were too small to completely cover the sensor head aperture. Porometer measurements were taken on both leaf surfaces at approximately the middle of each blade. Four different blades were selected for each hourly sampling period and the same blade was not sampled twice if it was damaged in an earlier measurement. All measurements were downloaded from the microcomputer to a cassette tape.

Chapter 3

Theory and Model Development

In this chapter, the theory surrounding the measurement and modelling of evaporation from the site will be discussed.

3.1 Theory of Measurement

Two approaches for calculating evaporation were used in this study. The Bowen ratio-energy balance method calculates the sensible and latent heat fluxes by determining their ratio and using it to apportion the available energy at the surface. The aerodynamic method calculates the fluxes by considering the turbulent activity of the atmosphere near the surface. Both methods require profile measurements of air temperature and humidity while the Bowen ratio approach needs net radiation and ground heat flux measurements and the aerodynamic approach needs measurement of the vertical wind profile.

Both methods assume that the similarity principle applies to the profile measurements, such that

$$K_v = K_h = K_m \tag{3.1}$$

where K_v, K_h and K_m are the eddy diffusion coefficients for latent heat, sensible heat and momentum respectively. This simplifies the flux calculations by assuming that the same eddy can carry all of these properties at the same time.

3.1.1 The Bowen Ratio Energy Balance Approach

The energy balance at the earth's surface follows the law of conservation of energy such that

$$Q^* = Q_e + Q_h + Q_g \tag{3.2}$$

where Q^* is net radiation, Q_e is the latent heat flux, Q_h is the sensible heat flux and Q_g is the ground heat flux. The convective fluxes Q_e and Q_h can also be related through the Bowen ratio, β, where

$$\beta = \frac{Q_h}{Q_e} \tag{3.3}$$

Q_e and Q_h can be determined using a time-averaged flux-gradient approach, where

$$Q_e = -\frac{\rho C_p}{\gamma} \cdot K_v \cdot \frac{de}{dz} \tag{3.4}$$

$$Q_h = -\rho\, C_p \cdot K_h \cdot \frac{dT}{dz} \tag{3.5}$$

where ρ is the density of air, C_p is the specific heat of air at constant pressure, γ is the psychrometric constant, z is height, e is vapour pressure and T is air temperature. If equations 3.4 and 3.5 are introduced into equation 3.3 and equation 3.1 is obeyed, then it follows that

$$\beta = \gamma \frac{dT}{de} \tag{3.6}$$

Combining β with equation 3.2 and solving for Q_e or Q_h gives

$$Q_e = \frac{Q^* - Q_g}{1+\beta} \tag{3.7}$$

$$Q_h = \beta \frac{Q^* - Q_g}{1+\beta}$$

This demonstrates that the convective fluxes can be calculated using measured Q^* and Q_g and measurements of vapour pressure and air temperature at a minimum of two heights.

3.1.2 The Aerodynamic Approach

The aerodynamic approach for calculating the convective fluxes assumes that under neutral conditions wind speed increases linearly with the natural logarithm of height, where

$$u_z = \frac{u^*}{k} \ln \frac{z-d}{z_o} \tag{3.9}$$

where u_z is the wind speed at height z, z_o is the surface roughness length, d is the zero plane displacement, k is von Karman's constant and u^* is the friction velocity, defined as

$$u^* = \left(\frac{\tau}{\rho}\right)^{\frac{1}{2}} \tag{3.10}$$

where τ is the momentum flux, given as

$$\tau = \rho \cdot K_m \cdot \frac{du}{dz} \tag{3.11}$$

where u is wind speed.

Equations 3.9 - 3.11 can be combined with equations 3.4 and 3.5 to give the sensible and latent heat fluxes under neutral atmospheric stability. However, neutral conditions are not common and usually only occur when the fluxes are small (Holtslag, 1984). In non-neutral conditions, the profiles are not log-linear due to buoyancy effects and must be corrected for stability. This correction is done using the stability functions for water vapour, heat and momentum, which are Φ_v, Φ_h and Φ_m respectively. In this study they are expressed as functions of the Richardson Number (Ri) (Dyer, 1974; Halliwell and Rouse, 1989) such that

$$\phi_v = \phi_h = (1-16Ri)^{-\frac{1}{2}} \tag{3.12}$$

$$\phi_m = (1-16Ri)^{-\frac{1}{4}} \tag{3.13}$$

for unstable conditions and

$$\phi_v = \phi_h = \phi_m = (1-5Ri)^{-1} \tag{3.14}$$

for stable conditions. The Richardson Number is calculated from the temperature and wind speed profiles such that

$$Ri = \frac{g}{T}\frac{\frac{dT}{dz}}{\left(\frac{du}{dz}\right)^2} \tag{3.15}$$

where g is the acceleration due to gravity. By combining equations 3.9 - 3.11 and the stability functions with the flux equations 3.4 and 3.5, the fluxes become

$$Q_e = -\frac{\rho C_p}{\gamma} k^2 \frac{du}{d\ln z} \frac{de}{d\ln z} (\phi_v \phi_m)^{-1} \qquad (3.16)$$

$$Q_h = -\rho C_p k^2 \frac{du}{d\ln z} \frac{dT}{d\ln z} (\phi_h \phi_m)^{-1} \qquad (3.17)$$

Equations 3.16 and 3.17 comprise the aerodynamic approach to calculating the convective fluxes, which is applicable under all stability conditions.

3.1.3 Data Manipulation

The Bowen ratio-energy balance and aerodynamic approaches were implemented in a Turbo Pascal program called "Profile", which is described by Halliwell (1989). Profile determines the sensible and latent heat fluxes by considering the log-height profiles of temperature, humidity, and wind speed. This was done for every half hour of the season for the two approaches.

Profile displayed five graphs in which air temperature, vapour pressure, wind speed and wet bulb depression were plotted against the natural logarithm of height and temperature was plotted against vapour pressure.

This assumed that temperature, vapour pressure and wind speed have a linear relationship with log height, which was true over the height interval of the mast instruments. The program also displayed the flux values, which were calculated using the gradients displayed by the graphs. The primary advantage of Profile is that it allows identification and removal of individual data values which are obviously in error, such as a higher than expected temperature produced from a wet bulb sensor because of a drying wick. When a data point was removed, the gradient of the profile changed and the sensible and latent heat fluxes were recalculated accordingly. However, the choice of which data points to eliminate is subjective (Halliwell and Rouse, 1989) and requires careful consideration.

On a half hour basis, the fluxes as calculated by the Bowen ratio-energy balance approach were chosen to represent the measured values of Q_e and Q_h for the remainder of this study. However, this method has been found to produce substantial errors in magnitude and sign of the fluxes when β approaches -1 (Ohmura, 1982; Halliwell and Rouse, 1989). This has been resolved in the past by replacing the Bowen ratio values with the corresponding aerodynamic values when this occurred. This was done for cases when $-1.4 < \beta < -0.7$, which occurred in only 2% of the half hour data periods of the season.

3.2 Theory of Combination Models

In this study, evaporation originates from three surface types: vegetation, bare soil and open water. The water availability for any one of these surfaces tends to change over time. The Bowen ratio and aerodynamic approaches do not consider these sources of water in their calculations of the latent heat flux. Instead, they assume that changes in surface wetness or stomatal conductance are accounted for in the temperature and vapour pressure profiles.

Combination models calculate the latent heat flux by assuming that evaporation is largely controlled by surface and aerodynamic resistances. These include the surface resistance caused by the regulatory role of the stomata on plant leaves. Since these resistances are controlled by hydrological, climatological and physiological processes, combination models have an advantage in that they can consider the various sources of water.

3.3 The Penman-Monteith (PM) Combination Model

Penman (1948) was one of the first to derive a physically based model which determined evaporation from any wet surface. The one-dimensional model combined the energy balance and aerodynamic methods in describing potential evaporation from open water using radiant energy, temperature, vapour pressure and wind speed. However the practical application of the potential evaporation calculation is limited, since it requires that the actual vapour pressure at the surface approximately equals the saturation vapour pressure at surface temperature, which seldom happens in nature. Furthermore, it does not consider the contribution from vegetation.

To accommodate these problems, Monteith (1965) modified the model and included surface and aerodynamic resistance terms. The stomatal resistance of vegetation was also included. The result of the derivation was a model which could calculate actual rather than potential evaporation. The model could also be used for vegetated surfaces. A schematic diagram of the model is given in figure 3.1. The Penman-Monteith (PM) combination model equation is defined as

$$Q_e = \frac{\Delta AE + \dfrac{\rho C_p D}{r_a}}{\Delta + \gamma\left(1 + \dfrac{r_c}{r_a}\right)} \tag{3.18}$$

where Δ is the slope of the saturation vapour pressure vs. temperature curve, AE is available energy, r_c is canopy resistance, r_a is aerodynamic resistance and D is vapour pressure deficit such that

$$D = e_w(T_z) - e_z \tag{3.19}$$

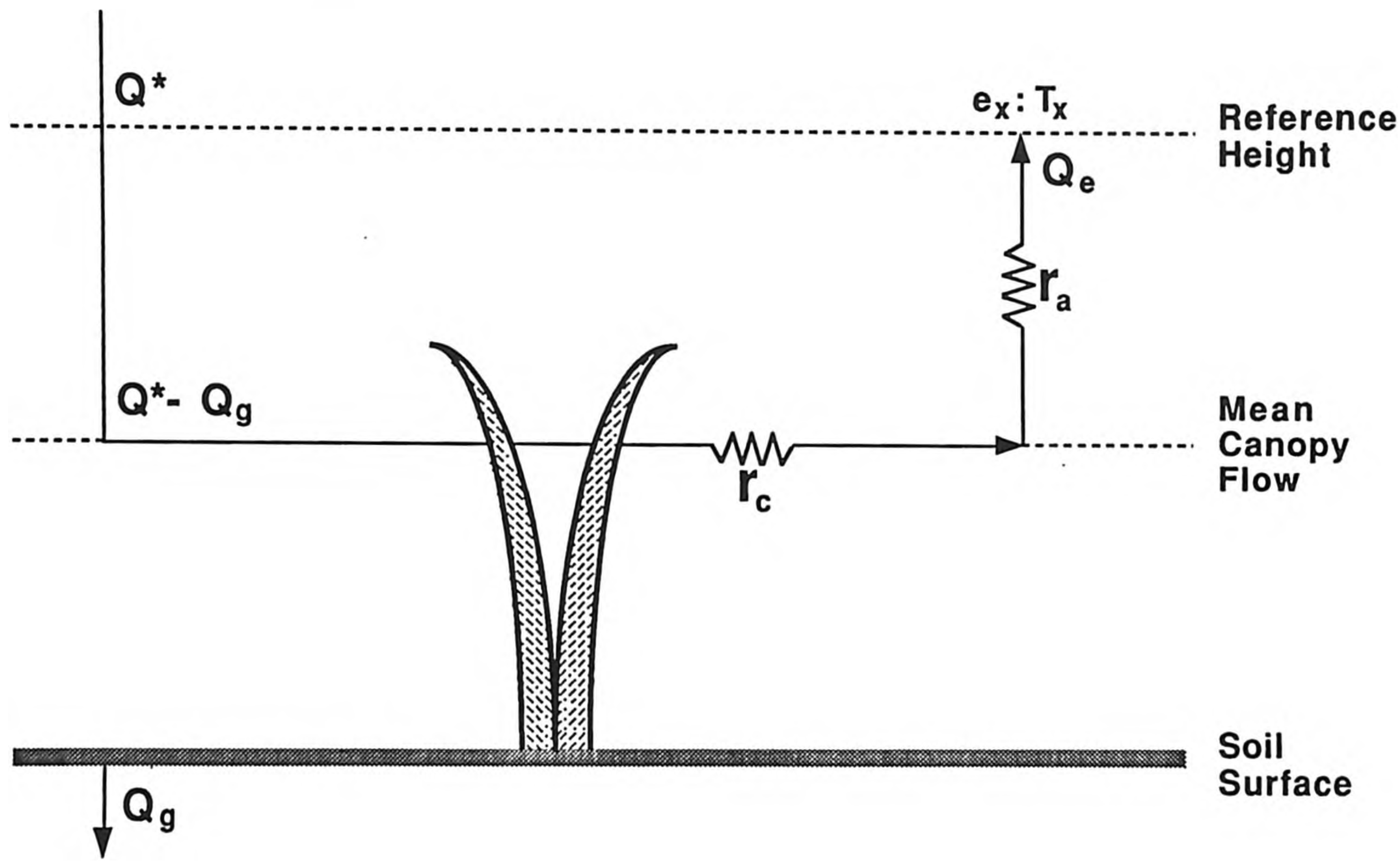

Figure 3.1 Schematic representation of the Penman-Monteith model.

where $e_w(T_z)$ is the saturation vapour pressure at temperature T_z at height z and e_z is the vapour pressure at height z. Available energy is defined as

$$AE = Q^{*} - Q_g \tag{3.20}$$

The reader is referred to the original paper for a full derivation of the model.

Equation 3.18 relies on the assumption that the canopy behaves as a single large leaf, with temperature and vapour pressure defined by values considered to be representative of the canopy. This further assumes that the sources of heat and water vapour are at the same level in the canopy. For an individual leaf surface, this is not entirely the case since heat originates from the leaf surface and water vapour originates from within the stomata. However, these sources are close enough to ignore this difference and the application of the "big-leaf" analogy of the canopy has not produced large errors in subsequent testings of the model.

The importance of the aerodynamic and surface resistances within the model has been stressed in past studies and will be discussed here.

3.3.1 Aerodynamic Resistance in the PM Model

The aerodynamic resistance term is derived as a measure of the resistance to momentum transfer (r_{am}) between the surface and a height z (Thom, 1975), where

$$r_{am} = \frac{u_z}{(u^*)^2} \qquad (3.21)$$

if equation 3.9 is rearranged for u^* and substituted into equation 3.21, r_{am} becomes

$$r_{am} = \frac{\left(\dfrac{\ln(z-d)}{z_o}\right)^2}{k^2 u_z} \qquad (3.22)$$

Some authors have suggested that equation 3.22 underestimates the true aerodynamic resistance since it does not take into account the excess resistance, r_{bb}, caused by bluff body forces (Thom, 1972; Monteith, 1973). To compensate for this, Thom (1975) described total aerodynamic resistance, r_a, as

$$r_a = r_{am} + r_{bb} \qquad (3.23)$$

where

$$r_{bb} = \frac{4}{u^*} \qquad (3.24)$$

Since equation 3.22 is dependent on a log-linear relationship with height, it is subject to error in non-neutral conditions due to buoyancy effects. As a result, correction for stability would normally be required. However, Bailey and Davies (1981a) have found that the combination model is relatively insensitive to error in r_a. No correction for stability was made in the present study.

3.3.2 **Canopy Resistance in the PM Model**

Monteith (1965, 1973) suggested that the canopy resistance of equation 3.18 is primarily a physiological control of water loss by a vegetative canopy. It is considered to be analogous to a parallel circuit, where all of the stomata in a canopy create a combined resistance such that

$$r_c = \frac{r_{st}}{LAI} \qquad (3.25)$$

where r_{st} is the mean stomatal resistance.

The limiting factors in equation 3.25 are the difficulties in determining r_{st} and LAI accurately, such that they are representative of the canopy as a whole. Measurement of r_{st} is tedious and the results may not be representative unless all dominant vegetation types are sampled. Modelling of r_{st} has seen mixed results (Bailey and Davies, 1981b; Lafleur and Rouse, 1990). Leaf area index measurement can be difficult and may not be representative if the canopy is spatially heterogenous, which is often the case in partial canopies.

Another problem with equation 3.25 is that it assumes that canopy transpiration is the only contributor to the latent heat flux. If bare soil and open water evaporation are not negligible, then r_c becomes a surface resistance and is no longer a true canopy resistance. A representative surface resistance from a site with many surface types is difficult to obtain and potentially highly erroneous.

In the cases where the PM model is used for a predictive purpose, canopy (or surface) resistance must be determined independently of the latent heat flux, as in equation 3.25. For simulating purposes, r_c can be found using

$$r_c = (\beta + 1)\, r_i + \left(\beta \frac{\Delta}{\gamma} - 1\right) r_a \qquad (3.26)$$

where

$$r_i = \frac{\rho\, C_p}{\gamma} \cdot \frac{D}{AE} \qquad (3.27)$$

in which r_i is the climatological resistance (Stewart and Thom, 1973). However, the accuracy of this approach requires that e_z and T_z be good estimates of vapour pressure and temperature at the surface of the leaves.

3.4 The Shuttleworth-Wallace (SW) Combination Model

The main limitation of the PM model is its assumption that beneath-canopy surface evaporation is negligible, which may not be applicable for partial canopies or wet surfaces. It has been shown that the heat and water vapour fluxes from the soil of sparse crops can greatly affect the result of the PM equation, particularly when the crop is short and has a small leaf area index (Bailey and Davies, 1981b; Wallace et al, 1990). To remedy this situation, Shuttleworth and Wallace (1985) developed a one-dimensional energy combination model which calculates evaporation from sparse canopies. It is based on the original PM equation except that it calculates bare soil evaporation and canopy transpiration separately and sums them to find the total evapotranspiration stream from the surface. The driving variable of available energy is used to partition the bare soil and canopy components. Separate aerodynamic and surface resistances are calculated for each surface type. The reader is referred to the original paper for a full derivation of the model but a brief description of it is warranted. A schematic diagram of the model is given in figure 3.2.

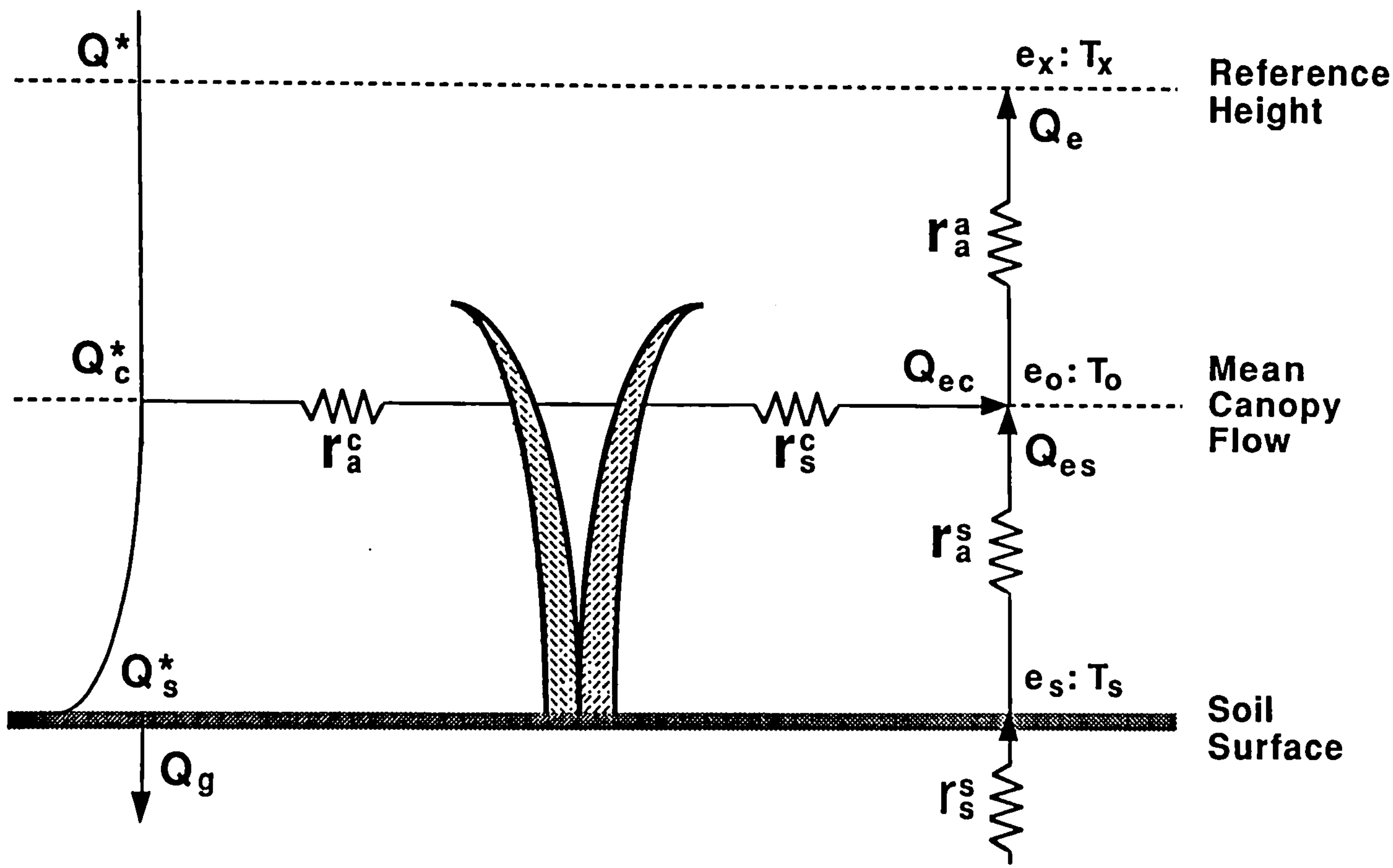

Figure 3.2 Schematic representation of the Shuttleworth-Wallace model.

The Shuttleworth-Wallace (SW) model is given as

$$Q_e = C_c PM_c + C_s PM_s \tag{3.28}$$

where C_c and C_s are model coefficients and PM_c and PM_s are the PM equations applied to canopy and bare soil respectively. The model coefficients are defined as

$$C_c = \frac{1}{1+\dfrac{R_c R_a}{R_s(R_c+R_a)}} \tag{3.29}$$

$$C_s = \frac{1}{1+\dfrac{R_s R_a}{R_c(R_s+R_a)}} \tag{3.30}$$

where

$$R_s = (\Delta+\gamma)\, r^{s}_{a} + \gamma r^{s}_{s} \tag{3.31}$$

$$R_c = (\Delta+\gamma)\, r^{c}_{a} + \gamma r^{c}_{s} \tag{3.32}$$

$$R_a = (\Delta + \gamma)\, r^a{}_a \qquad (3.33)$$

The PM equations are expressed as

$$PM_c = \frac{\Delta AE + \dfrac{\rho C_p D_x - \Delta r^c{}_a AE_s}{r^a{}_a + r^c{}_a}}{\Delta + \gamma\left(1 + \dfrac{r^c{}_s}{r^a{}_a + r^c{}_a}\right)} \qquad (3.34)$$

$$PM_s = \frac{\Delta AE + \dfrac{\rho C_p D_x - \Delta r^s{}_a (AE - AE_s)}{r^a{}_a + r^s{}_a}}{\Delta + \gamma\left(1 + \dfrac{r^s{}_s}{r^a{}_a + r^s{}_a}\right)} \qquad (3.35)$$

where

$$D_x = e_w(T_x) - e_x \qquad (3.36)$$

where AE_s is the available energy term for bare soil, $e_w(T_x)$ is the saturation vapour pressure at reference height temperature T_x, and e_x is the vapour pressure at a reference height (x).

Once the total evaporation from the surface has been determined, the resulting value of Q_e is used to calculate the in-canopy vapour pressure deficit, D_o, such that

$$D_o = D_x + \frac{[\Delta AE - (\Delta+\gamma) Q_e] r^a{}_a}{\rho C_p} \tag{3.37}$$

This is then used to find the component evaporation terms, Q_{ec} and Q_{es}, for the canopy and bare soil respectively, where

$$Q_{ec} = \frac{\Delta(AE - AE_s) + \dfrac{\rho\ C_p D_o}{r^c{}_a}}{\Delta + \gamma\left(1 + \dfrac{r^c{}_s}{r^c{}_a}\right)} \tag{3.38}$$

$$Q_{es} = \frac{\Delta\, AE_s + \dfrac{\rho C_p D_o}{r^s{}_a}}{\Delta + \gamma\left(1 + \dfrac{r^s{}_s}{r^s{}_a}\right)} \tag{3.39}$$

The physiological resistance terms $r^c{}_a$ and $r^c{}_s$ define bulk boundary layer and bulk stomatal resistances, respectively. The resistance term $r^s{}_s$ represents the soil surface resistance. The terms $r^a{}_a$ and $r^s{}_a$ are the aerodynamic resistances for two layers of the atmosphere below a reference height (x), with the boundary between the layers being the height of the canopy source height, which is defined at d + z_o. A definition of this height is required before an analysis of the resistances is considered.

3.4.1 Canopy Source Height

Aerodynamic resistance is divided between two layers of the canopy air stream, with the dividing boundary being the canopy source height (figure 3.2). This is assumed to be the height at which the mean conditions within the air stream occur. Shuttleworth and Wallace (1985) define this height at $d + z_o$, with

$$d = 0.63\ h \tag{3.40}$$

$$z_o = 0.13\ h \tag{3.41}$$

where h is the mean height of the canopy. The d and z_o terms were assumed to remain at this fixed fraction of canopy height after Monteith (1973).

However, this approach only considers the effects of canopy height and is independent of the canopy density, which tends to vary even while the height remains constant. This is especially the case in sparse canopies, where individual plants have small leaf areas and are far apart in relation to their height. As an alternative, Choudhury and Monteith (1988) and Shuttleworth and Gurney (1990) calculated d and z_o as functions of leaf area index after the theory of Shaw and Pereira (1982). In both cases, d and z_o were defined as

$$d = 1.1h \cdot \ln\left(1 + X^{1/4}\right) \tag{3.42}$$

and

$$z_o = z'_o + 0.3h\, X^{1/2} \quad \text{if } 0 < X < 0.2 \tag{3.43}$$

$$z_o = 0.3h\left(1 - \frac{d}{h}\right) \quad \text{if } 0.2 < X < 1.5 \tag{3.44}$$

where

$$X = C_d\, FAI \tag{3.45}$$

where z'_o is the roughness length of the bare substrate and C_d is the mean drag coefficient for the individual vegetative elements of the canopy. For the SW model, C_d was assumed to be constant at 0.2 after Choudhury and Monteith (1988).

Shuttleworth and Gurney (1990) suggested that this method of calculating d and z_o is superior to that of Monteith (1973) and they recommended that it be used in any application of the SW model. Dolman and Wallace (1991) supported this by stating that this approach was the most physically realistic of any used in the models they examined. For these reasons, it was applied in this study to the calculation of the canopy source height for both the SW model and its modified version, the MSW model.

3.4.2 Aerodynamic Resistance in the SW Model

The aerodynamic resistance terms, r^a_a and r^s_a, define the resistances for two atmospheric layers within the boundary layer. They are dependant on the location of the canopy source height since it determines the boundary between the two layers. The bottom layer is defined as the distance from the surface to the canopy source height and the top layer is the distance from the source height to the reference height above the canopy.

Soil evaporation is partially governed by aerodynamic resistance within these two layers. The resistance between the surface and the canopy source height, r^s_a, is assumed to vary between two asymptotic limits of foliage area index. The lower limit, when FAI is zero, is defined as $r^s_a(0)$ where

$$r^s_a(0) = \frac{\ln\left(\frac{x}{z'_o}\right)\ln\left(\frac{d+z_o}{z'_o}\right)}{k^2 u_x} \qquad (3.46)$$

where u_x is the wind speed at reference height. The upper limit, when FAI is at a maximum, is defined as $r^s_a(\alpha)$ where

$$r^{s}_{a}(\alpha) = \frac{\ln\left(\frac{x-d}{z_o}\right)}{k^2 u_x} \cdot \frac{h}{n(h-d)} \cdot \left\{\exp n - \exp\left[n\left(1-\frac{d+z_o}{h}\right)\right]\right\} \quad (3.47)$$

where n is an eddy diffusivity decay constant, which is defined later. It is as yet unknown how r^s_a behaves so it is assumed to vary linearly between these two limits. Thus

$$r^{s}_{a} = \frac{1}{0.28} FAI\, r^{s}_{a}(\alpha) + \frac{1}{0.28}(0.28 - FAI)\, r^{s}_{a}(0) \quad (3.48)$$

This approach was accepted by Choudhury and Monteith (1988) but they considered it to be a source of limitation to modelling until additional research suggested an improvement or an alternative.

The aerodynamic resistance between the canopy source height and the reference height, r^a_a, follows the same approach as r^s_a where

$$r^{a}_{a}(0) = \frac{\ln^2\left(\frac{x}{z'_o}\right)}{k^2 u} - r^{s}_{a}(0) \quad (3.49)$$

$$r^a_a(\alpha) = \frac{\ln\left(\frac{x-d}{z_o}\right)}{k^2 u}\left\{\ln\left(\frac{x-d}{h-d}\right) + \frac{h}{n(h-d)}\left[\exp\left(n\left\{1-\frac{d+z_o}{h}\right\}\right)-1\right]\right\} \qquad (3.50)$$

and

$$r^a_a = \frac{1}{0.28} FAI\ r^a_a(\alpha) + \frac{1}{0.28}(0.28-FAI)\, r^a_a(0) \qquad (3.51)$$

All of these individual aerodynamic resistances are results of an integration over height. The $r^s_a(\alpha)$ term was integrated from the surface to the canopy source height, $d + z_o$. The $r^s_a(0)$ term was integrated over the same height except that the lower limit was the bare soil surface roughness length z'_o, instead of the surface. The $r^a_a(\alpha)$ term was the sum of two integrations involving the height ranges from $d + z_o$ to the height of the canopy, h, and from h to the reference height, x. The final result is that $r^a_a(\alpha)$ represents the height range from the canopy source height to the reference height. The $r^a_a(0)$ term was the result of the difference between two integrations, where the height range from z'_o to $d + z_o$ was subtracted from the range from z'_o to x. This resulted in $r^a_a(0)$ representing the height range from $d + z_o$ to x. The reader is referred to Shuttleworth and Wallace (1985) for a more complete derivation of these resistances.

3.4.3 Canopy Resistance in the SW Model

Canopy resistance is comprised of the bulk boundary layer resistance of the canopy, r^c_a, and the bulk stomatal resistance of the canopy, r^c_s. They follow the same approach as equation 3.25 where

$$r^c_a = \frac{r_b}{FAI} \tag{3.52}$$

$$r^c_s = \frac{r_{st}}{LAI} \tag{3.53}$$

where r_b is the mean boundary layer resistance, defined by Choudhury and Monteith (1988) as

$$r_b = \frac{1}{\dfrac{0.02}{n'}\left(\dfrac{u_h}{Lw}\right)^{\frac{1}{2}}\left[1-\exp\left(\dfrac{-n'}{2}\right)\right]} \tag{3.54}$$

where u_h is the wind speed at the top of the canopy, Lw is the mean leaf width and n′ is an attenuation coefficient for wind speed. Equations 3.52 and 3.54 assume that molecular diffusion through a laminar layer adhering to the surface of the leaves is the only process of energy exchange within the boundary layer of the vegetation. It is also assumed that the attenuation coefficient decays at the same rate within the canopy as the eddy diffusivity constant, n. Following Lafleur and Rouse (1990), these constants are calculated in this study as

$$n = n' - b(FAI^{a}) \qquad (3.55)$$

where a and b are dimensionless coefficients with values of 0.36 and 2.6 respectively.

Equation 3.55 was developed for a wet sedge meadow and is believed to be the first attempt to determine n and n′ for developing canopies. The function gives the coefficients values ranging from 2.0 to 3.7 for LAI values ranging from 0.4 to 2.5. In this study, equation 3.55 was extrapolated and applied to the values of FAI which ranged from 0.14 to 0.28.

3.4.4 Resistances of Dead Vegetation

Dead vegetation, particularly dead sedges and grasses, covers as much as one-sixth of the study site (table 2.1) and is expected to contribute to the total aerodynamic resistance. This vegetation was factored into the model through the addition of DAI to LAI (equation 2.6). Hence, FAI was used in all of the equations calculating aerodynamic resistance. The only equation not requiring DAI was the bulk stomatal resistance of the canopy. This was the only physiological resistance and required living vegetation with a stomatal conductance.

3.4.5 Soil Surface Resistance

The soil surface resistance, r^s_s, is the limiting factor in practical applications of the model, considering that it is a difficult variable to measure in the field. Total Q_e as calculated by the SW model is strongly influenced by the surface condition of the soil and demands an accurate determination of r^s_s (Shuttleworth and Wallace, 1985). However, there is very little information available concerning typical values of r^s_s.

Shuttleworth and Wallace (1985) calculated evaporation using the SW model by assuming that r^s_s was constant. They ran their model for three values of r^s_s: 0, 500 and 2000 sm^{-1}. A value of 0 sm^{-1} was said to correspond to saturated soil or open water and 2000 sm^{-1} represented a typically dry soil, according to Fuchs and Tanner (1967). The value of 500 sm^{-1} was chosen as an intermediate value representing that of dry vegetation. Shuttleworth and Gurney (1990) used the same assumed value of 500 sm^{-1}. Lafleur and Rouse (1990) assumed that r^s_s was zero at all times since the wetland surface being studied was constantly saturated.

The mathematical definition of r^s_s has been given as

$$r^s_s = \frac{\left(\frac{\rho C_p}{\gamma}\right) \cdot D_s}{Q_{es}} \tag{3.56}$$

where Q_{es} is the evaporation from the soil and D_s is the vapour pressure deficit at the soil surface where

$$D_s = e_w(T_s) - e_s \tag{3.57}$$

where $e_w(T_s)$ is the saturated vapour pressure at soil temperature T_s, and e_s is the vapour pressure at the soil surface. However, Fuchs and Tanner (1967) examined the effectiveness of equation 3.56 in modelling surface resistance and found that the approach was physically unacceptable.

A more detailed analysis of surface resistance is given in chapter 4. However, for the initial purposes of this study, r^s_s was assumed to be constant for the entire season. This assumption was considered to be acceptable since soil moisture never changed appreciably over the course of the measurement period. However, a constant value of zero as assumed by Lafleur and Rouse (1990) was not applicable since all of the soil was never saturated. Instead, r^s_s was initially considered to be 500 sm^{-1} as assumed by Shuttleworth and Wallace (1985), which is a value that was only used in the hourly comparison of the four models. For the daily comparison, an iterative process was implemented with the data from the hourly values and a more representative constant r^s_s value was determined. This process is described in chapter 4.

3.4.6 Available Energy

The dividing of the SW model into bare soil and canopy evaporation is done through the partitioning of available energy. The available energy equations for the site, AE, and bare soil, AE_s, are

$$AE = Q^* - Q_g \tag{3.58}$$

$$AE_s = Q^*{}_s - Q_g \tag{3.59}$$

where Q^*_s is the net radiation over bare soil. The available energy for the canopy is considered to be the difference between AE and AE_s. Q^*_s is found using Beer's law where

$$Q^*{}_s = Q^* \exp(-C_a FAI) \tag{3.60}$$

where C_a is the canopy attenuation coefficient. In this study, a constant value of 0.55 was assigned to C_a after Lafleur and Rouse (1990), who used it for a subarctic, sedge canopy. Uchijima (1976) used a value of 0.56 for a rice canopy with a LAI of 0.22, which closely resembled the sedge canopy in this study.

3.5 The Modified Shuttleworth-Wallace (MSW) Model

As was mentioned earlier, the PM model was designed to model evaporation for canopies where surface evaporation is negligible, which limits its use to applications with full canopies. The SW model assumes that the only source of non-canopy evaporation is bare soil. This assumption would seem to be inapplicable to surfaces where open water is present. In the present study, open water covered as much as 76% of the surface (figure 2.3). To account for this extra source of evaporation, a modified version of the SW combination model (MSW) was designed to include contributions from canopy, bare soil and open water. The MSW model follows the same logic as the SW model except that C_w and PM_w terms are added for open water in the derivation. The reader is referred to Appendix I for the full derivation of the MSW model but a brief description is given here. A schematic diagram of the model is given in figure 3.3.

The MSW model is given as

$$Q_e = C_c PM_c + C_s PM_s + C_w PM_w \qquad (3.61)$$

where C_w is the model coefficient and PM_w is the PM equation applying to open water. The model coefficients are given as

$$C_c = \frac{1}{1 + \dfrac{R_c R_a (R_w + R_s)}{R_w R_s (R_c + R_a)}} \qquad (3.62)$$

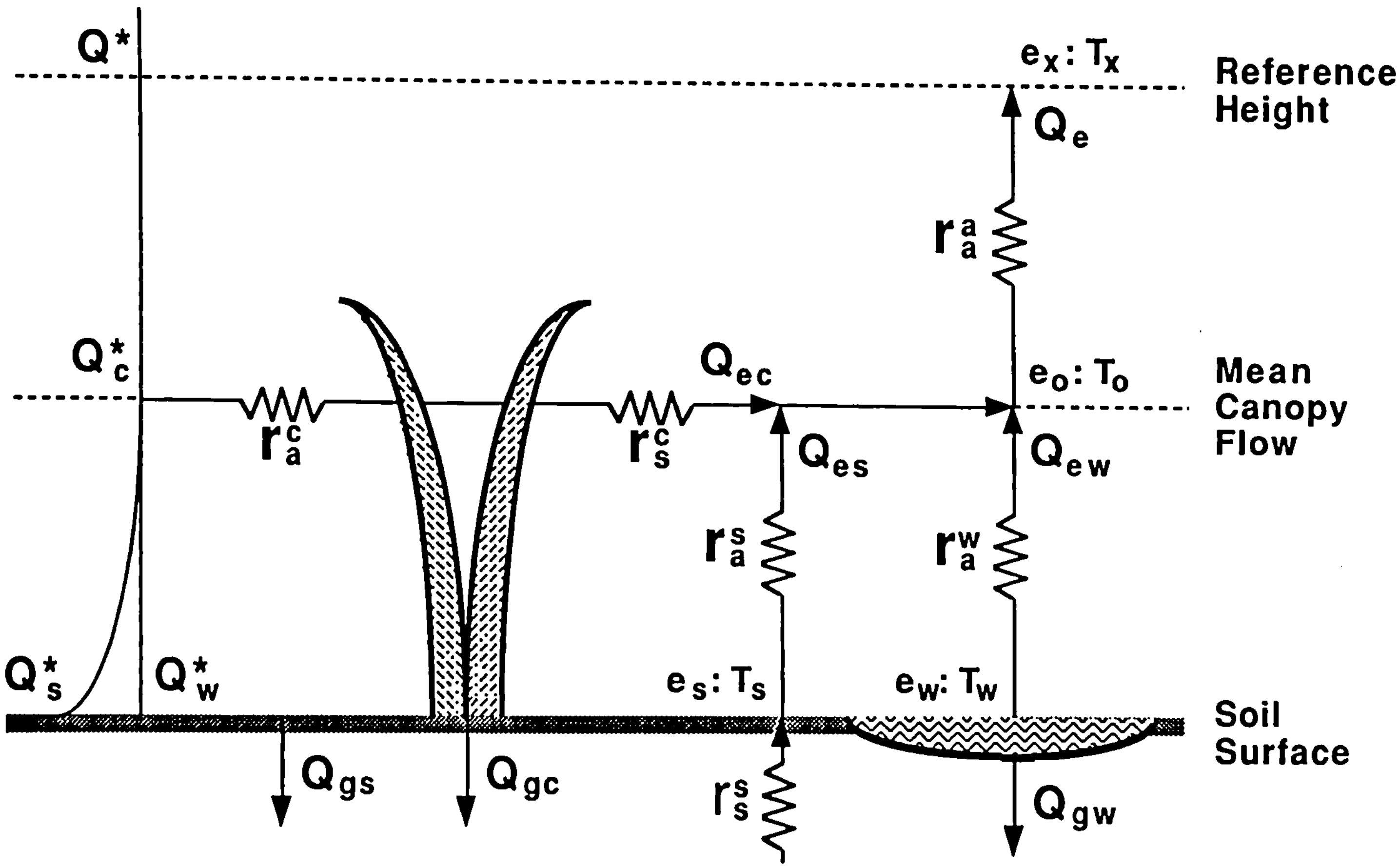

Figure 3.3 Schematic representation of the Modified Shuttleworth-Wallace model.

$$C_s = \frac{1}{1 + \dfrac{R_s R_a (R_w + R_c)}{R_w R_c (R_s + R_a)}} \tag{3.63}$$

$$C_w = \frac{1}{1 + \dfrac{R_w R_a (R_c + R_s)}{R_c R_s (R_w + R_a)}} \tag{3.64}$$

where R_s, R_c and R_a are the same as defined earlier and R_w is defined as

$$R_w = (\Delta + \gamma)\ r^w{}_a \tag{3.65}$$

where $r^w{}_a$ is the aerodynamic resistance between the open water surface and the canopy source height. The PM equations are expressed as

$$PM_c = \frac{\Delta AE + \dfrac{\rho C_p D_x - r^c{}_a \Delta (AE - AE_c)}{r^a{}_a + r^c{}_a}}{\Delta + \gamma\left(1 + \dfrac{r^c{}_s}{r^a{}_a + r^c{}_a}\right)} \tag{3.66}$$

$$PM_s = \frac{\Delta AE + \dfrac{\rho C_p D_x - r^s{}_a \Delta (AE - AE_s)}{r^a{}_a + r^s{}_a}}{\Delta + \gamma\left(1 + \dfrac{r^s{}_s}{r^a{}_a + r^s{}_a}\right)} \tag{3.67}$$

$$PM_w = \frac{\Delta AE + \dfrac{\rho C_p D_x - r^w{}_a \Delta (AE-AE_w)}{r^a{}_a + r^w{}_a}}{\Delta + \gamma} \qquad (3.68)$$

where AE_c and AE_w are the available energy terms for canopy and open water, respectively.

The individual evaporation components Q_{ec} and Q_{es} are calculated using the same equations as those used by the SW model and the Q_{ew} component is calculated in a similar fashion using

$$Q_{ew} = \frac{\Delta AE_w + \dfrac{\rho C_p D_o}{r^w{}_a}}{\Delta + \gamma} \qquad (3.69)$$

3.5.1 Aerodynamic Resistance in the MSW Model

The aerodynamic resistance terms in the MSW model are the same as those for the SW model except that an extra term, $r^w{}_a$, is applied to open water. This term is used to describe the aerodynamic resistance over open water between the surface and the canopy source height. It is assumed to be equal to the aerodynamic resistance over a bare substrate, $r^s{}_a(0)$, which was defined in equation 3.46. Thus

$$r^{w}_{a} = \frac{\ln\left(\frac{x}{z'_{o}}\right)\ln\left(\frac{d+z_{o}}{z'_{o}}\right)}{k^{2}u_{x}} \tag{3.70}$$

3.5.2 Surface Resistance for Water

The Q_{ew} evaporation component for the MSW model assumes that there is negligible surface resistance for open water. As a result, the only resistances to open water evaporation are the aerodynamic terms r^{a}_{a} and r^{w}_{a}. It is therefore assumed that any diffusional resistance due to the presence of a thin laminar layer on the surface of the water has a negligible effect. When these assumptions are implemented into the MSW model, the open water component resembles a simple Penman formula for calculating potential evaporation.

3.5.3 Available Energy

The MSW model was partitioned into canopy, bare soil and open water evaporation through the partitioning of available energy, as for the SW model. The available energy equation for the site, AE, is the same as that defined in equation 3.58. The equations for the surface types are

$$AE_{c} = Q^{*}_{c} - Q_{gc} \tag{3.71}$$

$$AE_s = Q^*_s - Q_{gs} \qquad (3.72)$$

$$AE_w = Q^*_w - Q_{gw} \qquad (3.73)$$

where Q^*_c and Q^*_w are the net radiation terms for canopy and open water, respectively, and Q_{gc}, Q_{gs} and Q_{gw} are the soil heat flux terms for canopy, bare soil and open water, respectively. All of the soil heat flux terms were measured and weighted for surface area.

Net radiation was measured over the three surface types of hummock (Q^*_{hum}), hollow (Q^*_{hol}) and open water (Q^*_w) and weighted according to their surface areas. The total Q^*_s was calculated as the sum of net radiation over bare soil in hollows (Q^*_{hol}) and on hummocks (Q^*_{shum}), such that

$$Q^*_s = Q^*_{hol} + Q^*_{shum} \qquad (3.74)$$

Since the hummocks have a canopy, the Q^*_{shum} term was determined using Beer's Law as in equation 3.60, where

$$Q^*_{shum} = Q^*_{hum} \exp(-CFAI) \qquad (3.75)$$

The Q^*_c term was determined as a residual, such that

$$Q^*_c = Q^* - (Q^*_s + Q^*_w) \tag{3.76}$$

3.5.4 MSW Model Assumptions

As with all combination models, the MSW model requires a few basic assumptions in order to be used in practical applications. Most of these assumptions are applicable to both the SW and MSW models. Those assumptions not described earlier will be discussed here.

The MSW model assumes horizontal spatial uniformity, which is necessary for all one-dimensional models. Of course, in practice this is never entirely the case since three dimensional features of a canopy always exist. This is especially true with partial canopies, where aerodynamic effects tend to change with spatially heterogenous vegetation. However, in models of a Penman-Monteith type, all variables (such as the resistances and energy fluxes) are defined as horizontal averages. Essentially, this is only relevant where horizontal differences in the variables are minor over a given area so that representative horizontal averages are acceptable. However, implicit in the assumption of horizontal uniformity is the idea that a one-dimensional model can be applied to any surface regardless of the degree of spatial heterogeneity. Thus, the model is applicable to natural heterogenous surfaces as well as homogenous surfaces such as row crops. Using this reasoning, the measured variables at the Churchill study site are expected to be acceptable horizontal averages at a local scale, despite the relative heterogeneity of the surface.

The MSW model makes the assumption that a hypothetical mean canopy air stream exists which is sufficiently described by the meteorological variables of temperature, vapour pressure and wind speed. The relevance of this air stream depends on an adequate degree of aerodynamic mixing within the canopy. Aerodynamic mixing within a partial canopy is considered to be greater than that of a closed canopy (Shuttleworth and Wallace, 1985) and is likely to be applicable to the existence of a mean air stream in this study.

The bulk stomatal resistance is assumed to be representative of the entire site. In order for this to occur, the individual stomatal resistances within the canopy must be similar so that the overall sum is accurately described by the r_{st} term. This allows equation 3.53 to be applicable in practical situations. However, studies have shown that canopies with different types of plants will have a variety of stomatal resistances. In practice, each one of the plants must be sampled and an acceptable average must be determined. However, the dominance of Carex aquatilis in the very sparse canopy at the study site warranted the measurement of r_{st} from this vegetation type only. In addition to this, no other dominant living plant could be sampled accurately due to limitations of the porometer.

Both the SW and MSW models require that the surface types represented by the evaporation components must always exist, even if the evaporative flux is zero. This is due to the mathematical limitations of the resistance terms within the model coefficients C_c, C_s and C_w. For example, if no open water exists on the surface, then there is no aerodynamic resistance r^w_a and therefore R_w becomes zero and C_c and C_s become undefined. As a result, the SW and MSW models are limited for use only in applications where all of the surface components represented in the model are present. Thus, the MSW model cannot be applied in this study for days when the water table falls below the surface.

Provided that all of the components are present, both models have correctly defined asymptotic limits. If there is no canopy transpiration, r^c_s is infinite and PM_c is zero. Similarly, if surface evaporation is zero then r^s_s becomes infinite and PM_s becomes zero. However, since it is assumed that open water has no surface resistance, water will always contribute to the total evaporation stream as long as the water table remains at the surface.

3.6 The Weighted Penman-Monteith (WPM) Model

A fourth approach to modelling evaporation from a site which has more than one surface type is through the application of the PM model to each evaporation source and weighting the final Q_e values by surface area. This approach is henceforth called the Weighted Penman-Monteith (WPM) model. A schematic diagram of the model is given in figure 3.4. The WPM model is defined as

$$Q_e = LAI \cdot Q_{ec} + S \cdot Q_{es} + W \cdot Q_{ew} \tag{3.77}$$

where S and W are the proportions of bare soil and open water, respectively.

The individual Penman-Monteith components of the WPM model differ only in their treatment of available energy and surface resistance. The canopy component of the model is defined exactly as given in equation 3.18 for the PM model except that the available energy term represents only energy produced by the canopy, AEC. AEC differs from AE_c in that the latter is a surface-weighted available energy term whereas the former represents the available energy expected if the entire site was covered by a canopy. Thus the Penman-Monteith calculation for a canopy, Q_{ec}, can be defined as

$$Q_{ec} = \frac{\Delta AEC + \frac{\rho C_p D_x}{r_a}}{\Delta + \gamma\left(1 + \frac{r_{cs}}{r_a}\right)} \tag{3.78}$$

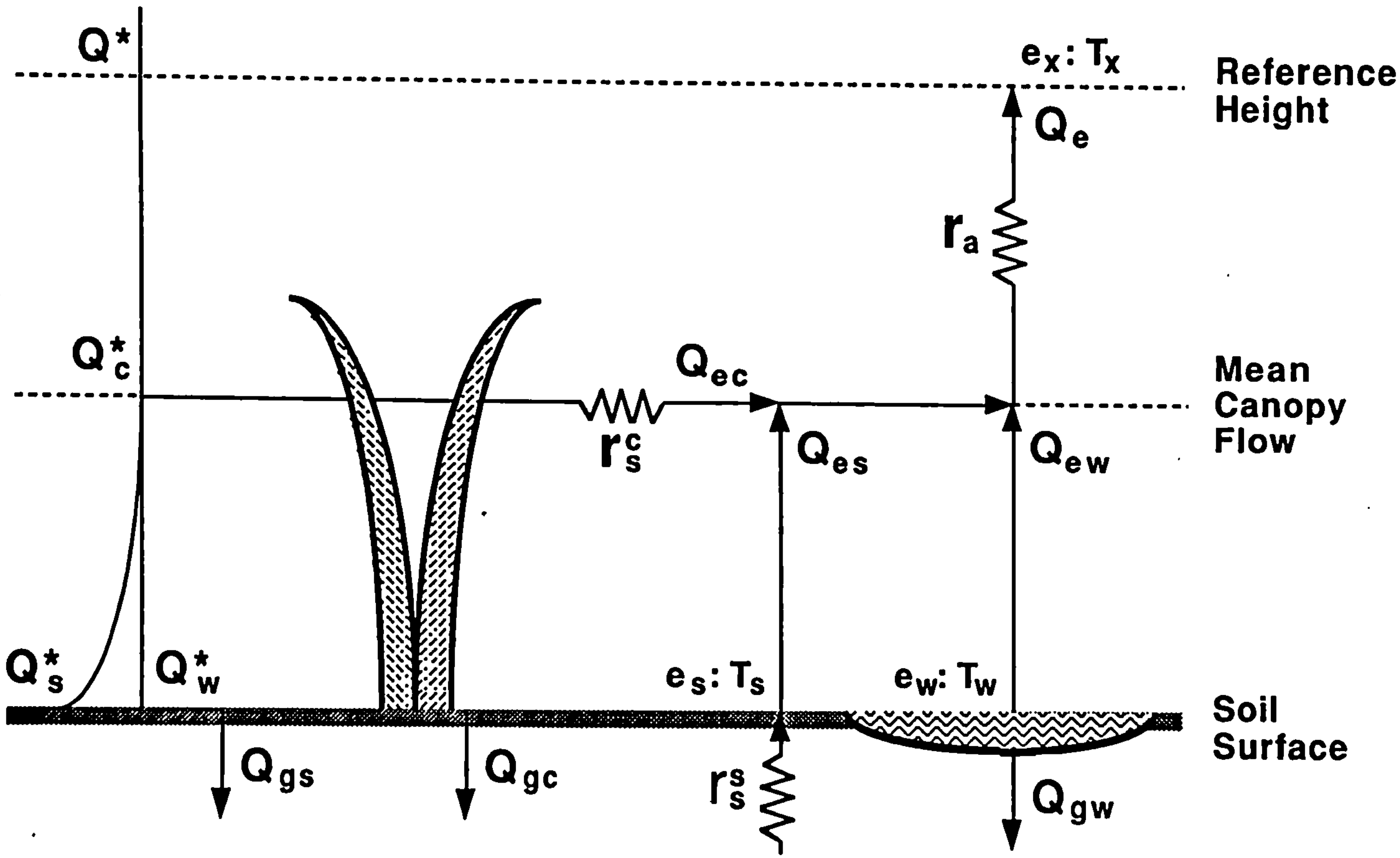

Figure 3.4 Schematic representation of the Weighted Penman-Monteith model.

Similarly, the bare soil component of the WPM model, Q_{es}, can be defined as

$$Q_{es} = \frac{\Delta AES + \frac{\rho C_p D_x}{r_a}}{\Delta + \gamma\left(1 + \frac{r_{ss}}{r_a}\right)} \tag{3.79}$$

where AES is the available energy produced only from bare soil. The r^s_s term is the same soil surface resistance term defined for the SW and MSW models. It is assumed to be a constant value of 500 sm^{-1} for the hourly analysis of the WPM model.

The open water component, Q_{ew}, follows the same approach as the canopy and soil components except that the surface resistance is assumed to be zero. Thus

$$Q_{ew} = \frac{\Delta AEW + \frac{\rho C_p D_x}{r_a}}{\Delta + \gamma} \tag{3.80}$$

where AEW is the available energy produced only from open water.

Although the WPM model is similar to the MSW model, the former is a much simpler approach and requires fewer parameters and variables. In addition to this, the three dimensional nature of the WPM model seems to provide a better representation of a sparse heterogenous canopy than the MSW model, since the WPM model weights the final evaporation terms instead of the available energy terms.

Chapter 4

Model Testing and Analysis

There are three objectives pursued in this chapter. The first is to analyze the results of the hourly simulation from each model for the days when stomatal resistances were measured. The second is to determine the sensitivity of each modelled Q_e to the driving variables and the resistances. The third objective is to compare the models in their simulation of daily average evaporation.

4.1 Initial Conditions for Hourly Simulations

Each of the four models has characteristics which must be considered before it can be applied in any simulation. Since not all of the models have a true application to a typical tundra wetland surface, certain initial conditions must be established to allow any valid comparison of the models to take place. These are described as follows.

4.1.1 Adaptation of Model Analogy to the Wetland Surface

All four models were designed individually and for different applications. As a result, the theory of one or more of the models may not be entirely analogous to the study site. This restriction requires an analysis and suitable adjustments in the conceptual approach of each model.

The PM (Penman-Monteith) model was originally designed to simulate transpiration from a closed vegetative canopy with negligible surface evaporation. This concept is not valid for a wetland surface with a sparse canopy. However, if a surface resistance can be factored into the model to represent the surface contribution to the evaporation stream, then the PM model has at least a theoretical application to a wetland surface. For the hourly comparison of the four models, the PM model was used as originally presented by Monteith (1965), in order to examine the effects caused by the misrepresented surface. The results of the simulation were then used to determine a more accurate surface resistance, which was assumed to represent the entire surface in the daily comparison.

The conceptual approach of Shuttleworth and Wallace (1985) in the development of the SW model was to describe evaporation for a surface consisting of bare soil and a sparse canopy. No allowance for open water was considered and, hence, application of the model is limited to sites where open water contribution to evaporation is negligible. To adapt the SW model for use in this study, the bare soil and open water surfaces were combined and represented by the PM_s and Q_{es} terms in the model. Although this approach has obvious potential problems, the model can still be effectively applied to the hourly and daily comparisons.

Both the MSW (Modified Shuttleworth-Wallace) and WPM (Weighted Penman-Monteith) models were developed for the study site and both consider all three surface types in the wetland environment. As a result, no adjustments were required in either model for any of the simulations.

4.1.2 The Determination of Surface Resistance

In the hourly simulation, the surface resistance of the PM model is represented by the canopy resistance, r_c. This variable can be determined for each hour of the simulation by using measured r_{st} values with equation 3.25.

However, surface resistance is the only variable required by the other three models that was not measured or calculated. This is due to the fact that r^s_s is difficult to determine experimentally and very little information is available concerning typical values in the literature. As a result, surface resistance is one of the most important limiting variables in the practical application of the models. In order for any of the models to simulate evaporation effectively, the surface resistance must be determined as accurately as possible.

A precise mathematical definition of soil surface resistance was given in equation (3.56) and is repeated here:

$$r^s_s = \frac{\left(\frac{\rho C_p}{\gamma}\right) D_s}{Q_{es}} \tag{4.1}$$

This definition is a simplified approach to the drying of a bare soil and implies that r^s_s is primarily dependant on soil evaporation and the vapour pressure deficit at the soil surface. Monteith (1981) described this resistance using a conceptual approach, where evaporation occurs from a wet soil which is covered by a dry, isothermal soil layer of finite thickness. The boundary between the wet and dry soil is considered to be at the level of water vapour saturation and represents the source of water vapour in the soil. Thus, equation 4.1 is the resistance of the dry layer to water vapour transfer. This approach is considered to be conceptually acceptable and consistent with observation (Shuttleworth and Wallace, 1985). However, Fuchs and Tanner (1967) found that equation 4.1 was physically unreasonable. This was primarily due to the fact that the sources of water vapour are not found in a well defined boundary but occur in a thicker layer between the wet and dry soil. Since the water vapour sources were well distributed and not confined in one plane, the assumption of constant isothermy within the dry soil becomes unrealistic and assists in reducing the validity of the equation.

Shuttleworth and Gurney (1990) also acknowledged the difficulty of determining r^s_s. In order to develop a submodel of the SW model to calculate r^c_s, they had to assume a constant value for r^s_s of 500 sm^{-1} after Shuttleworth and Wallace (1985). Tests of the submodel showed that r^c_s was relatively insensitive to changing r^s_s at large values of LAI. However, for small LAI values, r^c_s was highly sensitive to changes in r^s_s. This indicates that the behaviour of r^s_s in the present study, particularly during wetting and drying periods, can greatly vary the value of r^c_s. This can have significant effects on the total evaporation calculated from a site if the canopy is an important contributor to the latent heat flux. One of the conclusions of Shuttleworth and Gurney (1990) was that the most important requirement to determining bulk stomatal resistance, using present theory, was the need to improve the estimation of r^s_s. They suggested a simple method of calculating r^s_s using an analogous equation developed from the submodel for r^c_s, such that

$$r^s_s = \frac{\left(\frac{\rho C_p}{\gamma}\right)\left[e_w(T_s) - e_o\right]}{AE_s - \frac{\rho C_p (T_s - T_o)}{r^s_a}} - r^s_a \tag{4.2}$$

where T_s and T_0 are temperatures at the substrate surface and canopy source height, respectively, and e_0 is the vapour pressure at the canopy source height. Application of equation 4.2 to the present study yielded poor results with r^s_s varying greatly and sometimes becoming negative. These bad results are probably partly due to error in the estimates of the surface temperature, which is difficult to measure with acceptable accuracy in the field. Further investigation of equation 4.2 is required with improved estimates of T_s.

Wallace et al (1990) calculated r^s_s through an iterative process involving the main equations of the SW model. They substituted an arbitrary value of r^s_s into the PM_s equation 3.35 and calculated total evaporation using equation 3.28. The resulting total Q_e was then used to solve for D_0 in equation 3.37 which was substituted into equation 3.39 to find Q_{es}. This calculated Q_{es} was then compared to a measured value of soil evaporation as determined by microlysimeters. The r^s_s value was adjusted and the process repeated until the calculated and measured Q_{es} agreed. The resulting D_0 was substituted into equation 3.38 to find Q_{ec}, which was the flux required in their study. Of course, this method of determining r^s_s cannot be implemented if soil evaporation is desired. As a result, it was not attempted in this study.

Since no feasible surface resistance could be determined for this study for the SW, MSW and WPM models, a constant value of 500 sm^{-1} as suggested by Shuttleworth and

Wallace (1985) was used for the hourly simulations. The results of the simulations were then used to determine a more representative surface resistance for each model for the daily comparison.

4.2 Error in Measured Q_e

The absolute error in the measured evaporation, δQ_e, is largely dependant on the measurement errors of Q^*, Q_g and the Bowen ratio β. In this study, the measurement errors were assumed to be the same as those assigned by Lafleur (1988), who used the same methods and types of instruments as employed in the present study. Thus, Q^*, Q_g and β were assigned errors of ±7%, ±20% and ±4%, respectively. Following Lafleur (1988), δQ_e was calculated as

$$\delta Q_e = \left[\left(\frac{\partial Q_e}{\partial Q^*}\delta Q^*\right)^2 + \left(\frac{\partial Q_e}{\partial Q_g}\delta Q_g\right)^2 + \left(\frac{\partial Q_e}{\partial \beta}\delta \beta\right)^2\right]^{\frac{1}{2}} \qquad (4.3)$$

where

$$\frac{\partial Q_e}{\partial Q^*} = \frac{1}{1+\beta} \qquad (4.4)$$

$$\frac{\partial Q_e}{\partial Q_g} = -\frac{1}{1 + \beta} \tag{4.5}$$

$$\frac{\partial Q_e}{\partial \beta} = -\frac{Q^{*} - Q_g}{(1 + \beta)^2} \tag{4.6}$$

The absolute error in Q_e ranged from 0.5 Wm^{-2} to 35.2 Wm^{-2} over the three day hourly simulation and from 0.5 Wm^{-2} to 13.4 Wm^{-2} for the daily averages in the daily simulation. The relative error in Q_e is defined as $\delta Q_e/Q_e$ and ranged from 9% to 21% for the three day simulation and from 5% to 11% for the daily simulation.

4.3 **Hourly Comparison**

Stomatal resistance was measured on an hourly basis for the three days of July 8, July 25 and August 4. The availability of a measured r_{st} allows for an hourly calculation of r_c in the PM model and r^c_s in the SW, MSW and WPM models. This conveniently avoids the unrealistic assumption that bulk stomatal resistance is constant through time, which must be made when data for r_c or r^c_s are not available. As a result, the three models can be compared with soil surface resistance being the only unknown variable.

A substantial range in surface cover occurred on the three days, which provides the opportunity to compare the models under various surface conditions. On July 8, the surface was relatively dry and consisted of 5% open water and 95% bare soil with a canopy FAI of 0.25. On July 25, the surface was wet with 63% open water, 37% bare soil and an FAI of 0.28. On August 4, the surface was moderately wet with 39% open water, 61% bare soil and an FAI of 0.28. In general, a high percentage of open water indicates that the water table is at or above the surface and therefore the surface is wetter than when there is a lower percentage of open water.

The simulations of total evaporation using the four models are shown in figure 4.1. The WPM model provides the best overall simulation of the total measured Q_e (table 4.1), followed by the MSW model, the PM model and the SW model. The relative performances of each model can be easily determined using the "index of agreement", d_i, which is a descriptive measure defined by Willmott and Wicks (1980) from the mean square error, where

$$d_i = 1 - \left[\frac{\sum_{i=1}^{N} (P_i - O_i)^2}{\sum_{i=1}^{N} \left(|P'_i| + |O'_i| \right)^2} \right] \qquad (4.7)$$

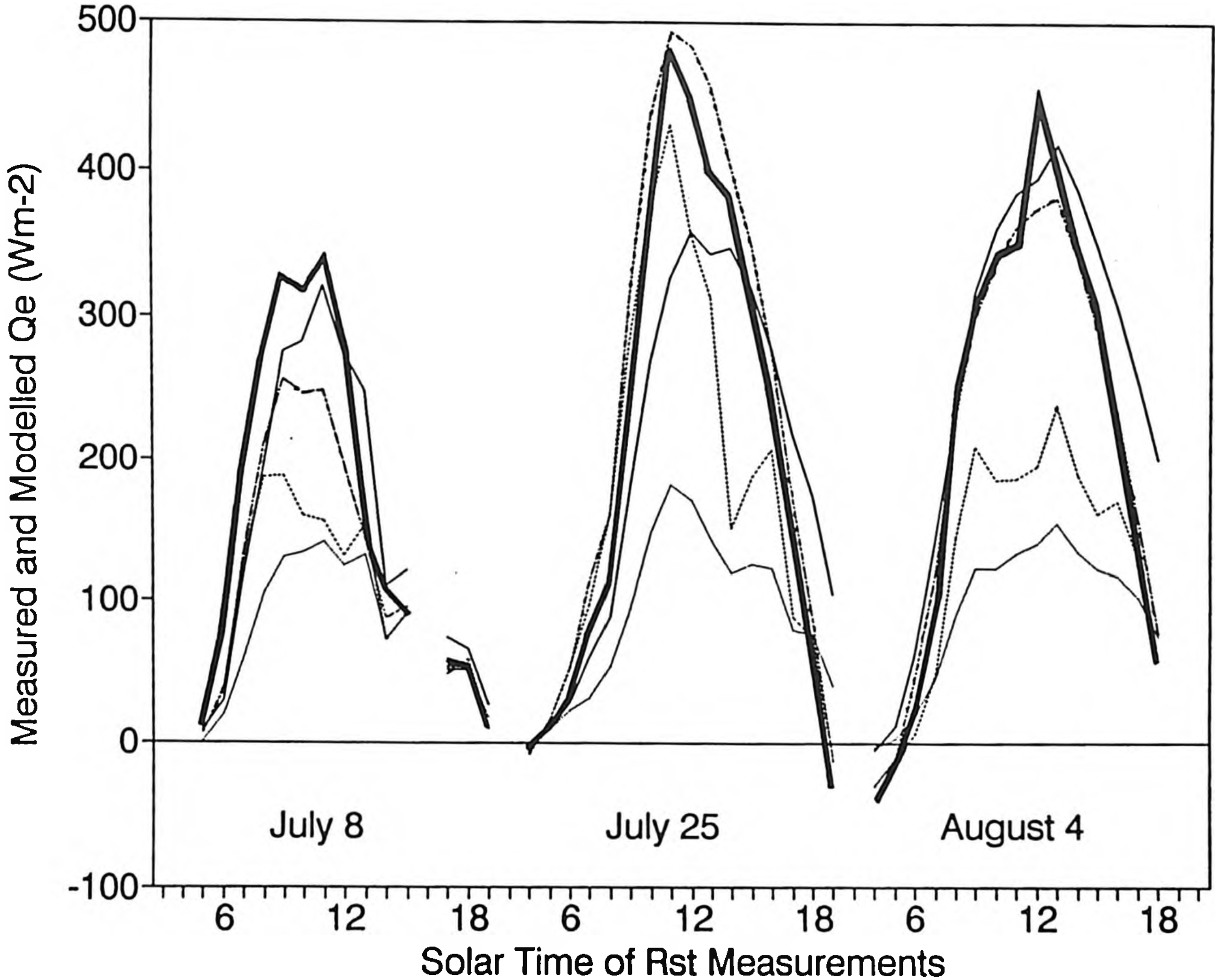

Figure 4.1 Comparison between measured Q_e (heavy solid) and the PM model (dashed), the WPM model (centerline), the SW model (dotted) and the MSW model (solid) for the hourly comparison. All r_s and r^s_s values were 500 sm^{-1} and r_{st} was measured.

		PM	WPM	SW	MSW
a)	N	47	47	47	47
	RMSE	97.3	38.3	150.1	61.4
	MBE	-58.4	-1.5	-103.3	6.8
	Observed	188.1	188.1	188.1	188.1
	Predicted	129.7	186.6	84.8	194.9
	d_i	0.87	0.98	0.67	0.95
b)	N	15	15	15	15
	RMSE	87.5	48.1	111.5	44.8
	MBE	-57.4	-33.9	-76.5	-8.3
	Observed	152.1	152.1	152.1	152.1
	Predicted	94.7	118.2	75.6	143.8
	d_i	0.80	0.95	0.68	0.96
c)	N	16	16	16	16
	RMSE	80.4	38.4	165.5	72.2
	MBE	-32.0	30.9	-117.2	-11.6
	Observed	206.8	206.8	206.8	206.8
	Predicted	174.8	237.7	89.6	195.2
	d_i	0.93	0.99	0.66	0.94
d)	N	16	16	16	16
	RMSE	119.1	25.6	164.7	62.9
	MBE	-85.7	-3.4	-114.4	39.4
	Observed	203.2	203.2	203.2	203.2
	Predicted	117.5	199.8	88.8	242.6
	d_i	0.82	0.99	0.67	0.96

Table 4.1 Evaluation of model performance for all a) three days involved in the hourly simulations, b) July 8, c) July 25 and d) August 4. Observed and Predicted refer to the means of the observed and predicted values, N refers to the total number of hours simulated and d_i is the index of agreement. All values except N and d_i are in Wm^{-2}.

where N is the number of cases, P_i and O_i are the predicted and observed variables and P'_i and O'_i are defined as

$$P'_i = P_i - \bar{O} \quad (4.8)$$

$$O'_i = O_i - \bar{O} \quad (4.9)$$

where $\bar{O}$ is the mean of the observed variables. The "index of agreement" varies between 0 and 1 and is entirely relative, such that the model with the highest value of d_i is considered to have the best simulation.

The good agreement between predicted and observed evaporation during the morning and evening hours for all four models is most likely due to the relatively small available energy which corresponds to these periods. The small measured evaporation fluxes that result would tend to correlate well with the small predicted fluxes since both observed and predicted evaporation are strongly influenced by AE.

4.3.1 The PM Model

For most of the time during the three days, the PM model badly underestimated the measured Q_e. In fact, the predicted evaporation was often only half of the observed. The main reason for this trend is most likely due to the influence of the canopy resistance term.

Since the PM model assumes that the entire surface conforms to the "big-leaf" analogy, it is assuming that the total surface resistance is described by the canopy resistance as calculated in equation 3.25. However, figure 4.2 shows that r_c is highly sensitive to small values of LAI. Since the minimum LAI for the site for the three simulated days was 0.11, r_c often exceeded 1000 sm^{-1} which substantially lowered the predicted Q_e (figure 4.3). However, since there is evaporation from the surface, the canopy resistance cannot be a true representative of total surface resistance. In fact, when the PM model is rearranged and solved for r_c using the measured Q_e values, the resulting resistance is the total representative surface resistance of the site and is much lower than r_c (figure 4.4). In this light, the "big-leaf" analogy is not applicable and the PM model is not a useful approach to estimating true wetland evaporation.

The diurnal pattern of predicted Q_e follows the general trend of measured Q_e for all three days, where both approaches produce a relatively small Q_e on the day with the smallest proportion of surface water (July 8) and a larger value on the wetter days. The best simulated day by the PM model was July 25, on which the predicted evaporation reached its maximum for the three days. Not surprisingly, the peak in the morning corresponds to the lowest values of canopy resistance for the measurement period (figure 4.3B). This pattern demonstrates that the PM model is highly sensitive to

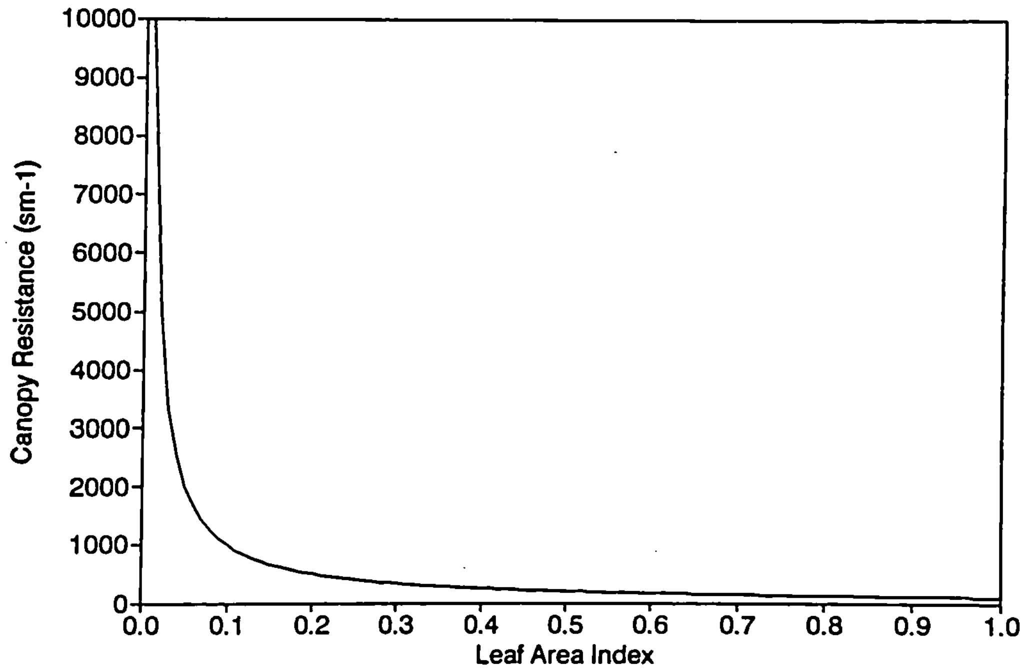

Figure 4.2 Sensitivity of canopy resistance to LAI using equation 3.25 with a constant value of r_{st} of 100 sm^{-1}.

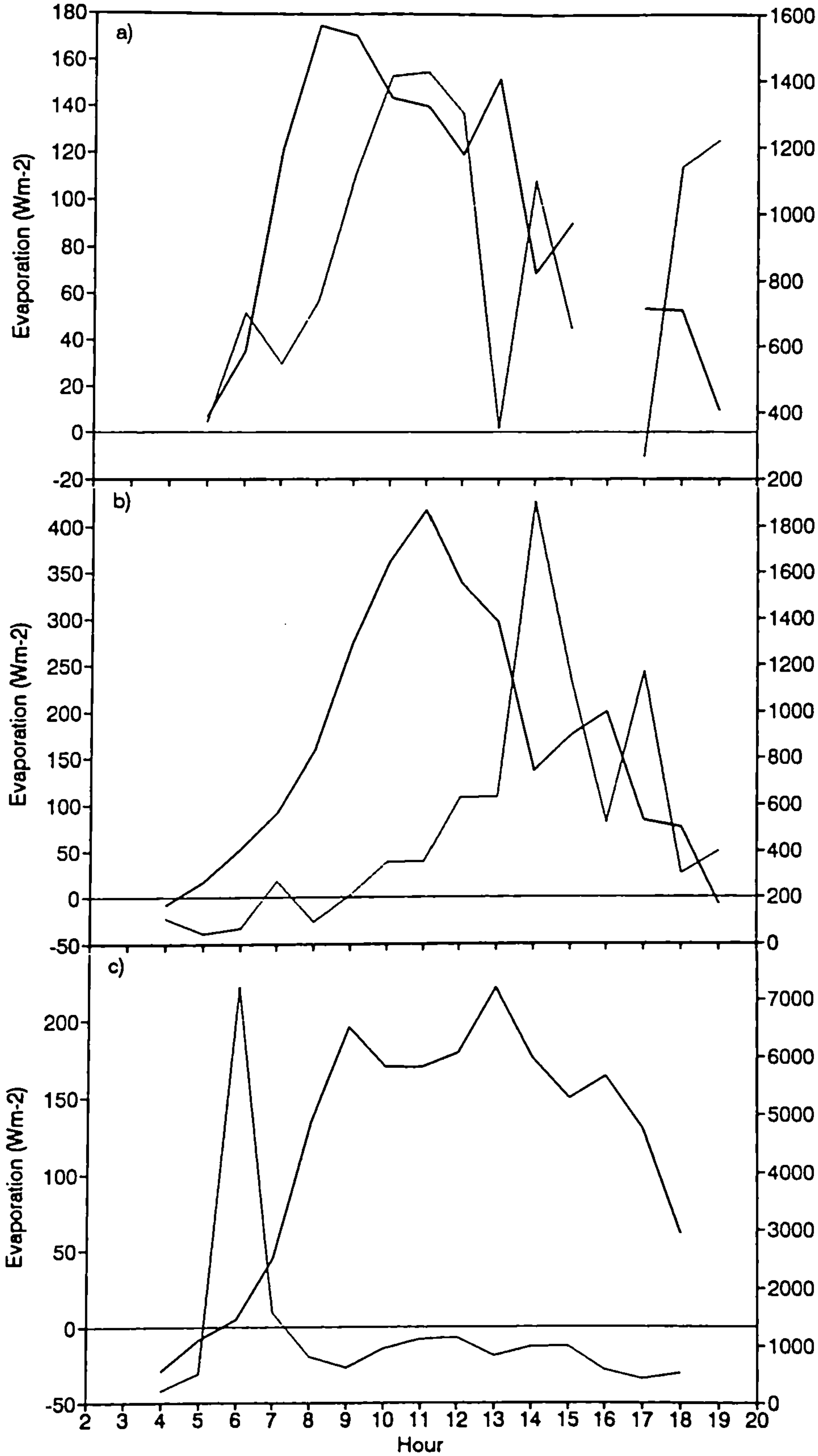

Figure 4.3 Daily trends of evaporation (solid) and canopy resistance (dotted) from the PM model for a) July 8, b) July 25 and c) August 4.

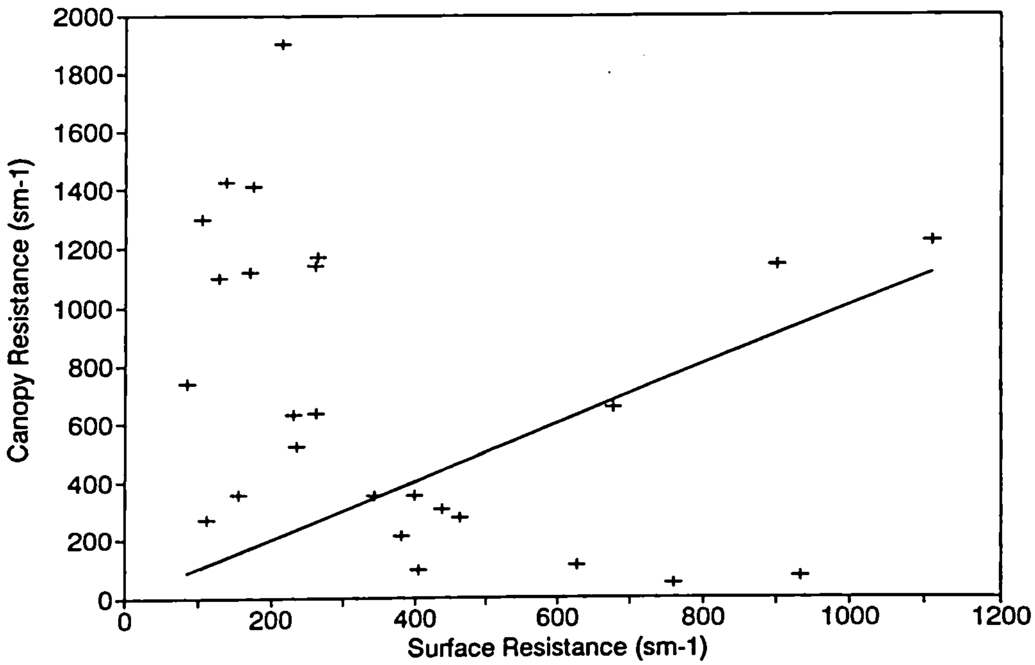

Figure 4.4 Comparison of canopy resistance to surface resistance for the three days from the hourly comparison. The line is 1:1.

the physiological resistances. This strong dependence is disadvantageous if the model is used for surfaces where the canopy is a minor component of the evaporative stream.

4.3.2 The SW Model

In all respects, the SW simulation clearly gave the worst results of the four models. On average, predicted evaporation underestimated the observed values by more than 50%. The SW model consistently underestimated the PM model as well, which is conceptually unrealistic considering that the former deals with a canopy component only whereas the latter adds to this an additional component for soil/water. In addition to this, the SW model gives a much smaller response than the PM model to the proportion of surface water, with SW total evaporation showing little variation throughout the three days. As with the PM model, the unknown surface resistance is the most likely source of error in the SW simulation. Problems with the concept of the model are related to this and will also contribute to the error.

In both the SW and MSW models, the soil evaporation component PM_s was subjected to a constant surface resistance of 500 sm^{-1}. This might be a reasonable approximation for the MSW model, which shows better results, but it is almost certainly too high for the SW model. This would be expected considering that PM_s in the MSW model only represents bare soil whereas PM_s in the SW model represents a combined bare soil/open water component. This forces the SW model to assume that open water and bare soil evaporate at the same rate and that they both have the same constant surface resistance of 500 sm^{-1}. This is an obviously unreasonable assumption considering that open water has essentially no surface resistance and would therefore evaporate more freely than bare soil under the same climatological conditions.

For partial canopy applications, the apparent response of the SW model to r^s_s is largely determined by the soil/water component since the contribution to the total Q_e by the vegetation is often small (figure 4.5A). As a result, the total evaporation stream will be highly dependent on the sensitivity of the soil/water component to the meteorological and surface conditions.

4.3.3 The MSW Model

The MSW model provides the best simulation of the four models for the driest day (July 8) but underestimates measured evaporation for the wettest day (July 25). In addition to this, the morning periods of each day show a much more accurately simulated Q_e than the afternoon periods (table 4.2), when the model tends to overestimate the measured evaporation. The source of error is in the response of the water component, which is the main contributor to the total predicted Q_e (figure 4.5B).

The overestimation of Q_e in the afternoon periods of

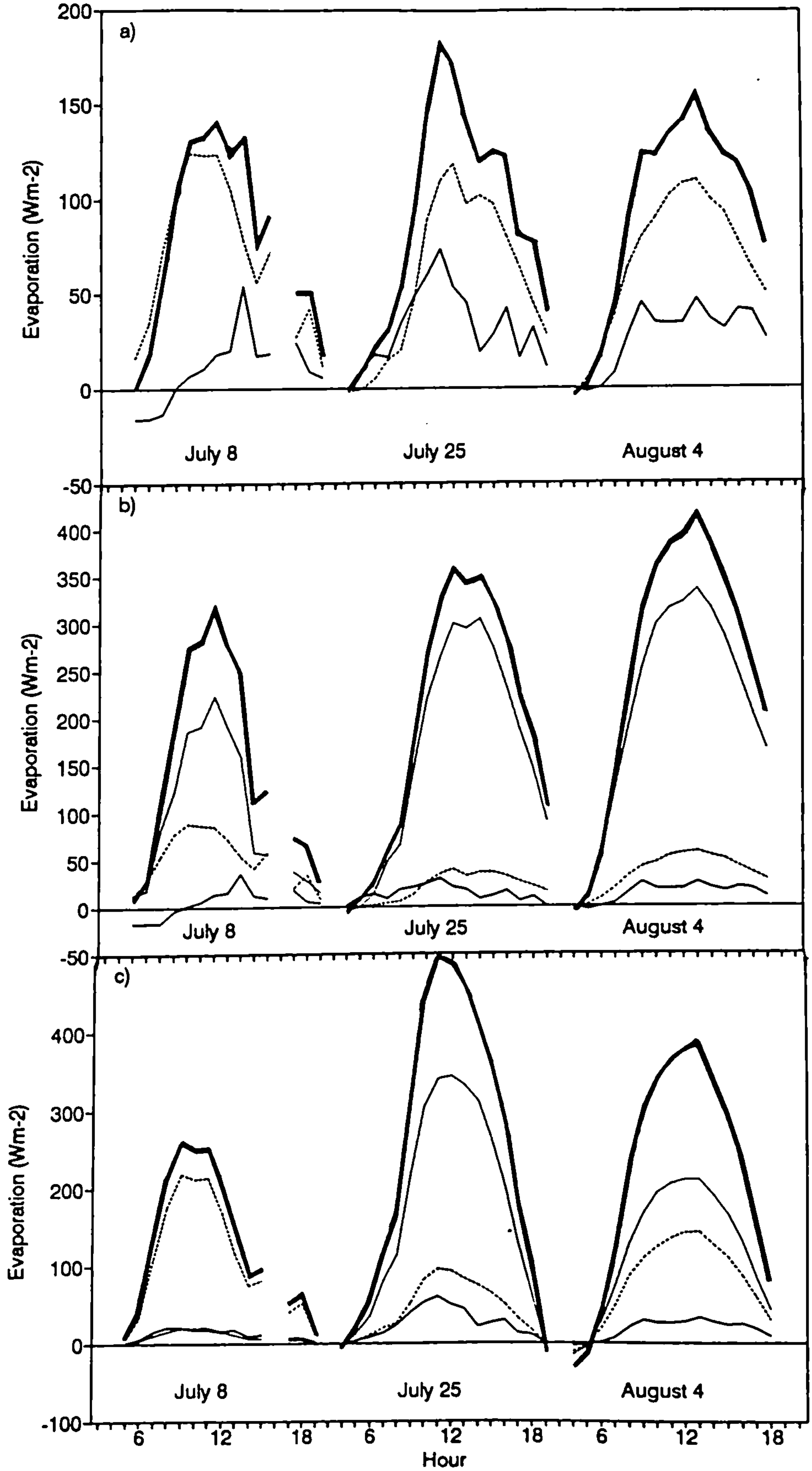

Figure 4.5 Comparison of total Q_e (heavy solid) to Q_{ec} (solid), Q (dashed) and Q_{ew} (dotted) for a) the SW model, b) the MSW model ar c) the WPM model from the hourly comparison.

Day	Period	N	RMSE	MBE	OBS	PRED	d_i
Jul 8	3:30-12:00 12:00-19:00	9 6	43.3 47.4	-33.0 33.0	201.6 77.8	168.6 110.8	0.97 0.84
Jul 25	4:00-12:00 12:00-19:00	9 7	69.5 78.4	-47.7 37.3	194.7 222.4	147.0 259.7	0.95 0.89
Aug 4	4:00-12:00 12:00-20:00	9 7	33.7 89.8	12.3 76.5	201.1 205.9	213.4 282.4	0.99 0.91
All	3:30-12:00 12:00-20:00	27 20	51.1 75.2	-22.8 49.7	199.1 173.2	176.3 222.9	0.97 0.92

Table 4.2 Evaluation of MSW model performance for the morning and afternoon of July 8, July 25, August 4 and the entire three day period. OBS and PRED refer to the means of the observed and predicted values, N refers to the total number of hours simulated and d_i is the index of agreement. All values except N and d_i are in Wm^{-2}.

all three days indicates a prominent diurnal pattern of surface resistance. This is expected since surface resistance is strongly responsive to the vapour pressure deficit (Rouse et al, 1992), which has an obvious diurnal pattern. In this case, r^s_s would be expected to be close to a minimum when D_x is relatively small and Q_e approaches a maximum, which is commonly in the late morning of each day. As a result, the overestimation in the afternoons could be due to an underestimation of the actual r^s_s when employing the constant value which was assumed in the simulation.

However, this cannot be the only reason for the overestimation since r^s_s primarily affects soil evaporation, which is a relatively minor component in the MSW model for the three simulated days. A more likely explanation can be found in the comparison of the diurnal trends of the measured and modelled Q_e with the trends in available energy and vapour pressure deficit. Figure 4.6A shows that measured Q_e follows available energy closely for each day whereas the modelled Q_e tends to overestimate both measured Q_e and AE in the afternoon. Instead, modelled Q_e tends to respond to vapour pressure deficit, which peaked in the late afternoon on the wetter days when the model overestimated measured Q_e (figure 4.6B). Indeed, the MSW model is much more sensitive to changes in D_x than in AE (figures 4.7 and 4.8). However, the response of total modelled Q_e ranges from a sensitivity to AE on the driest day to a sensitivity to D_x on the wetter days.

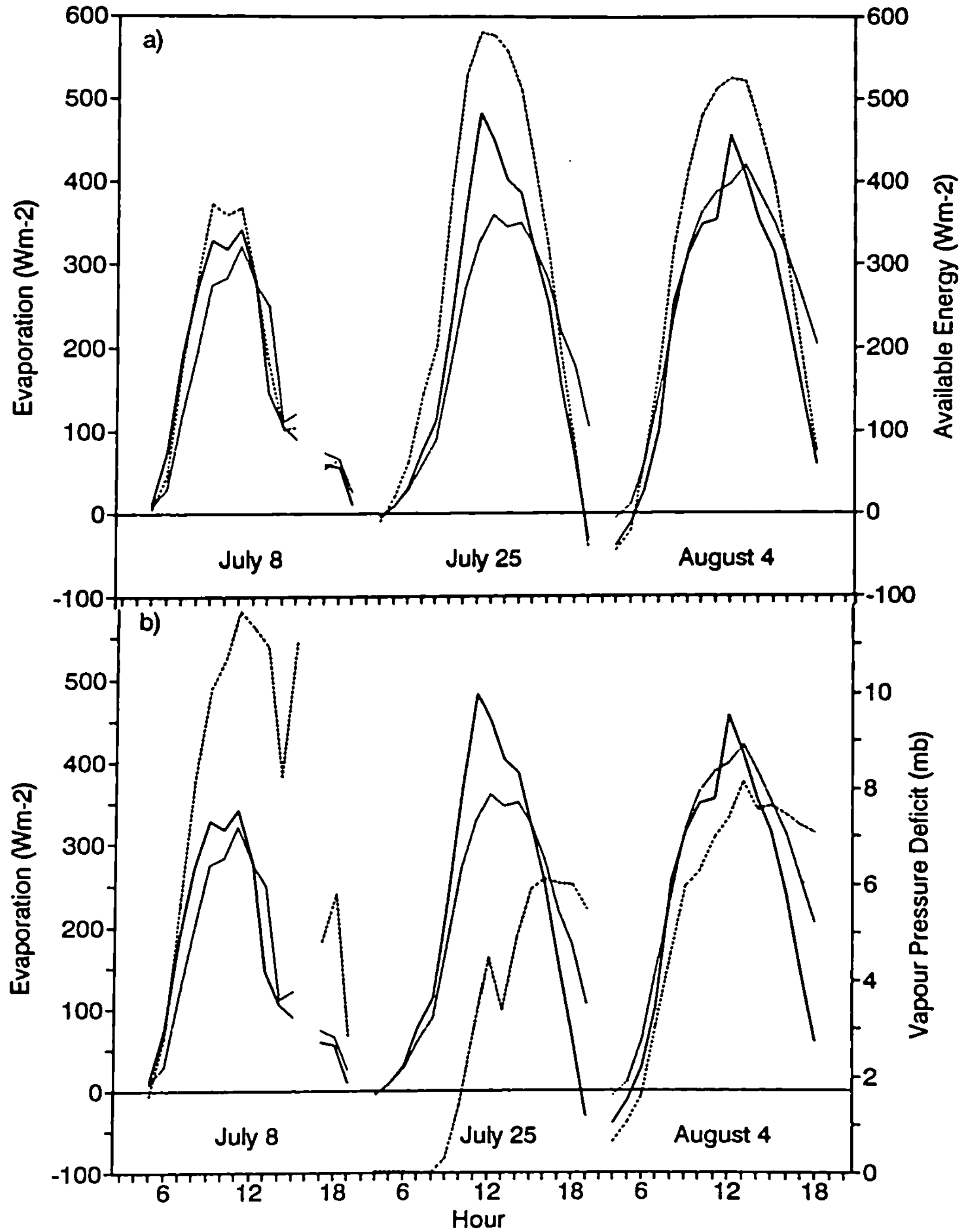

Figure 4.6 Measured Q_e (solid) and modelled Q_e from the MSW model (dotted) plotted against a) available energy and b) vapour pressure deficit (both dashed).

This seems to indicate that the presence of water can have a substantial effect on the source of the sensitivity of the model since the Q_{ew} term increases its effect on total Q_e as the proportion of surface water increases.

As a result, the behaviour of the measured Q_e tends to follow the typical pattern for grassland surfaces as first suggested by McNaughton and Jarvis (1983). They suggested that the grassland environment was typically poorly coupled to the atmosphere, which meant that the evaporation from the canopy was closely linked to net radiation. The opposite was true for a forest canopy, which was found to be closely linked to the vapour pressure deficit. Thus, the MSW total evaporation is in contrast with McNaughton and Jarvis (1983). However, in a comparison of atmospheric coupling between tundra and forest, LaFleur et al (1992) found that wet tundra had a higher sensitivity than forest to vapour pressure deficit, which they attributed to small canopy Q_e in the latter. This suggests that atmospheric coupling can vary widely between the two extremes of sensitivity. This is supported by LaFleur and Rouse (1988) who found that three wetland surfaces ranged from being moderately coupled to very poorly coupled to the atmosphere during the growing season. These results tend to add credibility to the results of the MSW model simulation.

4.3.4 The WPM Model

The modelled Q_e as simulated by the WPM model gives the lowest error and closest overall agreement to measured Q_e. This is especially evident for the August 4 simulation, where the average measured and modelled Q_e agreed to within 4 Wm^{-2}. The worst simulated day was the driest day, where the model underestimated total Q_e.

In conceptual terms, the WPM model would be expected to give virtually the same simulation as the MSW model, considering that these are two Penman-Monteith type models which place the most emphasis on the apparently dominant water evaporation term. However, the main difference between the two models is in the methods of partitioning the individual evaporation components using surface area. The MSW model partitions the components through the AE term, with the results showing that water evaporation was the dominant component on all three days. This was even evident on the driest day, when water covered only 5% of the surface. The WPM model partitions the components directly through evaporation, so that the results of each component Q_e are inherently more credible (figure 4.5C), with soil Q_e being substantial when bare soil is the dominant surface type. Thus, the dominance of the WPM soil term on July 8 caused the total Q_e to underestimate that of the MSW model, which placed more emphasis on the water term during dry periods. On July 25, water covered 63% of the surface and both models simulated high water evaporation. However, the WPM model showed a higher contribution of soil Q_e than the MSW model and provided a better overall diurnal simulation.

The WPM model only slightly overestimated measured Q_e in the late afternoon periods. As with the MSW model, this overestimation is most likely due to the high sensitivity of the model to vapour pressure deficit (figure 4.8). However, the WPM model is more sensitive to AE than the MSW model (figure 4.7), which would be expected to reduce the degree of overestimation by the former.

4.4 Determination of Optimal Surface Resistance

The main difficulty in determining the potential sources of error in the daily comparison is due to the effect of the unknown surface resistance in each model. Surface resistance is a vitally important variable which must be determined accurately, especially when considering partial canopies (Shuttleworth and Wallace, 1985). Since this resistance is a limiting variable in each model, it is necessary to determine a more representative surface resistance than the assumed 500 sm^{-1} before any seasonal simulations are attempted. The inability to calculate or measure this resistance means that it must remain constant throughout each simulation. It is also imperative to determine the sensitivity of each model to surface resistance, which will be examined in a later section.

The determination of the optimal surface resistances for each model was done using the data from the daily simulations. Optimal values were found for each day as well as for the entire three day period and are shown in table 4.3. The values of r_s from the PM model and r^s_s from the SW, MSW and WPM models were found in each case by adjusting the value of surface resistance until the model simulated the measured Q_e with the lowest possible mean bias error.

The optimal r^s_s values for the SW model represent the surface resistance of the combined soil/water term. As a result, they are lower than the r^s_s of soil for the MSW and WPM models and much lower than the previously assumed value of 500 sm^{-1} (table 4.3A). The optimal value used in the daily simulations for the SW model was assumed to be 51 sm^{-1}, which represents the value for the entire three day period.

The optimal values would be expected to reflect the moisture conditions of the surface. This is best demonstrated in the SW model by the fact that the lowest value of r^s_s occurred on July 25, the wettest of the three days. However, July 8 had only the second highest r^s_s, even though it was the driest day. The daily average vapour pressure deficits suggest that July 8 should have the highest surface resistance. However, the slightly lower value of r^s_s on July 8 could have been an indirect result of a small rain event which occurred during the mid-afternoon of this day. The 1 mm of rain which fell onto the drying soil might have temporarily

	Day	OBS	PRED	RMSE	MBE	r^s_s
a)	Jul 8	152.1	152.2	36.5	0.10	59
	Jul 25	206.8	206.8	67.5	0.01	10
	Aug 4	203.2	203.2	57.6	0.02	78
	All	188.1	188.1	57.9	0.02	51
b)	Jul 8	152.1	152.1	43.1	0.01	363
	Jul 25	206.8	206.8	71.9	-0.02	190
	Aug 4	203.2	220.0	59.6	16.8	∞
	All	188.1	188.1	63.5	-0.01	910
	Jul 8 Jul 25	180.3	180.3	59.9	0.01	287
c)	Jul 8	152.1	152.1	17.5	0.02	133
	Jul 25	206.8	206.8	18.3	0.05	324
	Aug 4	203.2	203.3	22.8	0.06	249
	All	188.1	188.2	21.7	0.05	251
d)	Jul 8	152.1	152.1	18.1	0.04	81
	Jul 25	206.8	206.8	24.6	0.02	4200
	Aug 4	203.2	203.2	23.8	-0.02	451
	All	188.1	188.1	37.5	0.02	472
	Jul 8 Aug 4	178.5	178.5	26.7	0.01	264

	% Water	D_x
July 8	5	7.1
July 25	63	3.0
Aug 4	40	5.4
All	--	5.1

Table 4.3 Comparison of measured Q_e to a) the SW model, b) the MSW model, c) the PM model and d) the WPM model for the determination of optimal surface resistances for July 8, July 25, August 4 and the entire three day period. OBS and PRED refer to the means of the observed and predicted values. All values except D_x and r^s_s are in Wm^{-2}. D_x is in mb and r^s_s is in sm^{-1}.

decreased the surface resistance for a period of time. Indeed, the vapour pressure deficit decreased from 7.8 mb prior to the rain event to 4.5 mb following it.

The optimal r^s_s values for the MSW model represent the resistance for soil only and are much more variable than those for the SW model (table 4.3B). Once again, the wettest day had the lowest r^s_s and, in this case, the driest day had the highest calculated r^s_s. However, the value for August 4 could not be determined as it tended to infinity, which suggested that soil evaporation approached zero. The r^s_s representing all three days was also higher than expected since it far exceeded the 500 sm^{-1} value that Shuttleworth and Wallace (1985) assumed for a drier surface. Neither of these unusually high values can be explained by a small rain event. Instead, they strongly indicate that the error in the modelled Q_e is not due to the unknown surface resistance only. As a result of the undetermined value on August 4, the constant optimal value used in the seasonal simulation for the MSW model was assumed to be 287 sm^{-1}, which represents the optimal r^s_s value for the period which combined July 8 and July 25.

Surface resistance as determined by the PM model represents the combined resistance of all of the surface types. However, the model produced a pattern of r_s which is opposite to the trend expected when related to surface wetness, with the smallest r_s occurring on the driest day instead of on the wettest (table 4.3C). Again, this demonstrates that the sources of model error are not found only in the unknown surface resistance. The optimal value assumed for the seasonal simulation for the PM model is 251 sm^{-1}, which is the value representing the entire three day period.

The optimal r^s_s values for the WPM model showed a high variability from day to day (table 4.3D). As with the PM model, the trend was opposite from that which was expected since the driest day showed the lowest resistance and the wettest day produced the highest. The value representing all three days was only slightly lower than the 500 sm^{-1} assumed in the daily simulations. However, the large r^s_s associated with July 25 far exceeds the typical maximum values for very dry soil. As with the other models, this shows that the model is subject to errors other than the uncertainty in r^s_s. The optimal value of r^s_s which was chosen for the seasonal simulation of Q_e was 264 sm^{-1}, which represents the value for the period which combined July 8 and August 4.

4.5 Sensitivity Analysis

In order to understand the characteristics of a model, the relative role of each variable within the model must be assessed. This requires a sensitivity analysis. The sensitivity of evaporation in each model to an independent variable x_i was determined by keeping all variables other than x_i constant at their mean seasonal values (table 4.4) and a)

AE	116.8	Wm^{-2}
Q^*	126.5	Wm^{-2}
Q_g	9.6	Wm^{-2}
D_x	16.4	mb
T_x	14.4	°C
u_x	3.3	ms^{-1}
u^*	0.3	ms^{-1}
LAI	0.13	
FAI	0.27	
Soil	74.7	%
Water	25.3	%

b)

r_a	58.6	sm^{-1}
r_{bb}	12.9	sm^{-1}
r_s	251	sm^{-1}

c)

r_a	58.6	sm^{-1}
r_{bb}	12.9	sm^{-1}
r_c^s	770.0	sm^{-1}
r_s^s	264	sm^{-1}

d)

AE_c	0.2	Wm^{-2}
Q^*_c	3.6	Wm^{-2}
Q_{gc}	3.4	Wm^{-2}
AE_s	84.5	Wm^{-2}
Q^*_s	87.9	Wm^{-2}
Q_{gs}	3.4	Wm^{-2}
AE_w	32.1	Wm^{-2}
Q^*_w	35.0	Wm^{-2}
Q_{gw}	2.9	Wm^{-2}
r^a_a	43.2	sm^{-1}
r_b	11.0	sm^{-1}
r^c_a	40.5	sm^{-1}
r^c_s	770.0	sm^{-1}
r^s_a	60.5	sm^{-1}
r^w_a	68.4	sm^{-1}
r^s_s	287	sm^{-1}

e)

AE_c	0.2	Wm^{-2}
Q^*_c	3.6	Wm^{-2}
Q_{gc}	3.4	Wm^{-2}
AE_s	116.6	Wm^{-2}
Q^*_s	122.9	Wm^{-2}
Q_{gs}	6.3	Wm^{-2}
r^a_a	43.2	sm^{-1}
r_b	11.0	sm^{-1}
r^c_a	40.5	sm^{-1}
r^c_s	770.0	sm^{-1}
r^s_a	60.5	sm^{-1}
r^s_s	51	sm^{-1}

Table 4.4 Seasonal averages used as constants in the sensitivity analysis for a) all four models, b) the PM model, c) the WPM model, d) the MSW model and e) the SW model. The seasonal average measured Q_e is 92.3 Wm^{-2}.

applying a step change to x_i. This approach has been used frequently in the past with meaningful results and it is best used when the complexity of a model prevents the use of a simpler approach. A simpler method of evaluating sensitivity is through a differentiation of the model, which is a process that has been well documented for the Penman equation and the PM model (McCuen, 1974; Saxton, 1975; Beven, 1979).

However, both of these approaches have a limited representation of reality since the evaporation response to a changing x_i is assumed to be independent of feedbacks from other variables in the model. For example, the changes in wind speed and vapour pressure deficit as a result of a change in temperature are ignored since u_x and D_x are held constant. In addition to this, any transient responses of the unperturbed variables while steady state is reachieved are not considered. As a result, recent research has attempted to account for feedbacks from the surface and planetary boundary layers in a sensitivity analysis for the PM model (Jacobs and De Bruin, 1992). However, for the sake of brevity, only the non-feedback, non-derivative approach is used in this study.

4.5.1 Available Energy

Since available energy is one of the main driving variables in each model, the sensitivity of Q_e to changes in AE must be determined.

The sensitivity of total Q_e to available energy is virtually the same for the PM and WPM models (figure 4.7). This is not surprising considering that the WPM model simply consists of three components with the Penman-Monteith format and that all the components are driven by AE in the same manner. Since it has been shown in the past that the PM model is very sensitive to changes in Q^* (Beven, 1979) and Q^* is the predominant variable in the calculation of AE, it follows that any AE perturbations or errors can cause important fluctuations in Q_e.

The sensitivity of evaporation to changes in AE is similar for the SW and MSW models but lower than that for the PM and WPM models. The similarity between the SW and MSW sensitivities indicates that the effect of AE on Q_e was maintained throughout the derivation of the MSW model from the original SW model. However, it follows that the derivation of the SW model from the PM model did not maintain the same degree of sensitivity.

As a result, the lower sensitivity of both the SW and MSW total evaporation as compared to that of the PM and WPM models indicates that sensitivity is dampened when AE is partitioned among the Q_e components. Table 4.5 shows that for the WPM model, the sensitivity of each component Q_e is virtually the same as the sensitivity of the total Q_e. However, for the SW and MSW models, the individual sensitivities of the components are variable, with the highest sensitivity belonging to Q_{ec} and the lowest belonging to Q_{es}.

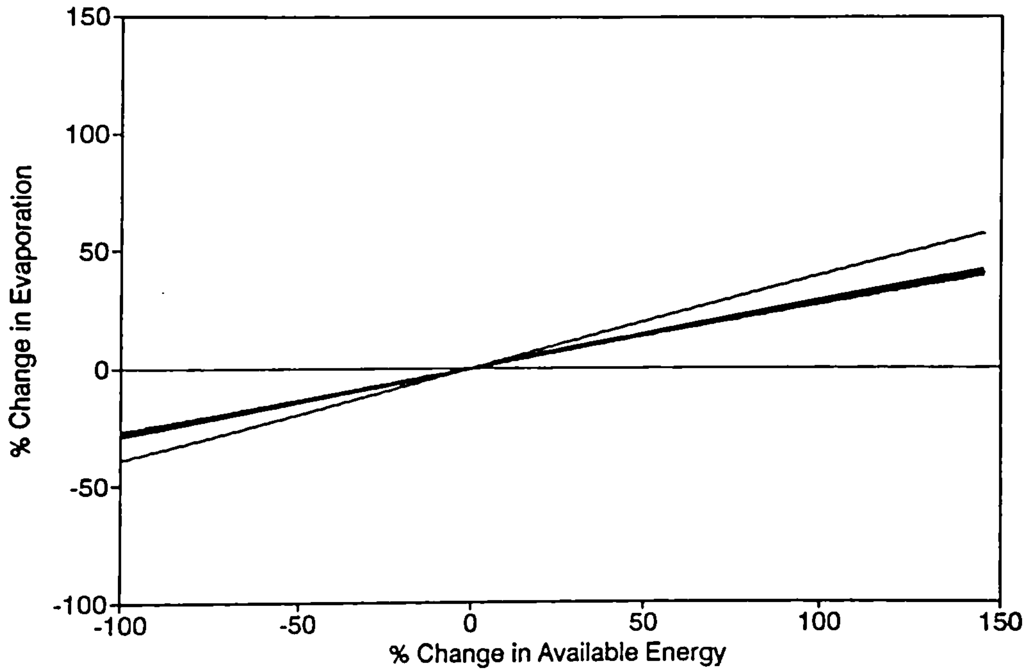

Figure 4.7 Sensitivity of modelled Q_e to changes in available energy for the PM model (solid), the WPM model (dashed), the SW model (dotted) and the MSW model (heavy solid). Q_e from the PM and WPM models overlap for the entire range of AE.

	AE	ΔAE	Q_e	Q_{ec}	Q_{es}	Q_{ew}
a)	116.8	1 x	51.1			
	233.6	2 x	71.2 (39.3)			
	58.4	½ x	41.0 (-19.8)			
b)	116.8	1 x	80.5	5.2	28.9	46.4
	233.6	2 x	112.2 (39.4)	7.3 (40.4)	40.3 (39.4)	64.6 (39.2)
	58.4	½ x	64.5 (-19.9)	4.2 (-19.2)	23.2 (-19.7)	37.1 (-20.0)
c)	116.8	1 x	118.7	9.5	109.2	
	233.6	2 x	150.6 (26.9)	19.7 (107.4)	130.9 (19.9)	
	58.4	½ x	102.6 (-13.6)	4.4 (-53.7)	98.2 (-10.1)	
d)	116.8	1 x	127.8	8.7	38.1	81.0
	233.6	2 x	163.1 (27.6)	12.0 (37.9)	46.6 (22.3)	104.5 (29.0)
	58.4	½ x	110.0 (-13.9)	7.0 (-19.5)	33.9 (-11.0)	69.1 (-14.7)

Table 4.5 Sensitivity of a) the PM model, b) the WPM model, c) the SW model and d) the MSW model to halving and doubling of AE. The numbers in the brackets are the % change of Q_e from the unperturbed value. All values are in Wm^{-2}.

Since the Q_{es} flux is a predominant component of the total evaporation stream in these two models, its lower sensitivity to AE will have a large weighting in the total Q_e sensitivity.

4.5.2 Vapour Pressure Deficit

The second driving variable is the vapour pressure deficit at the reference height, D_x. Figure 4.8 shows that the sensitivity of Q_e to D_x is similar for all of the models, with slightly lower responses in the SW and MSW models.

The sensitivities of Q_e to D_x for the PM and WPM models are exactly the same (table 4.6). Following the same reasoning as with the sensitivity to available energy, this trend would be expected since each component of the WPM model is in a Penman-Monteith format. In each case, D_x is used in the same manner to calculate Q_e.

In the SW model, Q_e has a distinctly lower response to changes in D_x than the PM and WPM models. This is most likely due to a dampening of the sensitivity of the Q_{es} component as a result of the soil resistance. Since Q_{es} is the dominant component of the model, the strong influence of r^s_s will act to reduce total evaporation even with an increase in D_x. This reasoning can also be applied to the MSW model, which also shows a lower sensitivity to D_x in its Q_{es} term. However, since Q_{es} in the MSW model involves only soil, r^s_s has a lower influence on total Q_e and the dampening effect will not be as evident.

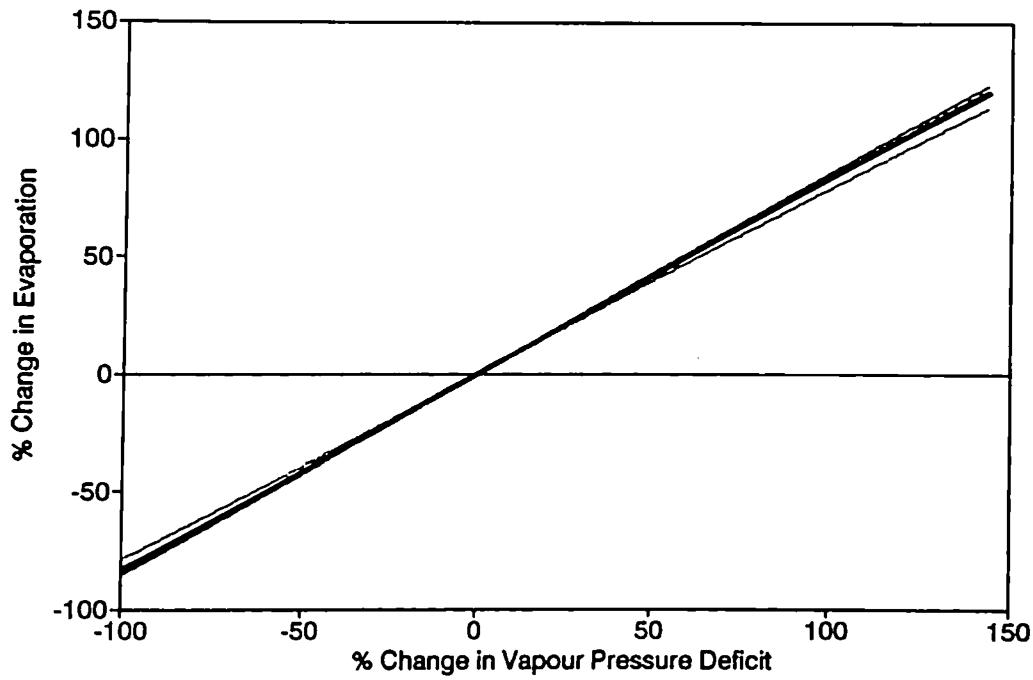

Figure 4.8 Sensitivity of modelled Q_e to changes in vapour pressure deficit for the PM model (solid), the WPM model (dashed), the SW model (dotted) and the MSW model (heavy solid). Q_e from the PM and WPM models overlap for the entire range of D_x.

	D_x	ΔD_x	Q_e	Q_{ec}	Q_{es}	Q_{ew}
a)	16.4	1 x	51.1			
	32.8	2 x	94.9 (85.7)			
	8.2	½ x	29.2 (-42.8)			
b)	16.4	1 x	80.5	5.2	28.9	46.4
	32.8	2 x	149.5 (85.7)	9.7 (85.7)	53.7 (85.7)	86.2 (85.7)
	8.2	½ x	46.0 (-42.8)	3.0 (-42.8)	16.5 (-42.8)	26.5 (-42.8)
c)	16.4	1 x	118.7	9.5	109.2	
	32.8	2 x	212.5 (79.0)	18.8 (97.6)	193.0 (76.7)	
	8.2	½ x	71.8 (-39.5)	4.9 (-48.4)	67.4 (-38.3)	
d)	16.4	1 x	127.8	8.7	38.1	81.0
	32.8	2 x	235.4 (84.2)	16.9 (94.2)	67.5 (77.1)	150.5 (85.8)
	8.2	½ x	74.0 (-42.1)	4.6 (-47.1)	23.4 (-38.6)	46.3 (-42.9)

Table 4.6 Sensitivity of a) the PM model, b) the WPM model, c) the SW model and d) the MSW model to halving and doubling of D_x. The numbers in the brackets are the % change of Q_e from the unperturbed value. All values are in Wm^{-2} except D_x which is in mb.

The absence of feedbacks in the sensitivity analysis of Q_e with D_x is very evident, especially in the SW, MSW and WPM models. By holding r^s_s and r^c_s constant while increasing D_x, it is assumed that there is no surface response to the perturbation. In reality, this is not the case. If D_x is increased, an increase in Q_e from the soil would be expected to be dampened by an increase in r^s_s as the soil dries, unless the supply of water to the soil is nonlimiting. Similarly, the stomata within the canopy components will tend to close, thus increasing r^c_s, in response to an increased loss of Q_e (Choudhury and Monteith, 1986). However, this is not applicable to the water components of the MSW and WPM models since no surface resistance is available to counteract the increased evaporation.

4.5.3 Surface Resistance

The sensitivity of Q_e to changes in surface resistance is non-linear in all four models and is substantial when r_s and r^s_s are decreased from their reference values (figure 4.9). The reference surface resistances that were used in the sensitivity analysis were the optimal values which were determined from the hourly comparison of the four models and which will be used in the daily comparison. As a result, the PM model was tested with a reference r_s value of 251 sm^{-1} and the SW, MSW and WPM models had reference r^s_s values of 51, 287 and 264 sm^{-1}, respectively. The reduction by 100% of any of

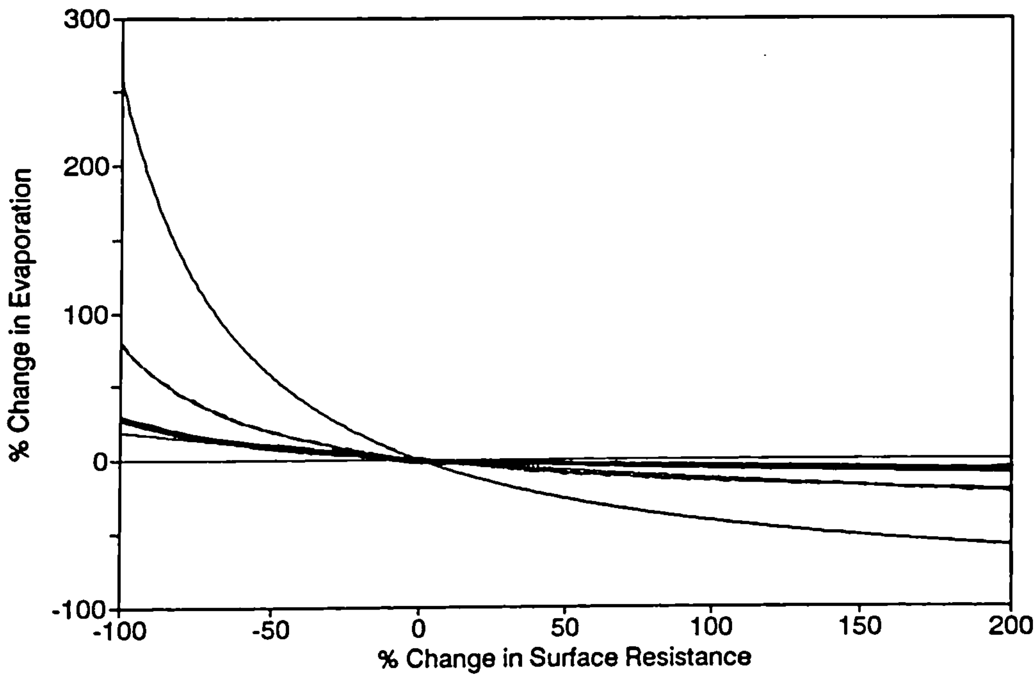

Figure 4.9 Sensitivity of modelled Q_e to changes in surface resistance for the PM model (solid), the WPM model (dashed), the SW model (dotted) and the MSW model (heavy solid). The surface resistance is represented by r_s for the PM model and by r^s_s for the WPM, SW and MSW models.

these values means that the surface resistance is zero.

All four models showed a small sensitivity to large surface resistance. In physical terms, this demonstrates that a critical point can be reached where evaporation is approaching a minimum and is hardly affected by any further increase in surface resistance. For the vegetation component, this point is reached under conditions when the stomata have essentially closed and restriction to transpiration is largest (Jarvis and Morison, 1981; Choudhury and Monteith, 1986). For bare soil, the critical point occurs when the soil has dried and is no longer supplied with moisture from deeper layers in the substrate.

The PM model showed the largest sensitivity to changes in r_s. However, since r_s represents the combined resistance of all of the surface types of a complex surface, it is difficult to determine the effect of the perturbation in physical terms. This is when the differentiation method of sensitivity analysis becomes advantageous. By using this method in their analysis of sensitivity without feedbacks, Jacobs and De Bruin (1992) showed that the sensitivity of Q_e to surface resistance in the PM model was dependant on temperature and on the ratio of r_a/r_s. These variables indirectly affect r_s through their effect on evaporation. High temperature conditions tend to increase evaporation, which then forces an increasing surface resistance to take place within the soil and vegetation components. High wind speeds create a low r_a, which then increases evaporation and, hence, surface resistance increases.

The relatively low sensitivity of total Q_e to r^s_s in the SW and MSW models is not due as much to the response of the soil component as to the opposite response of the water and canopy components (table 4.7). As r^s_s increases and soil evaporation decreases, both the water component in the MSW model and the canopy component in both models show an increase in evaporation. This is a result of the transfer of incident energy on the soil into sensible heat in response to the decrease in soil evaporation. The sensible heat is then used by the water and canopy components to increase evapotranspiration. Shuttleworth and Wallace (1985) also found that the transpiration of sparse crops can be altered substantially through a change in the surface resistance of the soil substrate and that this sensitivity increases for canopies with low LAI values. This was also supported by Shuttleworth and Gurney (1990), who found that the computation of the bulk stomatal resistance term, r^c_s, was highly complicated by r^s_s at small leaf areas.

The sensitivity of total Q_e to r^s_s in the WPM model is completely dependant on the soil component (table 4.7). This is a result of the complete independence of each component in the model with respect to each other in the calculation. The WPM model assumes that any interaction between the components takes place indirectly in the measured AE and D_x terms. This

	r^s_s	Δr^s_s	Q_e	Q_{ec}	Q_{es}	Q_{ew}
a)	251	1 x	51.1			
	502	2 x	29.7 (-41.9)			
	126	½ x	79.9 (56.4)			
b)	264	1 x	80.5	5.2	28.9	46.4
	528	2 x	68.7 (-14.7)	5.2 (0.0)	17.1 (40.8)	46.4 (0.0)
	132	½ x	95.7 (15.2)	5.2 (0.0)	44.1 (52.6)	46.4 (0.0)
c)	51	1 x	118.7	9.5	109.2	
	102	2 x	103.3 (-13.0)	10.9 (14.7)	92.4 (-15.4)	
	26	½ x	128.7 (8.4)	8.6 (-9.5)	120.1 (10.0)	
d)	287	1 x	127.8	8.7	38.1	81.0
	574	2 x	119.4 (-6.6)	9.4 (8.0)	23.7 (-37.8)	86.3 (6.5)
	144	½ x	137.5 (7.6)	7.8 (-10.3)	54.9 (44.1)	74.8 (-7.7)

Table 4.7 Sensitivity of a) the PM model, b) the WPM model, c) the SW model and d) the MSW model to halving and doubling of surface resistance. The numbers in the brackets are the % change of Q_e from the unperturbed value. All values are in Wm^{-2} except r^s_s which is in sm^{-1}.

relationship can be determined through a sensitivity analysis involving feedbacks. Otherwise, the lack of response by the water and canopy components can be considered to be unrealistic and is an important misrepresentation to be considered in any practical application of the model.

4.5.4 Aerodynamic Resistances

The sensitivity of Q_e to the aerodynamic resistances for all four models is depicted in figure 4.10. In every case, the sensitivity is low when the aerodynamic resistance is increased from its seasonal average value. With the exception of the WPM and MSW models, a similarly low sensitivity is found when the resistance is decreased. The substantially higher Q_e change with low resistance in the WPM and MSW models is the result of a lack of surface resistance in the Q_{ew} components.

The low overall sensitivity of Q_e to r_a in the PM model has been well established for forest (Tan and Black, 1976) and for crop (Bailey and Davies, 1981a). Tan and Black (1976) found that Q_e from a Douglas fir forest was essentially independent of r_a when the surface was aerodynamically rough and the ratio of r_s/r_a was large. Using this reasoning in the sensitivity analysis of the present study, a constant value of r_s of 251 sm^{-1} with r_a varying from 1 to 150 sm^{-1} tended to provide a small sensitivity within the PM model. This is supported by Bailey and Davies (1981a), who found that the

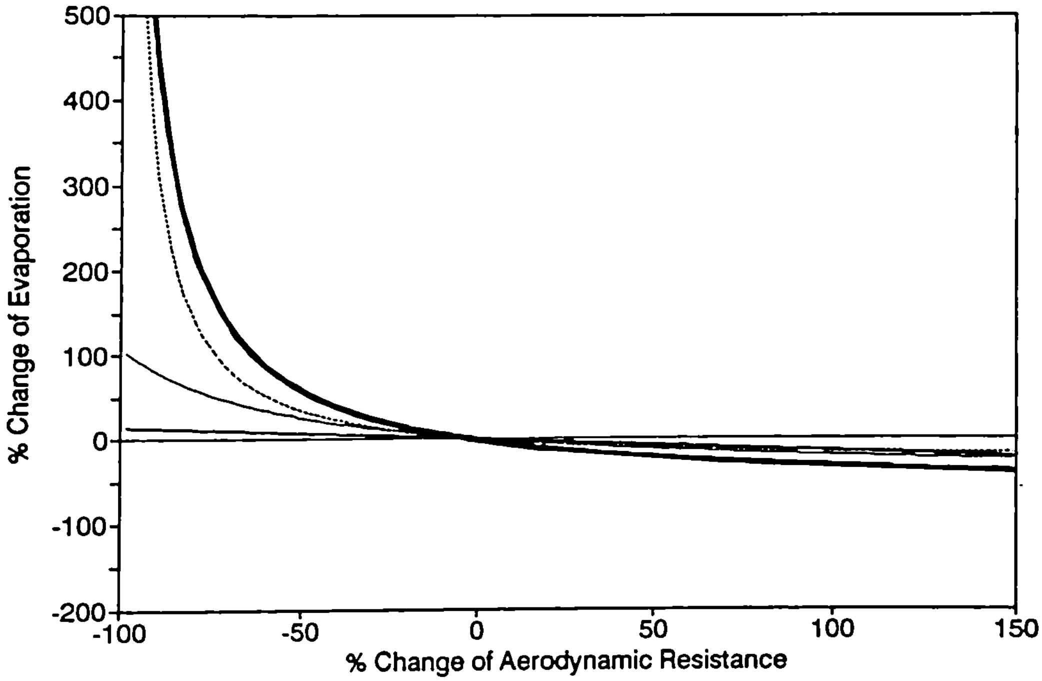

Figure 4.10 Sensitivity of modelled Q_e to changes in aerodynamic resistance for the PM model (solid), the WPM model (dashed), the SW model (dotted) and the MSW model (heavy solid). The aerodynamic resistance is represented by r_a for the PM and WPM models and by r^a_a for the SW and MSW models.

sensitivity was low for a soybean crop even under conditions of small values of r_c/r_a.

The high sensitivity of the WPM and MSW total Q_e to small values of aerodynamic resistance is unusual in light of the Penman-Monteith format of the model. The response of total Q_e in both models is strongly dependant on the Q_{ew} term (table 4.8), which assumes the form of a Penman potential evaporation equation with zero surface resistance. In effect, small values of aerodynamic resistance in combination with a lack of surface resistance leaves no restriction over the evaporation of water. The result of the aerodynamic resistance approaching zero is the forcing of Q_e to approach infinity. However, this does not represent reality and is an obvious flaw in the sensitivity analysis, since feedback of vapour pressure deficit is not considered. The expected climatological response to a decrease in aerodynamic resistance and an increase in Q_e is an increase in vapour pressure which would cause a negative feedback from the resulting decrease in D_x.

The dependence of the sensitivity of aerodynamic resistance to surface resistance is shown in figure 4.11. For both the WPM and MSW models, sensitivity was determined with an arbitrary water surface resistance value, which was held constant at 10 sm^{-1} in the Q_{ew} equations. The slight increase of surface resistance substantially decreased the sensitivity of Q_e to low values of aerodynamic resistance.

	r^a_a	Δr^a_a	Q_e	Q_{ec}	Q_{es}	Q_{ew}
a)	58.6	1 x	51.1			
	117.2	2 x	42.7 (-16.5)			
	29.3	½ x	54.8 (7.3)			
b)	58.6	1 x	80.5	5.2	28.9	46.4
	117.2	2 x	68.6 (-14.8)	6.4 (23.5)	30.7 (6.3)	31.9 (-31.3)
	29.3	½ x	109.2 (35.6)	4.5 (-13.7)	27.5 (-4.9)	76.3 (64.4)
c)	43.2	1 x	118.7	9.5	109.2	
	86.4	2 x	95.0 (-20.0)	8.2 (-14.0)	86.9 (-20.4)	
	21.6	½ x	163.3 (37.6)	10.7 (13.0)	138.7 (27.0)	
d)	43.2	1 x	127.8	8.7	38.1	81.0
	86.4	2 x	88.1 (-31.1)	8.4 (-3.7)	42.7 (12.2)	47.0 (-42.0)
	21.6	½ x	207.3 (62.2)	8.7 (0.0)	34.9 (-8.4)	146.5 (80.9)

Table 4.8 Sensitivity of a) the PM model, b) the WPM model, c) the SW model and d) the MSW model to halving and doubling of aerodynamic resistance. The numbers in the brackets are the % change of Q_e from the unperturbed value. All values are in Wm^{-2} except r^a_a which is in sm^{-1}.

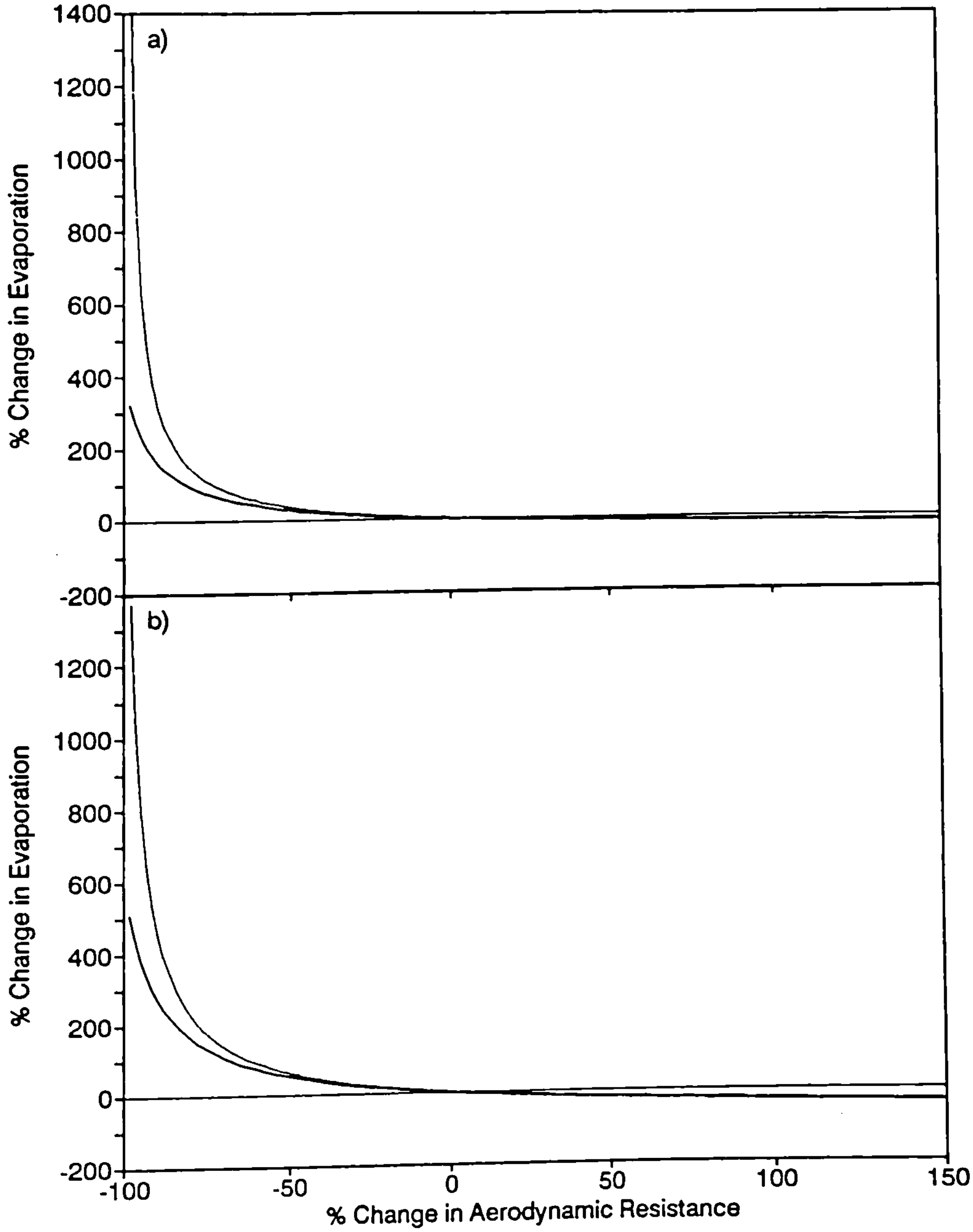

Figure 4.11 Sensitivity of modelled Q_e to a change in aerodynamic resistance for a) the WPM model and b) the MSW model, with no water surface resistance (dotted) and a resistance of 10 sm^{-1} (solid).

In the SW model, the high sensitivity of Q_e to low r^a_a is also the result of a low surface resistance. However, the sensitivity is much lower than that in the WPM and MSW models since the SW surface resistance represents a combined soil/water component and is greater than zero.

4.5.5 Bulk Stomatal Resistances

Bulk stomatal resistance was calculated in the WPM, MSW and SW models using equation 3.53 with a constant stomatal resistance and the seasonal average leaf area index. The constant r_{st} was the approximate average value for the three days of porometer measurements. The sensitivity of Q_e to r^c_s in the three models is illustrated in figure 4.12. The PM model was not examined in this analysis since the bulk stomatal resistance was assumed to be included in the total surface resistance term.

All three models showed a small Q_e sensitivity to increases in r^c_s from its reference value. This indicates that the stomata have essentially closed and that any further increase in r^c_s will not affect the total evapotranspiration stream. This trend was also seen in the sensitivity to r^s_s (figure 4.9). However, the high sensitivity of total Q_e at low values of r^c_s corresponds to the high sensitivity of the Q_{ec} components, such that even with small leaf areas the canopy seems to be a strong contributor to total Q_e. In reality, there have been no recorded cases of r^c_s approaching zero in

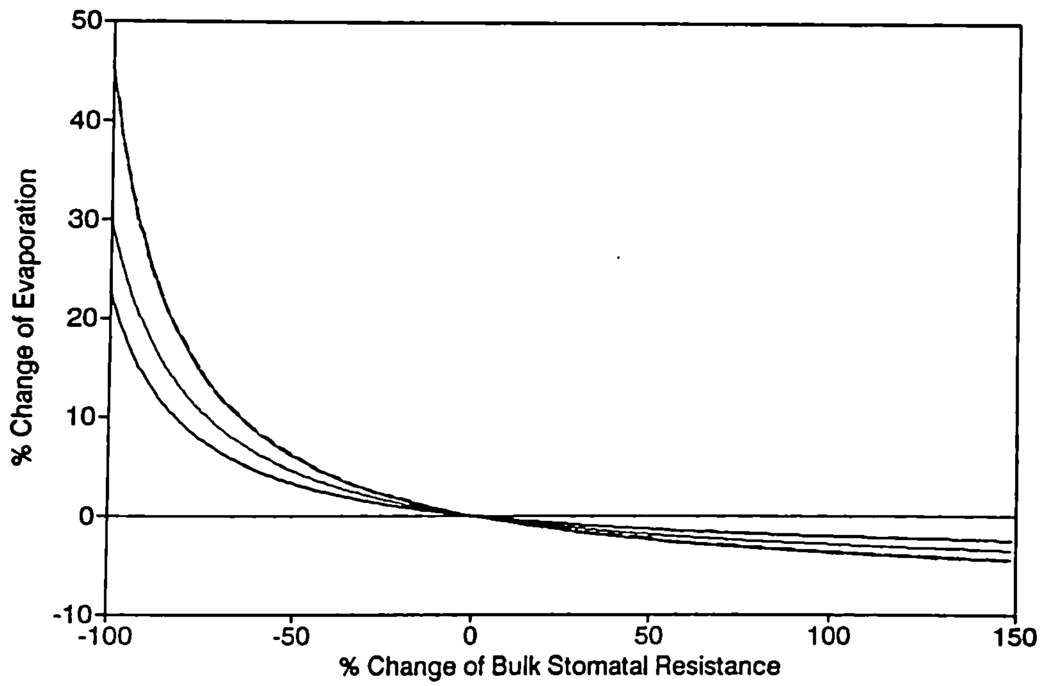

Figure 4.12 Sensitivity of modelled Q_e to changes in canopy resistance for the WPM model (dashed), the SW model (dotted) and the MSW model (heavy solid).

tundra vegetation since there is evidence that these plants have a maximum stomatal conductance (Korner et al, 1979), and therefore a minimum non-zero stomatal resistance. It would also seem unlikely that this situation is unique; maximum stomatal conductance is an established physiological characteristic which is often used as an indicator of maximum transpiration losses and CO_2 uptake (Lafleur, 1988).

The sensitivity of Q_e to r^c_s in the WPM model is only a result of the effect on the canopy component, since the bare soil and open water components are not responsive to the change (table 4.9). However, since the condition of the substrate tends to affect plant contribution to total Q_e, it is unreasonable to assume that the substrate is completely independent of vegetation changes (Waggoner, 1975), even when dealing with small canopies. Changes in transpiration rates due to drying soil can affect the vapour pressure deficit (Jarvis and Morison, 1981) which will then alter the evaporation rates of the surrounding bare soil and open water. In addition to this, increasing bulk stomatal resistance due to increasing D_x will reduce the level of uptake by roots (Rutter, 1975; Kaufmann and Fiscus, 1985) and increase water availability for substrate evaporation. As with the sensitivity analysis with r^s_s, the inability of the WPM model to couple the individual evaporation components together results in a misrepresentation of the true effect of r^c_s on total Q_e.

	r^c_s	Δr^c_s	Q_e	Q_{ec}	Q_{es}	Q_{ew}
a)	770.0	1 x	80.5	5.2	28.9	46.4
	1540.0	2 x	77.4 (-3.8)	2.8 (-47.0)	28.9 (0.0)	46.4 (0.0)
	385.0	½ x	85.2 (5.9)	72.7 (9.0)	28.9 (0.0)	46.4 (0.0)
b)	770.0	1 x	118.7	9.5	109.2	
	1540.0	2 x	115.3 (-2.9)	5.2 (-44.9)	111.1 (1.7)	
	385.0	½ x	124.0 (4.5)	16.2 (70.3)	106.3 (-2.7)	
c)	770.0	1 x	127.8	8.7	38.1	81.0
	1540.0	2 x	125.2 (-2.0)	4.8 (-45.4)	38.7 (1.6)	82.7 (2.1)
	385.0	½ x	132.0 (3.3)	15.0 (72.2)	37.1 (-2.6)	78.4 (-3.2)

Table 4.9 Sensitivity of a) the WPM model, b) the SW model and c) the MSW model to halving and doubling of bulk stomatal resistance. The numbers in the brackets are the % change of Q_{ec} from the unperturbed value of Q_e. All values are in Wm^{-2} except r^c_s which is in sm^{-1}.

The calculation of r^c_s using equation 3.53 has been considered to be an unrealistically simple approach to determining bulk stomatal resistance. Shuttleworth and Gurney (1990) note that r_{st} tends to vary in the vertical for a given canopy because of the difference in radiation interception by the leaves. Thus, they show that average r^c_s is not linear with leaf area index since an increase in LAI within a multilevel canopy causes a continually lower percentage of leaves within the canopy to intercept maximum available radiation. This problem has been avoided in past studies by dividing the canopy into distinct layers and calculating stomatal conductance for each layer (Jarvis et al, 1976; Squire and Black, 1981). However, leaves from a canopy with an LAI below unity are theoretically at the same level and therefore most of the vegetation will tend to receive the same amount of radiation. In this respect, despite the theoretical simplicity of the calculation, equation 3.53 would seem to be valid in practice for canopies with small LAI.

4.6 Daily Comparison

The comparison of modelled to measured daily averages of Q_e is shown in figure 4.13 and the seasonal averages and the RMSE and MBE errors are listed in table 4.10. The simulations cover 51 days from July 4 to August 23, inclusive. As with the hourly comparison, the percentage of open water varied such that there were three distinct periods of surface

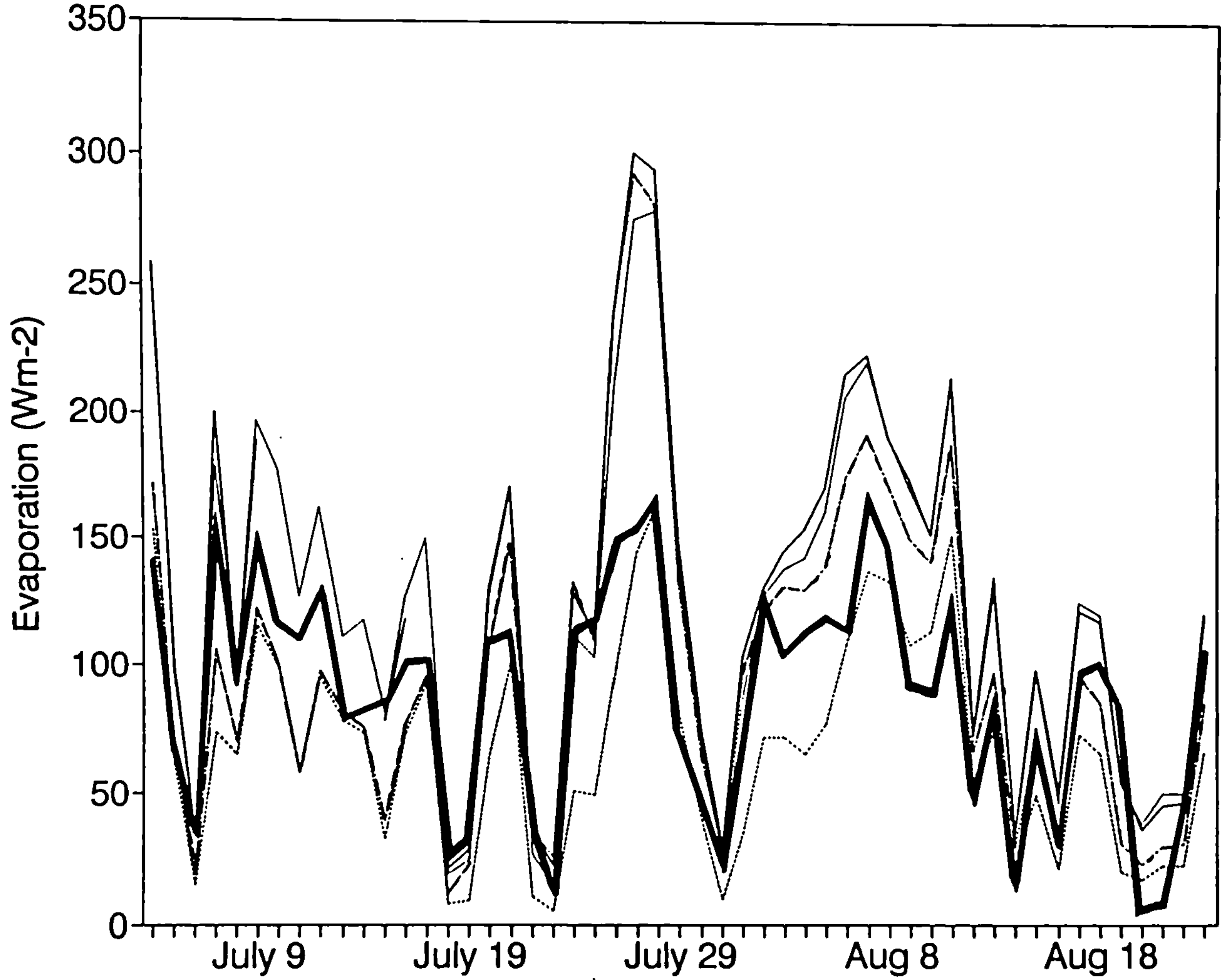

Figure 4.13 Comparison between measured Q_e (heavy solid) and the PM model (dashed), the WPM model (centerline), the SW model (dotted) and the MSW model (solid) for the daily comparison. All r_s and r^s_s values were the optimal resistances.

		PM	WPM	SW	MSW
a)	N	51	51	51	45
	RMSE	33.9	39.5	46.3	51.6
	MBE	-22.8	9.3	31.9	35.2
	Observed	92.3	92.3	92.3	90.8
	Predicted	69.5	101.6	124.3	126.0
	d_i	0.86	0.86	0.84	0.83
b)	N	15	15	15	9
	RMSE	36.0	29.6	42.2	44.3
	MBE	-26.7	-20.0	29.9	24.7
	Observed	100.0	100.0	100.0	97.4
	Predicted	73.3	80.0	129.9	122.1
	d_i	0.79	0.85	0.82	0.87
c)	N	12	12	12	12
	RMSE	35.8	61.1	57.2	67.6
	MBE	-26.4	38.3	35.2	46.2
	Observed	95.5	95.5	95.5	95.5
	Predicted	69.1	133.7	130.7	141.7
	d_i	0.88	0.82	0.84	0.80
d)	N	24	24	24	24
	RMSE	31.5	30.0	42.5	44.4
	MBE	-18.6	13.1	31.6	33.7
	Observed	85.9	85.9	85.9	85.9
	Predicted	67.3	99.0	117.5	119.6
	d_i	0.87	0.91	0.84	0.83

Table 4.10 Evaluation of model performance for a) the entire season, b) the dry period (July 4 to July 18), c) the wet period (July 19 to July 30) and d) the moderately wet period (July 31 to August 23). Observed and Predicted refer to the means of the observed and predicted values, N refers to the total number of hours simulated and d_i is the index of agreement. All values except N and d_i are in Wm^{-2}.

coverage. From July 4 to July 18, the surface was relatively dry with open water covering between 0% and 14% of the surface. From July 19 to July 30, the surface was very wet with water covering from 32% to 76% of the surface. From July 31 to August 23, the surface was moderately wet with water covering between 15% and 54% of the surface.

Of the two driving variables of evaporation, available energy had the strongest control over measured Q_e over all three periods (figure 4.14). The only times that the vapour pressure deficit had a strong influence was when D_x reached its peak values during the wet and moderately wet periods. Indeed, it has been demonstrated that Q_e shows a much stronger correlation with net radiation than with relative humidity for a typical grass wetland in Europe (Priban and Ondok, 1980).

4.6.1 The Dry Period

According to the index of agreement, the MSW model gives the best simulation for the dry period. However, the model was unable to simulate total Q_e on days when there was no open water since a zero value for r^W_a caused the coefficients C_c and C_s to become undefined. As a result, the MSW model was only able to simulate nine days of Q_e whereas the other three models simulated 15 days. This almost certainly increased the level of performance of the MSW model.

There is an obvious similarity between the simulations of the PM and WPM models, with both tending to follow the same

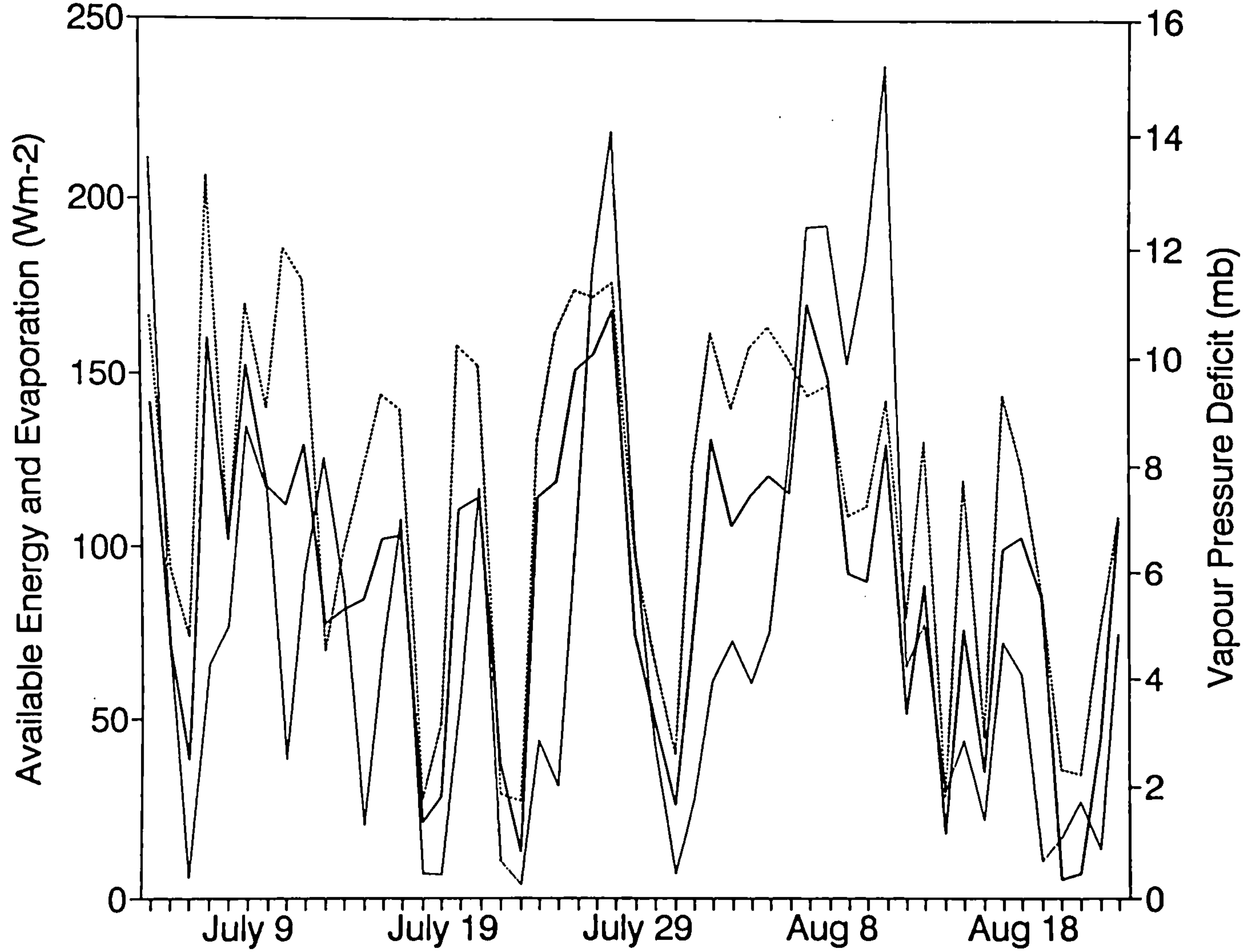

Figure 4.14 Comparison of measured Q_e (solid) to available energy (dashed) and the vapour pressure deficit (dotted) for the daily comparison.

pattern while consistently underestimating the measured Q_e. The underestimations could be a result of an overestimation of the surface resistance for the dry period. This would especially be expected for the WPM model since the soil term is the dominant component of the model during the dry period (figure 4.15) and therefore total WPM Q_e has a relatively high sensitivity to r^s_s. Similarly, the PM model has the highest sensitivity to surface resistance of the four models. However, the similarity between the two models in the simulation of Q_e for the dry period demonstrates that the underestimation in either case is not due primarily to a high surface resistance, since both models had a different sensitivity to r_s and r^s_s.

Instead, the trends of the PM and WPM models closely follow the seasonal pattern of vapour pressure deficit (figure 4.16). Available energy has minor but noticeable control over the modelled Q_e in both cases. It follows that the error in the relationship between the measured and modelled Q_e is mostly due to the driving variables, since the measured Q_e is largely driven by available energy and the PM and WPM Q_e values are driven by D_x.

The same reasoning can also be applied to the similarity between the SW and MSW simulations and the consistent overestimation of total evaporation by both models. In fact, the two simulations agree well enough during the dry period that the SW model could be used as a replacement for

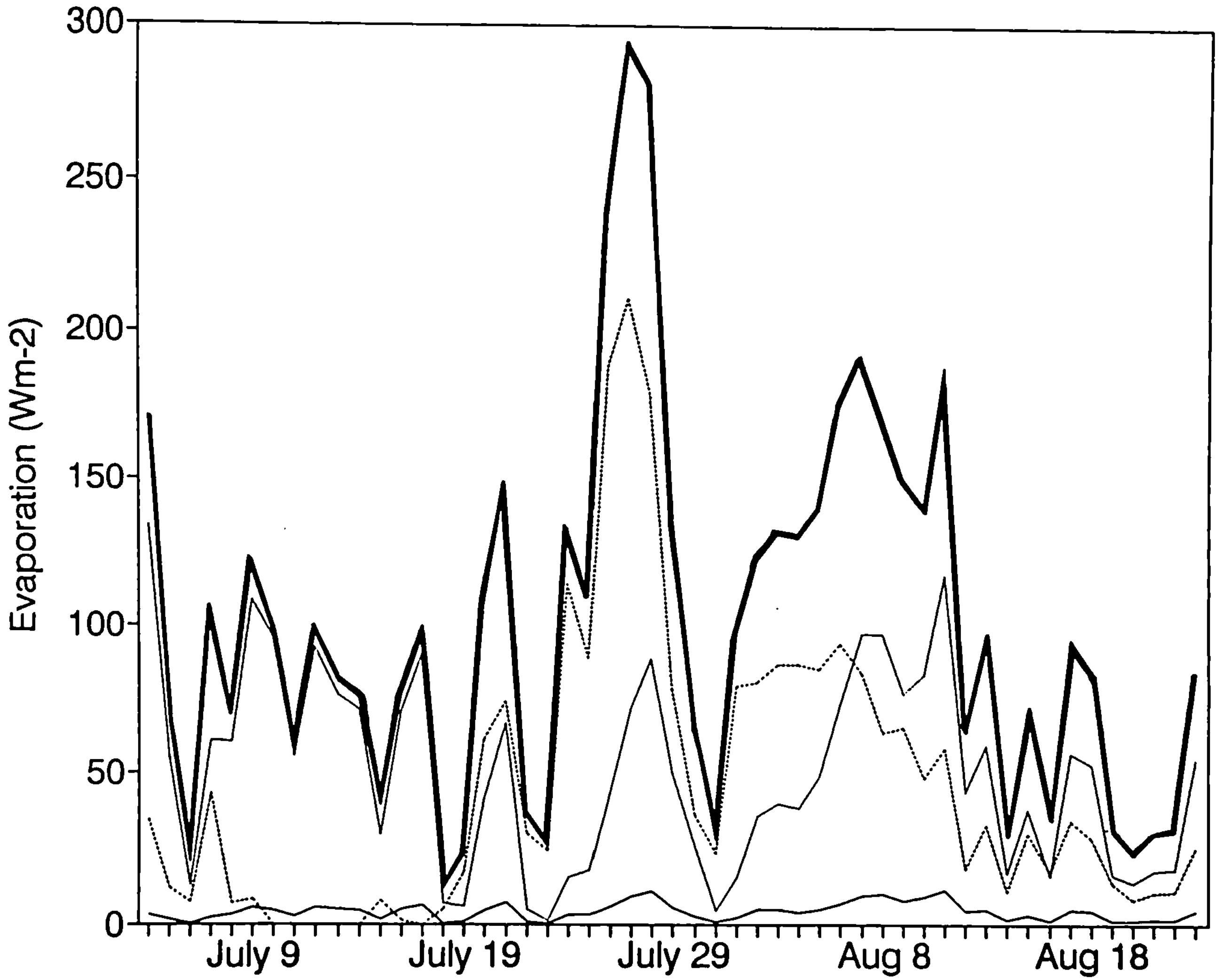

Figure 4.15 Comparison of total WPM modelled evaporation (heavy solid) to the canopy component Q_{ec} (solid), the bare soil component Q_{es} (dotted) and the open water component Q_{ew} (dashed).

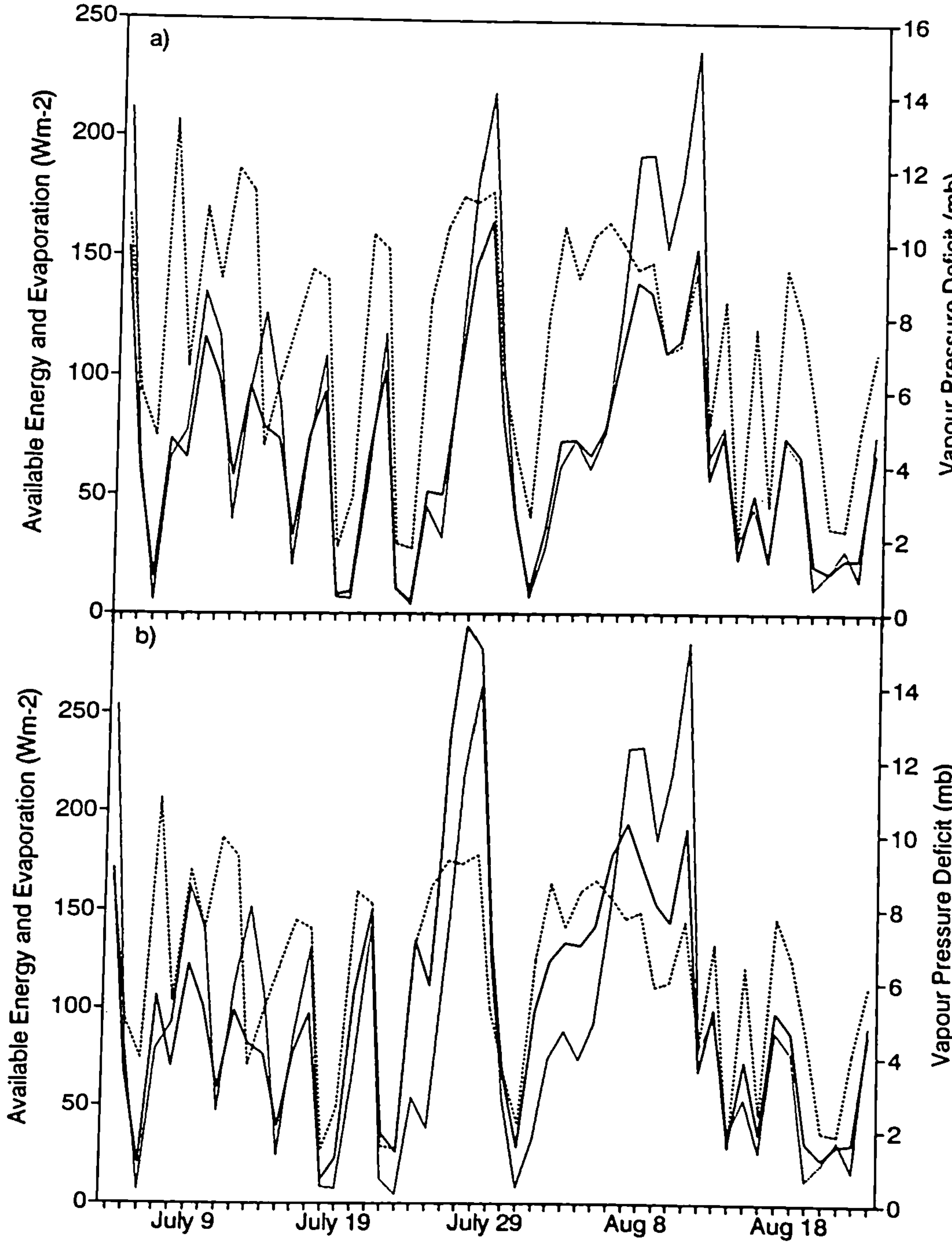

Figure 4.16 Comparison of evaporation from a) the PM model and b) the WPM model (both solid) to available energy (dashed) and vapour pressure deficit (dotted) for the daily comparison.

the MSW model when there is no surface water. As with the PM and WPM models, the higher sensitivity to D_x than to AE in the SW and MSW models (figure 4.17) is the most likely source of error in the comparison with measured Q_e. The fact that all four models do not give the same simulation could be partially due to their differences in sensitivity to available energy (figure 4.7).

As a result, since the Q_{ew} term of the MSW model has the largest contribution to the total modelled Q_e (figure 4.18B), it would be expected that open water is especially sensitive to D_x. This would also be the case with the dominant soil/water term in the SW model (figure 4.18A). However, the water component of the WPM model has a much smaller contribution to total Q_e than the SW and MSW models during the dry period, which indicates that one or all of the models are in error in the estimation of open water evaporation. Since the surface coverage of water is small or nonexistent, it would seem that the SW and MSW models have the larger error during this period.

4.6.2 The Wet Period

The PM model showed the smallest error and provided the best simulation for the 12 day wet period. However, this relatively strong performance of the PM model is mostly due to the large overestimation of total evaporation by the other three models, all of which temporarily estimated twice as much

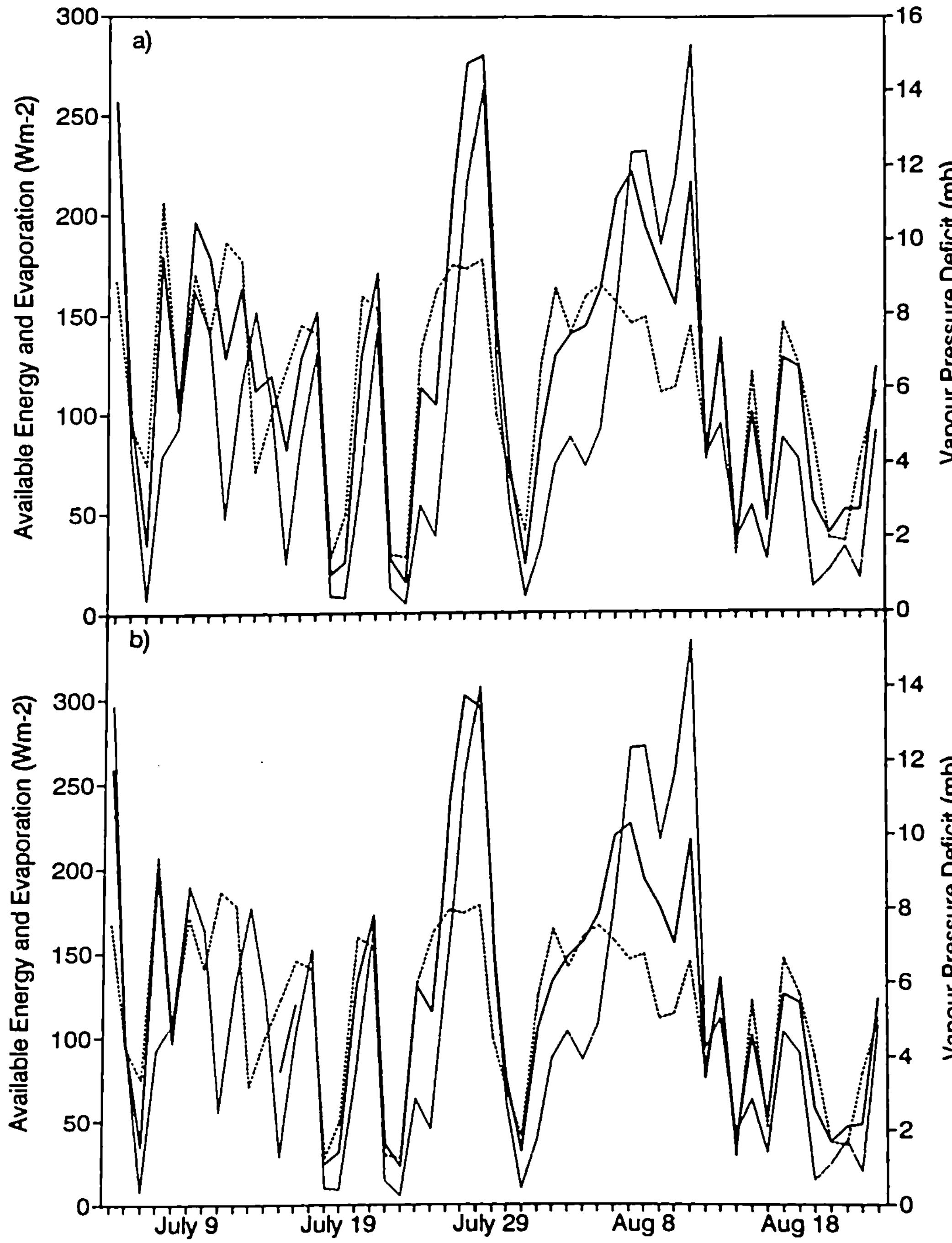

Figure 4.17 Comparison of evaporation from a) the SW model and b) the MSW model (both solid) to available energy (dashed) and vapour pressure deficit (dotted) for the daily comparison.

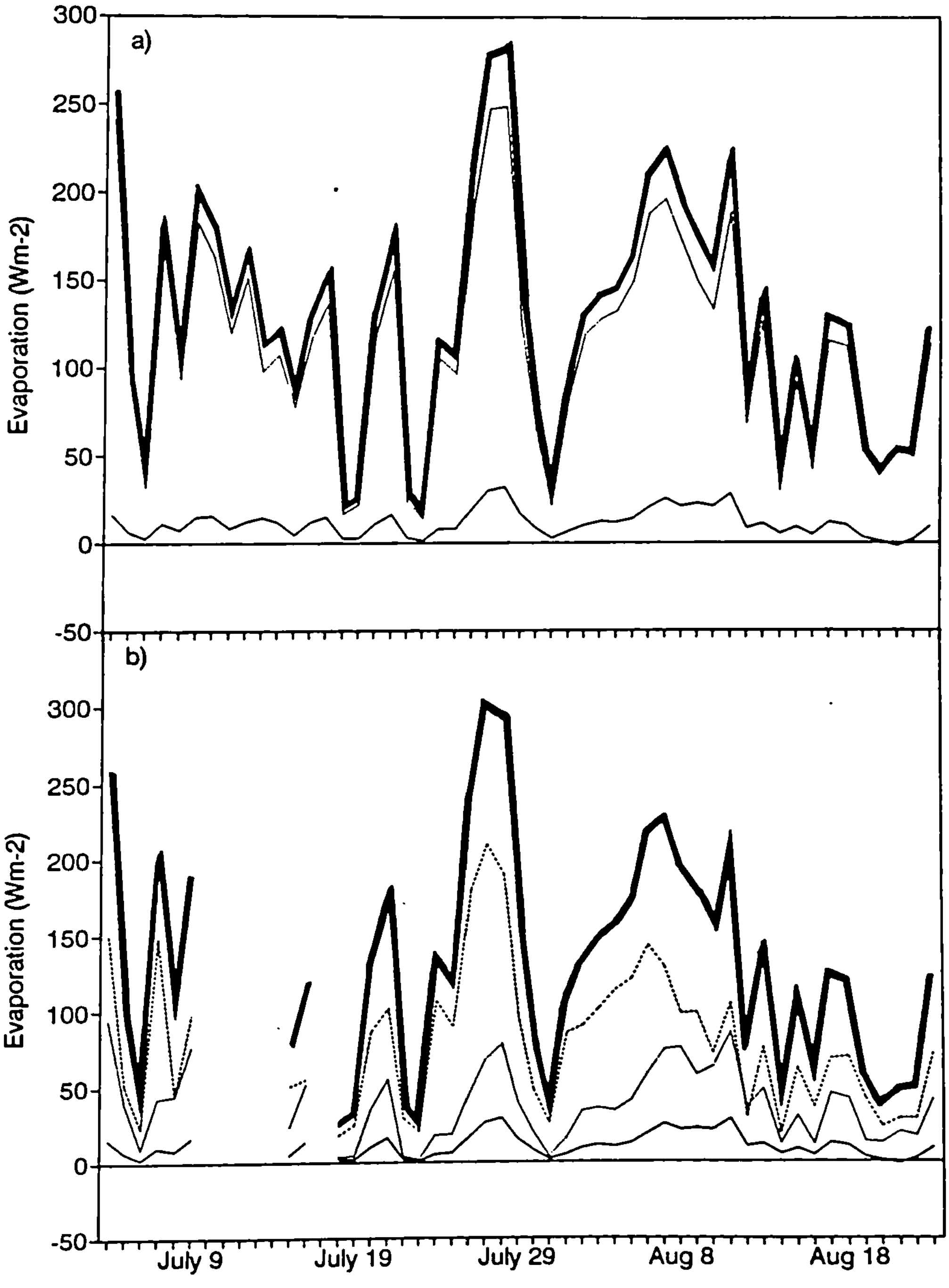

Figure 4.18 Comparison of total evaporation (heavy solid) to Q_{ec} (solid), Q_{es} (dotted) and Q_{ew} (dashed) from a) the SW model and b) the MSW model for the daily comparison.

Q_e as given by the measured values.

The overestimation by the SW and MSW models could possibly be due to the absence of a surface resistance term for water evaporation. If such a resistance actually existed and had a noticeable effect, it would mostly alter the dominant soil/water and water terms of the two models. In fact, it has been established that a thin gas layer exists over a typical water surface, within which the vapour pressure is at or near saturation (Jones, 1992). Evaporation from a water surface has been considered to be partially governed by the thickness of this diffusional layer, which varies with the degree of surface roughness. Since the ponds at the study site were small enough to allow the assumption of a 1 mm surface roughness length in the models, the relatively thick diffusional layer that might result could have a noticeable effect on the evaporation from water.

The SW and MSW models assume that all resistances which occur at the soil surface can be represented by the $r^s{}_s$ term. However, neither model accounts for any aerodynamic resistance which might occur between the surface and the 1 mm bare soil/open water surface roughness length. This is due to the fact that the aerodynamic resistance which exists below the canopy source height in both models was only integrated from the surface roughness length of bare soil and water to d + z_o, and not from the surface. In the case of the MSW Q_{ew} term, no surface resistance or diffusional resistance is considered. Thus, resistance to evaporation from open water is assumed to be entirely controlled by the values of r^w_a and r^a_a, which might not accurately represent reality.

However, the frequently used Penman potential evaporation model also assumes that no surface resistance exists and that the only resistance to Q_e is represented by the r_a term. The successful practical application of this model (Granger, 1989) tends to show the relative insignificance of a diffusional resistance.

The WPM model overestimates Q_e at the same time as the SW and MSW models. Since this period of overestimation occurs over the time that surface coverage of open water is highest, the error is most likely in the estimation of surface cover percentage. In figure 2.2, the relationship between the coverage of open water and the height of the water table depth was assumed to be linear. However, this might not be the case once the water table has risen to where all of the hollows have been completely covered. At this point, any further increase in the height of the water table will not change the coverage of open water, thus providing a non-linear relationship. Such a situation occurred during the wet period of the study season and the overestimation of water coverage during this time caused the models which were most sensitive to water evaporation to overestimate the measured Q_e.

The ultimate result of the high estimation of open water by the SW, MSW and WPM models is the increased sensitivity of total Q_e to a high vapour pressure deficit. Since the PM model was relatively insensitive to the percentage of open water cover, it did not respond to the same degree as the other three models.

4.6.3 The Moderately Wet Period

The modelled evaporation values in the moderately wet period followed similar patterns as those in the dry and wet periods. The WPM model provided the best simulation and had the lowest error.

For the first half of the period, the water table was high and the surface was covered with a substantial amount of open water. However, the coverage of open water decreased throughout the period until the surface was as dry as it was at the beginning of the season. Thus, the moderately wet period had a wet and dry period of its own. This was especially evident in the patterns of modelled evaporation.

The SW, MSW and WPM models strongly overestimated the measured Q_e for the first half of the moderately wet period as they did in the wet period. The PM model also continued the same trend by underestimating Q_e. Since the error in the surface cover estimation would still be high at this time, much of the overestimation by the SW, MSW and WPM models can be explained by this. Again, the result of this error is an increase in the influence of the water components of the models and a resulting increase in the sensitivity of total Q_e

to the high vapour pressure deficit which occurred during this period. The WPM model did not overestimate as much as the SW and MSW models because of the comparatively smaller weighting given to water evaporation by the former (figure 4.15).

The modelled Q_e values of the drier second half of the moderately wet period resembled the pattern of the dry period. The SW model showed almost exactly the same trend as the MSW model and both tended to overestimate measured Q_e whereas the PM model underestimated it. The WPM model produced the best simulation of all of the models in any of the three periods of the season. The main reason for these improved estimations of Q_e could be the direct result of an accurate estimation of surface cover. In addition to this, the vapour pressure deficit was smallest during this time of the season, which would be expected to reduce the degree of overestimation by the water-sensitive models.

4.6.4 Overall Seasonal Comparison

According to the index of agreement, all four models gave a similar quality of simulation for the entire season, with the WPM model producing the best agreement (table 4.10).

The trends in total Q_e from the SW and MSW models were almost exactly the same for the entire season. This strong relationship reflects the similar sensitivity of the models to the vapour pressure deficit, which is due to the large weighting by open water in both models. The occasional slight underestimation of the MSW model by the SW model seems to be a result of the assumption of a surface resistance on the SW soil/water component.

Both models consistently overestimated measured Q_e, especially during the wetter parts of the simulated period. Again, this would be due to the high weighting of the water components of the two models, even during the relatively dry periods. This resulted in the increase in the sensitivity of the total modelled Q_e to D_x. The apparent overestimation of surface water coverage tended to increase this sensitivity even further.

The PM model produced the only simulation which consistently underestimated Q_e. The strong sensitivity of the model to surface resistance is the most likely explanation for this pattern. However, at times of high D_x, the modelled Q_e approached the measured Q_e and provided the best simulation for the PM model for the entire season. In addition to this, the relatively close overall agreement to the measured Q_e is most likely a result of the comparatively stronger sensitivity of the PM model than the SW and MSW models to available energy, which is the variable to which the measured Q_e is most sensitive.

The general seasonal pattern of the WPM model involves an underestimation of measured Q_e during relatively dry periods and an overestimation during the wetter periods. The model has the same sensitivity as the PM model to D_x and AE but is less sensitive to surface resistance. Although the WPM Q_e tends to follow the seasonal trend of D_x, the model is most sensitive to the estimation of surface cover since this is used to weight the individual evaporation components. As a result, a more accurate determination of the surface coverage of the evaporating surfaces is needed before further simulation using the WPM model is attempted.

Chapter 5

Discussion and Conclusions

This study has focused on the ability of four physically-based, one-dimensional models to simulate evaporation from a subarctic wetland tundra. The purposes of this final chapter are threefold. The first is to outline the mathematical limitations within each model in order to delineate the minimum conditions required to use the model. The second is to outline the advantages and disadvantages of each model in their practical application. The third is to recommend future paths of research in order to improve the performance of each model.

5.1 Model Restrictions

The practical application of any of the four models discussed in this study is limited in several ways. The primary restriction for the PM, SW and MSW models is the simulation of evaporation from a site which has more surface types than the model was originally designed for. The WPM model was particularly designed to avoid this problem. This restriction within the other three models is directly related to the mathematical limitations within the models themselves. All of these restrictions are discussed as follows.

5.1.1 Restrictions in the PM and WPM Models

At present, the only surface type which can be described by the PM model using r_c as it was originally designed is one which has a relatively dense canopy. This requires that the LAI must be close to or greater than unity and that the surface contribution to the evaporation stream must be negligible. The model cannot be used for partial canopies within a wetland because of the large surface contribution and the unreliable results due to the high sensitivity of the canopy resistance to small LAI values.

In the case of partial canopies or surfaces with many surface types, the PM model might be employed if an accurate, representative surface resistance can be determined and substituted for r_c in the PM equation. However, in many cases the practical difficulty in obtaining a surface resistance that accurately defines a heterogenous and changing surface has prevented the application of this approach.

The PM model as defined by equation 3.18 can also be used to describe potential evaporation conditions over a surface cover of water or saturated soil. In this case, surface resistance is assumed to be zero and the result is an equation resembling that derived by Penman (1948). However, the concept of zero surface resistance may not be entirely correct unless resistance in the gaseous diffusion layer over the liquid surface can be considered to be negligible.

The PM and WPM models cannot be used under certain conditions which create calculation errors, such as when variables become zero. The aerodynamic and bluff body resistance equations, described by equations 3.22 and 3.24 respectively, become undefined when the roughness length or the wind speed at the reference height is zero. However, roughness length depends on wind speed and the height of the surface elements and rarely becomes zero under natural conditions.

5.1.2 Restrictions in the SW and MSW Models

Since the SW and MSW models are based on the PM equation, they have similar restrictions as the PM model. The SW model can only be used for surfaces which are comprised of both canopy and bare soil components. If either one of these surface types becomes negligible or is missing from the surface being modelled, the SW model becomes undefined. This restriction implies that the PM model should be substituted for the SW model under these conditions. Similarly, the MSW model cannot be used if any one of the three components of canopy, bare soil or open water are absent from the surface. The disappearance of open water from the surface due to a lowering of the water table is a common occurrence and can often happen in wetland environments. In this study, the water table dropped and remained below the surface for six days during the study period. Under conditions such as these, the failure of the MSW model suggests that the SW model should be used in its place.

These limitations within the SW and MSW models are strictly due to mathematical restrictions in the coefficients C_c, C_s and C_w. In order to prevent the coefficient calculations from becoming undefined, the R_c, R_s and R_w terms must never become zero. Since these terms are calculated using physiological, aerodynamic and surface resistances, this implies that these resistances must also be non-zero. As a result, the surface types which create these resistances (canopy, bare soil and open water) must be present on the surface being modelled. To obtain a better understanding of these limitations, an analysis of the coefficient terms is given as follows.

The R_c term (equation 3.32) depends primarily on a physiological resistance, r^c_s, and an aerodynamic resistance, r^c_a. The former is calculated using LAI only and the latter is calculated using FAI. Under conditions where there is no LAI and r^c_s is zero, R_c can still be calculated using FAI and r^c_a, provided that some form of foliage such as dead or woody material is present. However, if a living canopy exists and a plant canopy analyzer is used to measure FAI, the DAI and WAI (Woody Area Index) must be factored out so that only LAI is considered when calculating r^c_s (equation 3.53). However, since dead vegetation and woody material can create an aerodynamic resistance, these indices must be considered when determining r_b for the r^c_a calculation (equation 3.52). For both the SW and MSW models, the FAI must be greater than zero in order to satisfy equation 3.52.

The R_s term (equation 3.31) is calculated using a surface resistance, r^s_s, and an aerodynamic resistance, r^s_a. If r^s_s is considered to be zero under conditions where the surface is saturated, the R_s term must be non-zero as calculated using r^s_a. However, the absence of a soil surface causes r^s_a to become zero which forces the coefficients C_c and C_w to become undefined.

The R_w term (equation 3.65) is calculated using an aerodynamic resistance term, r^w_a, and does not consider a surface resistance. Following the same reasoning as for the R_s term, the R_w term must be calculated using a non-zero r^w_a.

5.2 Advantages and Disadvantages of the Models

One of the primary advantages of an evapotranspiration model is found in its ability to predict Q_e given a particular perturbation in the environment. However, the ability of the model to simulate measured evaporation is the first step in the development of a predictive model. Each of the four models has advantages and disadvantages in their ability to simulate evaporation from a tundra wetland surface.

5.2.1 The PM Model

The PM model is a practical approach to estimating evaporation from a particular surface type if an accurate, representative estimate of surface resistance is available. It is especially advantageous for situations where canopy evaporation is dominant and other sources of evaporation are minimal, which is the situation it was originally intended to represent. Apart from surface resistance, the model only requires measurements of temperature, vapour pressure and wind speed at a reference height and measurements of net radiation and ground heat flux. In this respect, the practical advantages of the PM model are comparable to that of the BREB approach in the estimation of total site evaporation. In addition to this, the model is grounded in essential physics and yet is still simple enough to be used in more complicated atmospheric models such as GCMs, where computer time is a significantly limiting factor.

The main disadvantage in applying the PM model is that an accurate representative r_s for a complex surface is difficult to determine at present. The typical wetland surface consists of canopy, bare soil and open water, all of which have a wide range of surface resistances which depend on a number of surface and meteorological variables. Consequently, the high sensitivity of the PM model to surface resistance is an important disadvantage in its practical application.

One of the less obvious disadvantages of all of the models is the accumulation of error. This is due to the fact that since each parameter and variable used in a model tends to have its own error, the sum total error within the model increases as more parameters and variables are added. By using this reasoning, the relatively small number of parameters and variables in the PM model, compared to the SW and MSW models, would be expected to produce a smaller total error in the calculation of evaporation.

5.2.2 The SW Model

The SW model was originally designed to simulate evaporation from a canopy which has a significant contribution from the soil surface. No allowance was made for evaporation from open water. As a result, the analogy of the model does not correspond to a typical wetland surface which produces substantial open water evaporation. If a complex model is required to describe the evaporation from a wetland surface, the more accurate analogy of the MSW model would warrant its use over that of the SW model. However, if an accurate representative surface resistance can be determined for a soil/water evaporation component, the SW model tends to become more practical.

The inability of the SW model to simulate evaporation when there is no canopy present is an obvious disadvantage. Thus, the model cannot be used prior to the growing season unless dead vegetation or woody mass exists. However, considering its strong correlation with the MSW model in the daily comparison, the SW model can be used as a surrogate to the MSW model when the latter fails to describe evaporation with no open water contribution.

5.2.3 The MSW Model

An obvious advantage of the MSW model over the PM and SW models is in its analogy, which allows the simulation of component evaporation from a site with three evaporation sources. Of course, the same holds true under one-source evaporation conditions with the PM model and two-source evaporation conditions with the SW model. However, typical sedge wetlands most often require the use of a three-stream approach. Even in cases where one of the streams is absent, the MSW model can still be used provided that the surface type from which the stream would normally originate is still in existence. It is only in the case when a surface type disappears, such as when the water table falls below the surface and the water contribution to evaporation is zero, that the MSW model fails and the SW model can be substituted.

However, the analogy of the MSW model is not completely sound considering the method by which the individual evaporation components are partitioned. The main similarity between the SW and MSW models is that both are partitioned through available energy. The difference is that the SW model was designed to partition available energy in a one-dimensional fashion using Beer's Law such that whatever net radiation was not intercepted by the canopy was used by the bare soil beneath. The MSW model assumes a two dimensional partition, where surface area becomes the primary determining factor in how much AE is used by the three components of the model. Thus, a two dimensional assumption in a one-dimensional model has potential problems and would seem to disqualify the practical use of the MSW model. However, the reasonably good performance of the MSW simulations compared to the other three models warrants further investigation.

As with the other models, the MSW model requires an accurate determination of the surface resistance for each of its evaporation components. The individual estimation of resistance for each component is inherently more accurate and representative of that particular surface type than a value used to represent the surface as a whole. Hence, the MSW model is advantageous in this respect and has the additional advantage of being relatively insensitive to surface resistance, which limits the error in total Q_e that might by caused by this variable. This is an important characteristic considering that the MSW model is the most complex of the four models studied and would consequently have the greatest total error.

One of the primary disadvantages in the complex SW and MSW models is that their use in actual measurement of evaporation is not feasible, even though they are more theoretically acceptable than the simpler PM model in most cases. The expense in time and money involved in measuring all of the parameters and variables required by the SW and MSW models is unnecessary, considering that the BREB approach is an acceptable method which can be used for any combination of surface types and requires only a few measurements. As a result, if the SW and MSW models can be improved in their ability to simulate a specified surface, their practical advantage would primarily be in a predictive role.

Both the SW and MSW models have an additional disadvantage in the establishment of a canopy source height. Shuttleworth and Wallace (1985) described the height in terms of d and z_0, both of which were determined as a function of canopy height only. However, the canopy in their study had a maximum LAI of 4, which would have a much more defined source height than the canopy of the present study which had a maximum FAI of 0.28. In addition to this, their study was intended to describe evaporation from a sparse crop canopy which was located on a flat surface. This allowed the assumption that the source height can remain constant at a fixed fraction of crop height and not be affected by the relief of the surface. This is not entirely the case with the surface described within this study, where a maximum sparse canopy height of 10 cm was often present on frost hummocks which themselves had a height of 44 cm.

5.2.4 The WPM Model

Perhaps the most prominent advantage of the WPM model is the ability to apply the model to any number of surfaces, providing that accurate estimates of surface resistance and surface cover percentage can be obtained. The model is especially advantageous under conditions when a surface type tends to appear on the surface, such as a canopy during the growing season, or disappear from the surface, such as the water table during a dry period. In cases where the surface cover proportion changes over the study period, the percentage of each surface type must be continuously monitored to maintain the level of accuracy required by the model.

The WPM model provided the best overall simulation of daily average evaporation of all four models. This is largely due to the method of surface weighting which is unique and inherently more accurate than that of the SW and MSW models. This is especially evident in the estimates of open water cover during the dry period of the study season, when the WPM model described total evaporation in terms of a dominant soil term whereas the SW and MSW models showed an unrealistically dominant water component even when open water was a minor surface type. Thus, the weighting of evaporation by surface area tends to produce a more accurate estimation of component evaporation than the weighting of available energy. However, the large overestimation of all three models during the wet period of the season demonstrates the need to accurately estimate surface cover percentage.

The apparent lack of interaction between the individual evaporation components of the WPM model is a potential source of error. This demonstrates an advantage of the SW and MSW models, both of which allowed each component to affect the others in the sensitivity analysis. In fact, Wallace et al (1990) noted that the ability of the SW model to determine the effects of soil evaporation on the transpiration and growth of the canopy was a significant characteristic of the model. However, the WPM model assumes that any interaction between canopy, bare soil and open water takes place through the available energy and vapour pressure deficit only. Indeed, it has been shown in this study that the exchange of energy and the change in vapour pressure caused by a perturbation of one surface type can be an important cause of the change of evaporation contribution from the other surface types. The inability of the sensitivity analysis to demonstrate this for the WPM model is a result of not considering feedbacks.

5.3 Recommendations for Future Research

According to the results of the daily comparison, any of the four models are capable of simulating total evaporation from a wetland surface provided that an accurate determination of surface resistance and surface cover proportion is obtained. This is required to provide a better assessment of each model and to assist in deciding which of the models is best in a predictive role. However, important conclusions can be reached from this present research which allow recommendations for directions in future studies.

One of the main sources of error which caused the simulated Q_e in all four models to deviate from the measured Q_e was the dependence of modelled evaporation on the vapour pressure deficit, since the measured Q_e was sensitive to available energy. A better understanding of this difference is required to determine the degree to which it affects total evaporation.

The PM model is the best model in terms of simplicity. If an accurate surface resistance can be obtained which is spatially and temporally representative of the general surface, it is expected that the simulation from the PM model will improve. It has been noted that surface resistance directly depends on vapour pressure deficit and soil moisture, which are partially governed by the height of the water table. The cause and effect of surface resistance are identified as important areas for future research.

The increased theoretical complexity of the SW and MSW models is an advantage over the PM model in that it allows a better description of sources, driving variables and resistances of evaporation. However, an increase in total error is expected to be the consequence. As a result, if the SW and MSW models are to be used in any practical application, it is imperative that all measurements be taken with emphasis placed specifically on the reduction of error. This will allow a better assessment of the simulations and determine the true effect of the bad analogy of the two models on their description of evaporation. Improvement is also needed in the estimation of the proportion of surface cover for the partitioning of the individual components of the SW and MSW models.

The WPM model is also highly dependent on the weighting of its components by surface area, which is the variable that is the most limiting in the model. This study assumed that the proportion of surface area could be obtained from a linear relationship between water table depth and surface cover percentage of water, which is not the case once the water table has risen enough to cover the hollows. It is expected that this relationship is largely non-linear and attention should be focused in determining the relationship for a given study site. Alternatively, surface area can be determined through maps and air photos, depending on the spatial scale desired. If surface resistance and the proportion of surface area can be obtained accurately, the WPM model would most likely give the best simulation of the four models and would have the highest potential for use in a predictive role.

Further analysis of the role of feedbacks in the models is recognized and is perhaps the most important direction for future study, particularly if a model is used to predict the effect of hydrological or climatic change. A sensitivity analysis which accounts for feedbacks is required so that a reliable comparison between measured and modelled feedback effects can be obtained. As a result, the feedbacks which occur within the tundra wetland must be assessed with acceptable accuracy.

Appendix One

The Derivation of the Modified Shuttleworth-Wallace Model

The description of energy partitioning within the boundary layer has prompted numerous studies designed to accurately estimate it. The theory resulting from these studies has been applied in a practical sense through the use of physically based models.

Penman (1948) was one of the first to derive a physically based, combination model to estimate evaporation from any wet surface. This model successfully combined the two most important processes which govern evaporation: the energy required to produce water vapour and the mechanism by which that water vapour is removed from the evaporating surface. The combination of these two processes allowed the calculation of potential evaporation. Since potential evaporation conditions are seldom found, Monteith (1965) modified the model, incorporated the physiological resistances caused by a vegetative canopy and defined the Penman-Monteith (PM) equation, given as

$$Q_e = \frac{\Delta AE + \frac{\rho C_p D}{r_a}}{\Delta + \gamma\left(1 + \frac{r_c}{r_a}\right)} \qquad \text{(A1.1)}$$

where Q_e is the latent heat flux, Δ is the slope of the saturation vapour pressure vs. temperature curve, AE is total available energy, ρ is the density of air, C_p is specific heat at constant pressure, γ is the psychrometric constant, r_a is aerodynamic resistance, r_c is canopy resistance and D is vapour pressure deficit such that

$$D = e_w(T_z) - e_z \qquad \text{(A1.2)}$$

where $e_w(T_z)$ is the saturation vapour pressure at temperature T_z at height z and e_z is the vapour pressure at height z.

Shuttleworth and Wallace (1985) adopted a similar approach to the PM model except that bare soil evaporation was added to canopy transpiration to give the total evaporation stream as would be found with a partial canopy. The resulting Shuttleworth-Wallace (SW) model was composed of two separate Penman-Monteith based equations which incorporated surface, aerodynamic and physiological resistances.

The development of the MSW sparse canopy combination model is similar to the procedure followed by Shuttleworth and Wallace (1985). The main difference is the inclusion of a third evaporation stream by the MSW model so that all three surface types from the study site are accounted for.

As with all combination models, each component of the MSW model is founded on an energy budget. The budgets for bare soil and open water are given by

$$AE_s = Q_{es} + Q_{hs} \tag{A1.3}$$

and

$$AE_w = Q_{ew} + Q_{hw} \tag{A1.4}$$

where Q_{es} and Q_{ew} are the latent heat fluxes, Q_{hs} and Q_{hw} are the sensible heat fluxes and AE_s and AE_w are the available energy terms for bare soil and open water respectively. The sum of the above canopy fluxes for the entire site, AE, is given by

$$AE = Q_e + Q_h \tag{A1.5}$$

or

$$AE = AE_c + AE_s + AE_w \tag{A1.6}$$

where AE_c is the available energy term for the canopy. AE_c is calculated with measured ground heat flux and net radiation determined as a residual from

$$Q^* = Q^*_c + Q^*_s + Q^*_w \tag{A1.7}$$

where Q^*, Q^*_c, Q^*_s and Q^*_w are net radiation terms for the entire site, canopy, bare soil and open water respectively.

Using the Penman-Monteith format from equation A1.1, Shuttleworth and Wallace (1985) derived the latent heat flux for the canopy, Q_{ec}, and Q_{es} such that

$$Q_{ec} = \frac{\Delta AE_c + \dfrac{\rho C_p D_o}{r^c_a}}{\Delta + \gamma\left(1 + \dfrac{r^c_s}{r^c_a}\right)} \tag{A1.8}$$

$$Q_{es} = \frac{\Delta AE_s + \dfrac{\rho C_p D_o}{r^s_a}}{\Delta + \gamma\left(1 + \dfrac{r^s_s}{r^s_a}\right)} \tag{A1.9}$$

where r^c_a is bulk boundary layer resistance of the canopy, r^c_s is the bulk stomatal resistance of the canopy, r^s_a is the aerodynamic resistance between the bare soil surface and the canopy source height $(d + z_o)$, r^s_s is soil surface resistance and D_o is the vapour pressure deficit at the canopy source height, which is defined as

$$D_o = D_x + \frac{\{\Delta AE - (\Delta + \gamma)Q_e\} r^a{}_a}{\rho C_p} \tag{A1.10}$$

where $r^a{}_a$ is the aerodynamic resistance between the canopy source height and the reference level (x) and D_x is the vapour pressure deficit at the reference height such that

$$D_x = e_w(T_x) - e_x \tag{A1.11}$$

The descriptions and equations for all resistances are defined in chapter 3.

Similarily, the latent heat flux over open water can be given as

$$Q_{ew} = \frac{\Delta AE_w + \dfrac{\rho C_p D_o}{r^w{}_a}}{\Delta + \gamma} \tag{A1.12}$$

where $r^w{}_a$ is the aerodynamic resistance between the water surface and the canopy source height. The total latent heat flux from the surface is

$$Q_e = Q_{ec} + Q_{es} + Q_{ew} \tag{A1.13}$$

Equation A1.12 assumes that open water behaves identically to bare soil except that water is assumed to have no surface resistance and a different value of aerodynamic resistance.

By substituting equations A1.10, A1.8, A1.9 and A1.12 into equation A1.13, the total latent heat flux becomes

$$Q_e = \frac{\Delta AE_c r^c{}_a + \rho C_p \left[D_x + \dfrac{\{\Delta AE - (\Delta+\gamma) Q_e\} r^a{}_a}{\rho C_p} \right]}{(\Delta+\gamma) r^c{}_a + \gamma r^c{}_s}$$

$$+ \frac{\Delta AE_s r^s{}_a + \rho C_p \left[D_x + \dfrac{\{\Delta AE - (\Delta+\gamma) Q_e\} r^a{}_a}{\rho C_p} \right]}{(\Delta+\gamma) r^s{}_a + \gamma r^s{}_s}$$

$$+ \frac{\Delta AE_w r^w{}_a + \rho C_p \left[D_x + \dfrac{\{\Delta AE - (\Delta+\gamma) Q_e\} r^a{}_a}{\rho C_p} \right]}{(\Delta+\gamma) r^w{}_a} \tag{A1.14}$$

After collecting the Q_e terms, equation A1.14 becomes

$$\begin{aligned}
Q_e \Big\{ & \left[(\Delta+\gamma) r^c{}_a + \gamma r^c{}_s\right]\left[(\Delta+\gamma) r^s{}_a + \gamma r^s{}_s\right]\left[(\Delta+\gamma) r^w{}_a\right] + \\
& + \left[(\Delta+\gamma) r^c{}_a + \gamma r^c{}_s\right](\Delta+\gamma) r^a{}_a (\Delta+\gamma) r^w{}_a + \\
& + \left[(\Delta+\gamma) r^s{}_a + \gamma r^s{}_s\right](\Delta+\gamma) r^a{}_a (\Delta+\gamma) r^w{}_a + \\
& + \left[(\Delta+\gamma) r^c{}_a + \gamma r^c{}_s\right]\left[(\Delta+\gamma) r^s{}_a + \gamma r^s{}_s\right](\Delta+\gamma) r^a{}_a \Big\} \\
= & \left[\Delta AE_s r^s{}_a + \rho C_p D_x + \Delta AE r^a{}_a\right]\left[(\Delta+\gamma) r^c{}_a + \gamma r^c{}_s\right](\Delta+\gamma) r^w{}_a + \\
& + \left[\Delta AE_c r^c{}_a + \rho C_p D_x + \Delta AE r^a{}_a\right]\left[(\Delta+\gamma) r^s{}_a + \gamma r^s{}_s\right](\Delta+\gamma) r^w{}_a + \\
& + \left[\Delta AE_w r^w{}_a + \rho C_p D_x + \Delta AE r^a{}_a\right]\left[(\Delta+\gamma) r^c{}_a + \gamma r^c{}_s\right]\left[(\Delta+\gamma) r^s{}_a + \gamma r^s{}_s\right]
\end{aligned} \tag{A1.15}$$

If we define

$$R_c = (\Delta+\gamma)\, r^{c}{}_{a} + \gamma r^{c}{}_{s} \qquad \text{(A1.16)}$$

$$R_s = (\Delta+\gamma)\, r^{s}{}_{a} + \gamma r^{s}{}_{s} \qquad \text{(A1.17)}$$

$$R_w = (\Delta+\gamma)\, r^{w}{}_{a} \qquad \text{(A1.18)}$$

$$R_a = (\Delta+\gamma)\, r^{a}{}_{a} \qquad \text{(A1.19)}$$

and substitute these into equation A1.15, it becomes

$$Q_e\,(R_cR_sR_w + R_cR_wR_a + R_sR_wR_a + R_cR_sR_a) = R_cR_w\left[\Delta A E_s r^{s}{}_{a} + \rho C_p D_x + \Delta A E r^{a}{}_{a}\right] + R_sR_w\left[\Delta A E_c r^{c}{}_{a} + \rho C_p D_x + \Delta A E r^{a}{}_{a}\right] + R_cR_s\left[\Delta A E_w r^{w}{}_{a} + \rho C_p D_x + \Delta A E r^{a}{}_{a}\right] \qquad \text{(A1.20)}$$

If we let

$$R_c + R_a = (\Delta+\gamma)\left(r^{c}{}_{a} + r^{a}{}_{a}\right) + \gamma r^{c}{}_{s} \qquad \text{(A1.21)}$$

$$R_s + R_a = (\Delta+\gamma)\left(r^{s}{}_{a} + r^{a}{}_{a}\right) + \gamma r^{s}{}_{s} \qquad \text{(A1.22)}$$

$$R_w + R_a = (\Delta+\gamma)\left(r^w{}_a + r^a{}_a\right) \tag{A1.23}$$

then

$$Q_e\ (R_c R_s R_w + R_c R_w R_a + R_s R_w R_a + R_c R_s R_a) =$$
$$PM_s R_c R_w (R_s + R_a) + PM_c R_s R_w (R_c + R_a) + PM_w R_c R_s (R_w + R_a) \tag{A1.24}$$

where

$$PM_c = \frac{\Delta AE + \dfrac{\rho C_p D_x - \Delta r^c{}_a (AE - AE_c)}{r^c{}_a + r^a{}_a}}{\Delta + \gamma\left[1 + \dfrac{r^c{}_s}{r^c{}_a + r^a{}_a}\right]} \tag{A1.25}$$

$$PM_s = \frac{\Delta AE + \dfrac{\rho C_p D_x - \Delta r^s{}_a (AE - AE_s)}{r^s{}_a + r^a{}_a}}{\Delta + \gamma\left[1 + \dfrac{r^s{}_s}{r^s{}_a + r^a{}_a}\right]} \tag{A1.26}$$

$$PM_w = \frac{\Delta AE + \dfrac{\rho C_p D_x - \Delta r^w{}_a (AE - AE_w)}{r^w{}_a + r^a{}_a}}{\Delta + \gamma} \tag{A1.27}$$

Solving for Q_e gives

$$Q_e = C_c PM_c + C_s PM_s + C_w PM_w \tag{A1.28}$$

where

$$C_c = \frac{1}{1+\dfrac{R_c R_a (R_s+R_w)}{R_s R_w (R_c+R_a)}} \tag{A1.29}$$

$$C_s = \frac{1}{1+\dfrac{R_s R_a (R_c+R_w)}{R_c R_w (R_s+R_a)}} \tag{A1.30}$$

$$C_w = \frac{1}{1+\dfrac{R_w R_a (R_c+R_s)}{R_c R_s (R_w+R_a)}} \tag{A1.31}$$

Appendix Two

Nomenclature

Upper Case Roman

AE	Total available energy (W m^{-2})
AE_c	Available energy of canopy (W m^{-2})
AEC	Available energy of canopy for WPM model (W m^{-2})
AE_s	Available energy of bare soil (W m^{-2})
AES	Available energy of bare soil for WPM model (Wm^{-2})
AE_w	Available energy of open water (W m^{-2})
C_a	Canopy attenuation coefficient (dimensionless)
C_c	SW and MSW model coefficient for canopy (W m^{-2})
C_d	Mean drag coefficient for vegetation (dimensionless)
CF	Correction factor for transducers (dimensionless)
C_p	Specific heat of air at constant pressure (J $kg^{-1} \cdot K^{-1}$)
C_s	SW and MSW model coefficient for bare soil (W m^{-2})
C	Heat capacity of water (J $kg^{-1} \cdot K^{-1}$)
C_w	MSW model coefficient for open water (W m^{-2})
D	Vapour pressure deficit (kPa)
DAI	Dead area index (dimensionless)
D_o	Vapour pressure deficit at canopy source height (mb)
D_s	Vapour pressure deficit at soil surface (mb)
D_x	Vapour pressure deficit at reference height (kPa, mb)

FAI	Foliage area index (dimensionless)
H_o	Proportion of surface area of hummocks (dimensionless)
H_u	Proportion of surface area of hollows (dimensionless)
K_h	Eddy diffusivity of sensible heat ($m^2\ s^{-1}$)
K_m	Eddy diffusivity of latent heat ($m^2\ s^{-1}$)
K_v	Eddy diffusivity of momentum ($m^2\ s^{-1}$)
LAI	Leaf area index (dimensionless)
Lw	Mean leaf width (m)
PM_c	PM equation for canopy in SW and MSW models ($W\ m^{-2}$)
PM_s	PM equation for bare soil in SW and MSW models ($W\ m^{-2}$)
PM_w	PM equation for open water in SW and MSW models ($W\ m^{-2}$)
Q^*	Net radiation ($W\ m^{-2}$)
Q^*_c	Net radiation over canopy ($W\ m^{-2}$)
Q^*_{hol}	Net radiation over hollows ($W\ m^{-2}$)
Q^*_{hum}	Net radiation over hummocks ($W\ m^{-2}$)
Q^*_s	Net radiation over bare soil ($W\ m^{-2}$)
Q^*_{shum}	Net radiation over bare soil on hummocks ($W\ m^{-2}$)
Q^*_w	Net radiation over open water ($W\ m^{-2}$)
Q_e	Latent heat flux ($W\ m^{-2}$)
Q_{ec}	Canopy evaporation ($W\ m^{-2}$)
Q_{es}	Soil evaporation ($W\ m^{-2}$)
Q_{ew}	Water evaporation ($W\ m^{-2}$)
Q_g	Ground heat flux ($W\ m^{-2}$)
Q_{gc}	Ground heat flux of canopy ($W\ m^{-2}$)
Q_{gs}	Ground heat flux of bare soil ($W\ m^{-2}$)
Q_{gw}	Ground heat flux of open water ($W\ m^{-2}$)

Q_{g1} Transducer measurement for canopy (W m^{-2})

Q_{g2} Transducer measurement for bare soil (W m^{-2})

Q_{g3} Transducer measurement for open water (W m^{-2})

Q_h Sensible heat flux (W m^{-2})

ΔQ_{st} Change in storage (W m^{-2})

Ri Richardson number (dimensionless)

S Proportion of surface area of bare soil (dimensionless)

T Temperature (°C)

T_o Temperature at canopy source height (°C)

T_s Temperature of substrate (°C)

T_w Temperature of open water (°C)

T_x Temperature at reference height (°C)

x Reference height (m)

W Proportion of surface area of open water (dimensionless)

Lower Case Roman

d Zero plane displacement (m)

d_w Depth of open water (m)

e Vapour pressure (kPa; mb)

e_s Vapour pressure at surface (mb)

e_x Vapour pressure at reference height (mb)

$e_w(T)$ Saturation vapour pressure at temperature T (kPa; mb)

g Acceleration due to gravity (m s^{-2})

h Height of canopy (m)

k von Karman's constant (dimensionless)

n Eddy diffusivity decay constant (dimensionless)

n' Attenuation coefficient for wind speed (dimensionless)

r_a Aerodynamic resistance for PM model (s m^{-1})

r_{aa} Aerodynamic resistance between canopy source height and reference height (s m^{-1})

$r_{aa}(0)$ Value of r_{aa} for minimum FAI (s m^{-1})

$r_{aa}(\alpha)$ Value of r_{aa} for maximum FAI (s m^{-1})

r_{am} Aerodynamic resistance to momentum (s m^{-1})

r_b Mean boundary layer resistance (s m^{-1})

r_{bb} Bluff body resistance (s m^{-1})

r_c Canopy resistance for PM model (s m^{-1})

r_{ca} Bulk boundary layer resistance of canopy (s m^{-1})

r_{cs} Bulk stomatal resistance of canopy (s m^{-1})

r_i Climatological resistance (s m^{-1})

r_s Surface resistance (s m^{-1})

r_{sa} Aerodynamic resistance between bare soil surface and canopy source height (s m^{-1})

$r_{sa}(0)$ Value of r_{sa} for minimum FAI (s m^{-1})

$r_{sa}(\alpha)$ Value of r_{sa} for maximum FAI (s m^{-1})

r_{ss} Soil surface resistance (s m^{-1})

r_{st} Stomatal resistance (s m^{-1})

r_{wa} Aerodynamic resistance between open water surface and canopy source height (s m^{-1})

u Wind speed (m s^{-1})

u^* Friction velocity (m s^{-1})

u_h Wind speed at height of canopy (m s^{-1})

u_x Wind speed at reference height (m s^{-1})

u_z Wind speed at height z (m s^{-1})

z height (m)

z_o Surface roughness length (m)

z'_o Surface roughness length of bare soil and water (m)

Greek

β Bowen ratio (dimensionless)

Δ Slope of saturation vapour pressure vs. temperature curve (kPa $°C^{-1}$, mb $°C^{-1}$)

ρ Density of air (kg m^{-3})

γ Psychrometric constant (kPa $°C^{-1}$)

τ Momentum flux (Pa)

ϕ_h Stability function for sensible heat (dimensionless)

ϕ_m Stability function for momentum (dimensionless)

ϕ_v Stability funciton for latent heat (dimensionless)

References

Bailey, W.G. and J.A. Davies, 1981a. The Effect of Uncertainty in Aerodynamic Resistance on Evaporation Estimates from the Combination Model. Boundary Layer Meteorol., 20:187-199.

Bailey, W.G. and J.A. Davies, 1981b. Bulk stomatal resistance control on evaporation. Boundary Layer Meteorol., 20:401-415.

Beven, K., 1979. A sensitivity analysis of the Penman-Monteith actual evapotranspiration estimates. J. Hydrol., 44:169-190.

Carlson, D.W., 1991. Energy balance of wet sedge tundra during summer drought and the influence of variable surface topography. M.Sc. thesis, McMaster University, Hamilton, 110pp.

Choudhury, B.J. and J.L. Monteith, 1986. Implications of stomatal response to saturation deficit for the heat balance of vegetation. Agric. and Forest Meteorol., 36:215-225.

Choudhury, B.J. and J.L. Monteith, 1988. A four-layer model for the heat budget of homogenous land surfaces. Quart. J. R. Met. Soc., 114:373-398.

Cowell, D.W., 1982. Earth Sciences of the Hudson Bay Lowland: Literature Review and Annotated Bibliography. Working Paper No. 18, Lands Directorate, Environment Canada, Burlington, Ontario, 309pp.

Dolman, A.J. and J.S. Wallace, 1991. Lagrangian and K-theory approaches in modelling evaporation from sparse canopies. Quart. J. R. Met. Soc., 117:1325-1340.

Dyer, A.J., 1974. A review of flux-profile relationships. Boundary-Layer Meteorol., 7:363-372.

Fuchs, M. and C.B. Tanner, 1967. Evaporation from drying soil. J. Appl. Meteorol., 6:852-857.

Granger, R.J., 1989. An examination of the concept of potential evaporation. J. Hydrol., 111:9-19.

Halliwell, D.H., 1989. A numerical model of the surface energy balance and ground thermal regime in organic permafrost terrain. Ph.d. thesis, McMaster University, Hamilton, 195pp.

Halliwell, D.H. and W.R. Rouse, 1987. Soil heat flux in permafrost: characteristics and accuracy of measurement. J. Climatol., 7:571-584.

Halliwell, D.H. and W.R. Rouse, 1989. A Comparison of Sensible and Latent Heat Flux Calculations Using the Bowen Ratio and Aerodynamic Methods. J. Atmos. Oceanic Technol., 6:563-574.

Holtslag, A.A.M., 1984. Estimates of diabatic wind speed profiles from near-surface weather observations. Boundary-Layer Meteorol., 29:225-250.

Jacobs, C.M.J. and H.A.R. de Bruin, 1992. The Sensitivity fo Regional Transpiration to Land-Surface Characteristics: Significance of Feedback. J. Climate, 5:683-698.

Jarvis, P.G. and J.I.L. Morison, 1981. The control of transpiration and photosynthesis by the stomata. In P.G. Jarvis and T.A. Mansfield (eds.) Stomatal Physiology. Cambridge University Press, Cambridge, pp.247-279.

Jarvis, P.G., G.B. James and J.J. Landsberg, 1976. Coniferous Forest. In J.L. Monteith (ed.) Vegetation and the Atmosphere, Volume 2, Case Studies. Academic Press, London, pp.171-240.

Johnson, K.L., 1987. Wildflowers of Churchill and the Hudson Bay Region. Manitoba Museum of Man and Nature, Winnipeg, 400pp.

Jones, F.E., 1992. Evaporation of Water - With Emphasis on Applications and Measurements. Lewis Publishers, Inc., Michigan, 188pp.

Kaufmann, M.R. and E.L. Fiscus, 1985. Water transport through plants - Internal integration of edaphic and atmospheric effects. Acta Horticulturae, 171:83-93.

Korner, Ch., Scheel, J.A. and Bauer, H., 1979. Maximum leaf diffusion conductance in vascular plants. Photosynthetica, 13:45-82.

LaFleur, P.M., 1988. Leaf conductance of four species growing in a subarctic marsh. Can. J. Bot., 66:1367-1375.

LaFleur, P.M. and W.R. Rouse, 1988. The influence of surface cover and climate on energy partitioning and evaporation in a subarctic wetland. Boundary-Layer Meteorol., 44:327-347.

LaFleur, P.M. and W.R. Rouse, 1990. Application of an energy combination model for evaporation from sparse canopies. Agric. and Forest Meteorol., 49:135-153.

LaFleur, P.M., W.R. Rouse and D.W. Carlson, 1992. Energy balance differences and hydrologic impacts across the northern treeline. Int. J. Climatol., 12:193-203.

McCuen, R.H., 1974. A sensitivity and error analysis of procedures used for estimating evaporation. Water Resour. Bull., 10:486-497.

McNaughton, K.G. and P.G. Jarvis, 1983. Predicting effects of vegetation changes on transpiration and evaporation. In T.T. Kozlowski (ed.) Water Deficits and Plant Growth, Academic Press, New York, pp.1-47.

Monteith, J.L., 1965. Evaporation and Environment. Symp. Soc. Exp. Biol., XIX, Cambridge University Press, London, 205-234.

Monteith, J.L., 1973. Principles of Environmental Physics. Edward Arnold, London, 241pp.

Monteith, J.L., 1981. Evaporation and surface temperature. Quart. J. R. Met. Soc., 107:1-27.

Morton, F.I., 1983. Operational estimates of areal evapotranspiration and their significance to the science and practice of hydrology. J. Hydrol., 66:1-76.

National Wetlands Working Group (NWWG) of the Canada Committee on Ecological Land Classification, 1987. The Canadian Wetland Classification System. Series No. 21, Lands Conservation Branch, Canadian Wildlife Service, Environment Canada, 18pp.

Ohmura, A., 1982. Objective Criteria for Rejecting Data for Bowen Ratio Flux Calculations. J. Appl. Meteorol., 21:595-598.

Penman, H.L., 1948. Natural evaporation from open water, bare soil and grass. Proc. Roy. Soc. London, Series A, 193:120-145.

Priban, K. and J.P. Ondok, 1980. The daily and seasonal course of evapotranspiration from a central European sedge-grass marsh. J. Ecology, 68:547-559.

Riley, J.L., 1982. Hudson Bay Lowland floristic inventory, wetlands catalogue and conservation strategy. Naturaliste canadien, 109:543-555.

Riley, J.L., 1990. The Vascular Plants of the Hudson Bay Lowland and their Postglacial Origins. Ontario Ministry of Natural Resources Parks and Recreational Areas Section, Central Region, Richmond Hill, 222pp.

Roulet, N.T. and M.K. Woo, 1986. Hydrology of a wetland in the continuous permafrost region. J. Hydrol., 89:73-91.

Rouse, W.R., 1984. Microclimate at the arctic treeline: 2. Soil microclimate of tundra and forest. Water Resour. Res., 20:67-73.

Rouse, W.R., D.W. Carlson and E.J. Weick, 1992. Impacts of summer warming on the energy and water balance of wetland tundra. Clim. Change, (in press).

Rutter, A.J., 1975. The Hydrological Cycle in Vegetation. In J.L. Monteith (ed.) Vegetation and the Atmosphere, Volume 1, Principles. Academic Press, London, pp.111-154.

Saxton, K.E., 1975. Sensitivity analyses of the combination evapotranspiration equation. Agric. Meteorol., 15:343-353.

Shaw, R.H. and A.R. Pereira, 1982. Aerodynamic roughness of a plant canopy: A numerical experiment. Agric. Meteorol., 26:51-65.

Shuttleworth, W.J. and R.J. Gurney, 1990. The theoretical relationship between foliage temperature and canopy resistance in sparse crops. Quart. J. R. Met. Soc., 116:497-519.

Shuttleworth, W.J. and J.S. Wallace, 1985. Evaporation from sparse crops - an energy combination theory. Quart. J. R. Met. Soc., 111:839-855.

Sims, R.A., J.L. Riley and J.K. Jeglum, 1979. Vegetation, flora and vegetational ecology of the Hudson Bay Lowland: a literature review and annotated bibliography. Department of the Environment, Canadian Forestry Service, Report O-X-297, 177pp.

Stewart, J.B. and A.S. Thom, 1973. Energy Budgets in a Pine Forest. Quart. J. R. Met. Soc., 99:154-170.

Squire, G.R. and C.R. Black, 1981. Stomatal behaviour in the field. In P.G. Jarvis and T.A. Mansfield (eds.) Stomatal Physiology. Cambridge University Press, Cambridge, pp.223-245.

Tan, C.S. and Black, T.A., 1976. Factors Affecting the Canopy Resistance of a Douglas-Fir Forest. Boundary-Layer Meteorol., 10:475-488.

Thom, A.S., 1972. Momentum, mass and heat exchange of vegetation. Quart. J. R. Met. Soc., 98:124-134.

Thom, A.S., 1975. Momentum, Mass and Heat Exchange of Plant Communities. In J.L. Monteith (ed.) Vegetation and the Atmosphere, Volume 1, Principles. Academic Press, London, pp.57-109.

Uchijima, Z., 1976. Maize and Rice. In J.L. Monteith (ed.) Vegetation and the Atmosphere, Volume 2, Case Studies. Academic Press, London, pp.33-64.

Waggoner, P.E., 1975. Micrometeorological Models. In J.L. Monteith (ed.) Vegetation and the Atmosphere, Volume 1, Principles. Academic Press, London, pp.205-228.

Wallace, J.S., J.M. Roberts and M.V.K. Sivakumar, 1990. The estimation of transpiration from sparse dryland millet using stomatal conductance and vegetation area indices. Agric. and Forest Meteorol., 51:35-49.

Weick, E.J., 1989. Energy advection in an arctic coastal environment, Churchill, Manitoba. M.Sc. thesis, McMaster University, Hamilton, 120pp.

Willmott, C.J. and D.E. Wicks, 1980. An Empirical Method for the Spatial Interpolation of Monthly Precipitation within California. Phys. Geog., 1:59-73.